

A COMPARISON BETWEEN DIAMICTITES AT THE WITTEBERG- DWYKA CONTACT IN SOUTHERN SOUTH AFRICA

by
MARELI GROBBELAAR

*Thesis presented in fulfilment of the requirements for the degree
of Master of Science in the Faculty of Science at Stellenbosch
University*



Supervisor: Prof Daniel Mikeš (Department of Geosciences, Nelson Mandela
Metropolitan University)
Co-supervisor: Prof Abraham Rozendaal (Department of Earth Science, Stellenbosch
University)

Maart 2015

DECLARATION

By submitting this thesis electronically, I declare that the entirety of the work contained therein is my own, original work, that I am the sole author thereof (save to the extent explicitly otherwise stated), that reproduction and publication thereof by Stellenbosch University will not infringe any third party rights and that I have not previously in its entirety or in part submitted it for obtaining any qualification.

Mareli Grobbelaar

Maart 2015

14620006

ABSTRACT

Diamictites are sedimentary deposits that originate from a number of different environments, the most common being associated with a glacial environment. Although this association is not, in all cases correct, it is still being used due to the lack of knowledge to confidently identify, classify and interpret a depositional environment for diamictite deposits.

During the late Carboniferous to early Permian, two diamictite deposits formed during the development of the Cape Basin and Main Karoo Basin in the southern margins of South Africa. These deposits are known as the Miller diamictite and Dwyka diamictite. The latter is well known and was deposited during the Karoo-deglaciation. The Dwyka diamictite is often referred to as Dwyka Tillite. This is an inappropriate reference owing to that not all of the Dwyka deposits are directly formed as a result of glacial contact. The origin of the Miller diamictite is uncertain, but there are suggestions that its origin can be traced to either a glacial or debris flow deposit formed in a deltaic environment, thus referred to by some as a tillite and others as a diamictite.

To establish the sedimentary environments of the above mentioned diamictite deposits in the study area, two facies models were presented with a notable bias for the second model. The first model represents a continuous sedimentation cycle between the closing of the Cape Basin and opening of the Main Karoo Basin, whereas the second model demonstrates an erosional break (hiatus) between the depositions of the above mentioned basins.

Derived from the use of the second model, it can be concluded that the Miller diamictite can indeed be classified as a diamictite from a textural interpretation. Both diamictites (Miller and Dwyka) cannot be referred to as tillite deposits since none show evidence of direct glacial contact. The Miller and the Dwyka are both diamictites, but were formed in different sedimentary environments. The Miller diamictite is a product of debris flow deposits from the slope of a braided delta, whereas the Dwyka diamictite represents distal glacio-marine "rain-out" deposits.

UITTREKSEL

Diamiktiete is sedimentêre neerslae afkomstig vanaf verskillende omgewings en dit word meestal met 'n glasiale omgewing geassosieer. Alhoewel hierdie assosiasie nie in alle gevalle korrek is nie, word dit nog steeds gemaak as gevolg van die gebrek aan kennis om diamiktiete met selfvertroue te identifiseer, te klassifiseer en 'n afsettingsomgewing vir die sedimente te interpreteer.

Gedurende die laat Karboon tot vroeë Permiese tydperk het twee diamiktiet afsettings gevorm gedurende die vorming van die Kaap Supergroep Kom en Karoo Kom in die suidelike grense van Suid-Afrika. Die afsetting staan bekend as die Miller diamiktiet en Dwyka diamiktiet. Laasgenoemde is redelik bekend en is gedurende die Karoo gletser ontvormings tydperk gesedimenteer. Die Dwyka diamiktiet word dikwels Dwyka Tilliet genoem, wat onvanpas is aangesien nie al die Dwyka neerslae direk gevorm het as gevolg van direkte glasiale kontak nie. Die oorsprong van die Miller diamiktiet is egter onseker. Dit word veronderstel dat die Miller diamiktiet óf deur 'n gletser, of puin vloeï neerslag gevorm het in 'n deltaïese omgewing, dus word daarna verwys as 'n tilliet of 'n diamiktiet.

Om die sedimentêre omgewings van die twee bogenoemde diamiktiet afsettings in die studie area te bevestig, is twee fasies modelle aangebied met 'n voorkeur aan die tweede model. Die eerste fasies model verteenwoordig 'n siklus van ongebroke sedimentasie tydens die sluiting van die Kaapse Kom en die opening van die Karoo Kom. Die tweede fasies model verteenwoordig 'n hiatus tussen die afsetting van die bogenoemde komme.

Gegronde op sy teksturele samestelling kan die Miller diamiktiet inderdaad as 'n diamiktiet geklassifiseer word. Beide diamiktiete (Miller en Dwyka) kan nie as tilliet neerslae beskou word nie, aangesien geen bewyse gelewer kan word van afsetting as gevolg van direkte glasiale kontak nie. Die Miller en Dwyka is 'n diamiktiet, maar is gevorm in verskillende afsettingsomgewings. Die Miller diamiktiet is 'n produk van die puin vloeï neerslag vanaf die helling van 'n delta, terwyl die Dwyka diamiktiet verteenwoordig 'n afgeleë glasio-mariene "uit-reen" neerslae.

ACKNOWLEDGEMENTS

My sincere thanks to the farming community of the Willowmore area for their hospitality and access to their beautiful farms during my field work period. Without their contribution this project would not have been possible.

I would like to thank my supervisors, Prof Mikeš and Prof Rozendaal for their assistance and guidance in the preparation of this thesis. Funding for the project was provided by Tullow Oil for which I am very grateful.

Finally I am grateful for the support of my family during my studies and want to acknowledge the contributions they made to guide me through this research project.

TABLE OF CONTENTS

	Pages
Abstract	I
Uittreksel	II
Acknowledgements	III
Table of contents	IV
List of figures	VII
List of tables	XIX
Chapter 1: Introduction	1
1.1 Background	1
1.2 Purpose of study	6
1.3 Methodology	7
1.3.1 Field work	7
1.3.1.1 Stratigraphic profiles	7
1.3.1.2 Sampling	13
1.3.2 Laboratory work	13
1.3.2.1 Petrography	13
1.3.3 Facies analysis	14
Chapter 2: Sedimentary systems	15
2.1 Classification and definitions of sediments	15
2.1.1 Texture	16
2.1.2 Composition	19
2.1.3 Source	19
2.1.4 Summary	19
2.2 Sedimentary processes	20
2.2.1 Gravity flow processes	20
2.2.1.1 Debris flow	20
2.3 Relevant environmental settings	24
2.3.1 Glacial systems	24

2.3.2	Deltaic systems	33
2.4	Linking sedimentary processes with environments	39
2.5	Facies analysis	42
2.5.1	Meaning of facies analysis	42
Chapter 3:	Regional and local geology	43
3.1	Plate tectonics of Cape – and Karoo Basin	43
3.2	Paleogeography	45
3.2.1	Basins	45
3.2.1.1	Witteberg Basin and Kommadagga Sub-basin	45
3.2.1.2	Karoo Basin	49
3.3	Facies analysis of local geology	52
3.3.1	Kommadagga Subgroup	52
3.3.2	Dwyka Group	58
3.4	Provenance	59
Chapter 4:	Descriptions of facies	62
4.1	Introduction	62
4.2	Facies A	62
4.2.1	Description	62
4.2.2	Interpretation	69
4.3	Facies B	69
4.3.1	Description	69
4.3.2	Interpretation	71
4.4	Facies C	71
4.4.1	Description	71
4.4.2	Interpretation	73
4.5	Facies D	75
4.5.1	Description	75
4.5.2	Interpretation	77
4.6	Facies E	79
4.6.1	Description	79
4.6.2	Interpretation	79
4.7	Facies F	82
4.7.1	Description	82

4.7.2 Interpretation	85
4.8 Facies G	85
4.8.1 Description	85
4.8.2 Interpretation	86
4.9 Facies H	86
4.9.1 Description	86
4.9.2 Interpretation	89
4.10 Facies I	89
4.10.1 Description	89
4.10.2 Interpretation	92
4.11 Facies J	94
4.11.1 Description	94
4.11.2 Interpretation	96
Chapter 5: Facies associations and model	97
5.1 Facies associations	97
5.1.1 Distal glacio-marine deposits (FA1)	97
5.1.2 Proximal slope deposits (FA2)	101
5.1.3 Beach barrier and tidal flats deposits (FA3)	101
5.1.4 Delta front and prodelta deposits (FA4)	103
5.2 Facies models	106
5.2.1 Model 1	108
5.2.2 Model 2	110
Chapter 6: Discussion and conclusion	114
References:	117
Appendix A:	126
Appendix B:	133
Appendix C:	134

LIST OF FIGURES**PAGE****CHAPTER ONE**

- Fig. 1.1: Location of the study area northeast of Willowmore indicating the Miller and Dwyka diamictite (not to scale) (Modified after Johnson, 1991). 2
- Fig. 1.2: Top - Late Palaeozoic glaciated basins; Bottom - maximum extent of glacially influenced marine conditions across Gondwana during Late Palaeozoic glaciations (Modified after Eyles, 1993). 3
- Fig. 1.3: Schematic reconstruction of the depositional setting for the valley and platform facies associations of Dwyka diamictites (Smith et al., 1993). 5
- Fig. 1.4: Map overview of main locations (Map1 and Map2) visited during fieldwork. 8
- Fig. 1.5a: Geological Map 1 indicating stratigraphic profile 1 at Volstruisleegte (A) and profiles 2 and 3 at Miller (B). 9
- Fig. 1.5b: Cross section A¹ – B¹ through study area at Volstruisleegte indicating stratigraphic profile 1 (Geological Map 1; Fig. 1.5a). 10
- Fig. 1.5c: Cross section A² – B² through area surrounding study area at Miller indicating stratigraphic profiles 2 and 3 (Geological Map 1; Fig 1.5a.). 10

Fig. 1.6a:	Geological Map 2 indicating stratigraphic profiles 4 and 5 at Swaylands (A) and profile 6 at Campherspoort (B).	11
Fig. 1.6b:	Cross section A ³ – B ³ through area surrounding study area at Swaylands indicating stratigraphic profile 4 and 5 (Geological Map 2, Fig. 1.6a).	12
Fig. 1.6c:	Cross section A ⁴ – B ⁴ through area surrounding study area at Campherspoort indicating stratigraphic profile 6 (Geological Map 2, Fig 1.6a).	12

CHAPTER TWO

Fig. 2.1:	Non-genetic classification of poorly sorted sediments with 50% as maximum proportion of gravel in diamict. The term "diamict" embraces both diamicton (unconsolidated) and diamictite (consolidated). "Mud" as used in this context, covers all fine sediments, i.e. mixtures of clay and silt Modified after Hambrey (1994).	17
Fig. 2.2:	Summary of the possible classifications of conglomerates with the main focus on terrigenous conglomerates.	21
Fig. 2.3:	Development of a debris flow in subaerial and subaqueous settings.	25
Fig. 2.4:	(A) Geometrical features of a debris flow, with distorted scale. (B) Sorting mechanisms and deposits of a debris flow (Bridge and Demicco, 2008).	26

Fig. 2.5:	Depositional structures of (A) strongly coherent debris flows and (B) moderate and weak coherent gravity flows (Marr et al., 2001).	25
Fig. 2.6:	Glacio terrestrial and glaciomarine depositional systems with associated facies (Eyles, 1993).	28
Fig. 2.7:	Summary of different glacial environments, indicating in which till deposits form.	31
Fig. 2.8:	Twelve prototype deltas, distinguished on the basis of a unique combination of four different type of feeder/distributary system and two ranges of basin depth. It also takes into account the variations due to inertia-friction and buoyancy-dominated river discharge (Postma, 1990)	34
Fig. 2.9:	Geometry of a delta. Modified after Boggs (2006) and Bridge and Demicco (2008)	35
Fig. 2.10:	Schematic representation of diamictite guideline.	40

CHAPTER THREE

Fig. 3.1:	Crustal evolution of southern Africa. N-N = Namaqua-Natal; K.C. = Kaapvaal Craton (Shone and Booth, 2005) with a description of the tectonic history (Modified after Tankard et al., 2009).	44
-----------	---	----

- Fig. 3.2: The Cape basin indicating the estimated boundaries from the opening (Table Mountain Group) of the basin towards the closing (Witteberg Group), as well as the northwards movement of the depo-axis during this period. (Modified after Dunley and Hiller, 1979). 46
- Fig. 3.3: Distribution of Witteberg Group. Marked area indicates the region which the Kommadagga Subgroup is confined to (Modified after SACS, 1980). 48
- Fig. 3.4: Paleogeographic (top) and paleotectonic (bottom) setting of Late Palaeozoic Dwyka Group (Eyles, 1993). 50
- Fig. 3.5: Sedimentary environments of pre-Karoo and Karoo Basin (Modified after Smith et al., 1993). 51
- Fig. 3.6: Flow direction of ice sheets during the Dwyka glaciation. Also show limits of marine conditions and extent of the Gondwana Ice sheet at about the Carboniferous-Permian boundary (Visser, 1997). 51
- Fig. 3.7: Schematic diagram of the deglaciation sequence in the Karoo Basin (A-D). A – Maximum extent of ice sheet over Karoo basin from north to south (Cambrian-Permian); B – Collapsing of ice margin allowing iceberg rafting in south. Active glaciation in north; C & D –Retreating phase of ice margin due to changes in climate with ice only restricted to the highlands in the north (Modified after Visser, 1997). 53

Fig. 3.8:	Stratigraphic column summarising lithology of Dwyka Group and Kommadagga Subgroup (Modified after Johnson (1991), Booth and Shone (2002), Johnson et al., (2006)).	54
Fig. 3.9:	Stratigraphic nomenclature changes of the Witteberg Group and Dwyka Group from 1953 to present (not to scale).	55
Fig. 3.10:	Distribution of Elandsvlei - and Mbizane Formations of Dwyka Group (Visser and Young, 1990).	60

CHAPTER FOUR

Fig. 4.1a:	Stratigraphic profile 1, 2 and 3.	64
Fig. 4.1b:	Stratigraphic profile 4, 5 and 6.	65
Fig. 4.2:	Texture of Dcm, a diamictite, indicating random sized clasts in a matrix. A – Weathered rock; B – Fresh rock	66
Fig. 4.3:	A - Plutonic rock fragment with interstitial material wrapping around clast. B - Overall view of clast-rich diamictite, Dcm, showing cleavage seams (arrows).	68
Fig. 4.4:	Outcrop of Sm at Miller showing veins and slickenside features on bedding.	68
Fig. 4.5:	A - Overview of Sm indicating coarse to medium sized grains which have point and concavo convex contact relation with each other. B - Schist rock fragment.	68

Fig. 4.6:	Ffd, fissile mudstone.	70
Fig. 4.7:	A – Lamination in Ffd wrapping around larger sand size grains. B - Lamination between silt (dark layers) and clay (light layers).	70
Fig. 4.8:	An outcrop of Dmm. Note small white clasts.	72
Fig. 4.9:	A - SEM image of igneous rock fragment in interstitial material. B - Overview of Dmm.	74
Fig. 4.10:	A - Overview of Smc with chlorite (cl) grains. B – SEM image of folded carbon streaks in Smc.	74
Fig. 4.11:	A - Grooves on bedding planes of Sl. B - Folding banded layers of quartzitic unit Sl.	76
Fig. 4.12:	Low angle planar lamination in Sl. Note the alternating white quartzitic and brown (iron oxide stained) bands defining the lamination.	76
Fig. 4.13:	Pebbles in bedding.	76
Fig. 4.14:	A – Overview of sandstone Sl. B - Lithic rock fragment in Sl.	78
Fig. 4.15:	Outcrop of Frc indicating ripple marks with strong interference of cleavage.	80

Fig. 4.16:	Ripple marks on bedding plane of lithological unit Frc.	80
Fig. 4.17:	SEM image indicating organic carbon streaks in between matrix of Frc.	81
Fig. 4.18:	A - Lenticular lamination of fine sand/silt lenses surrounded by clay in Frc. B - Close up of clay (Illite) layer in Frc.	81
Fig. 4.19:	Mixture of pebbles on the surface bedding plane of Smr.	83
Fig. 4.20:	Sample of Smr indicating the abrupt change in grain size from fine grained (below line) to coarse grained (above line). Arrow indicates "way up" of bedding.	83
Fig. 4.21:	Overview of gravelly quartz arenite Smr showing coarse sand grains surrounded by fine sand size grains.	83
Fig. 4.22:	Beds of Slr showing low angle horizontal lamination.	84
Fig. 4.23:	Bedding plane of Slr indicating small adhesion ripples.	84
Fig. 4.24:	Overview of quartz arenite Slr showing quartz with chlorite cement.	84
Fig. 4.25:	Overview of Smq quartzite indicating pressure solution and quartz overgrowth.	87

Fig. 4.26:	A - Overview of Fm. B - SEM close up image of Fm showing random distribution of silt grains.	87
Fig. 4.27:	Left - Horizontal - , cross lamination and carbonate bands in Fdp. Right - Nodule in Fdp.	88
Fig. 4.28:	Left – slumping in Fdp; Right – distorted horizontal lamination.	88
Fig. 4.29:	A - SEM image of Fdp showing clay grains wrapping around silt size grains. B - Mineralogy indicating silica content with bright orange colours being quartz grains. Green and blue and black are lower levels with black being the lowest.	90
Fig. 4.30:	Depositional structures in Frt.	90
Fig. 4.31:	Outcrop of Frt showing asymmetric current ripples on surface plane.	91
Fig. 4.32:	Surface marks (grazing trail marks) on bedding plane of Frt.	91
Fig. 4.33:	Left - Outcrop of Flp. Right – Close up view of alternating layers 1, 2 and 3.	93
Fig. 4.34:	Flame structures in mudstone Ffb, with bioturbation.	93
Fig. 4.35:	Low angle cross lamination (bottom, CL) and massive bed (top, M) in Slm.	95

Fig. 4.36: Low angle planar lamination in SIm. 95

Fig. 4.37: Overview of SIm. 95

CHAPTER FIVE

Fig. 5.1: The relations between the facies associations over the stratigraphic profiles at all four locations. Please note the difference in scale for each profile. Profiles can be viewed in more detail in Fig. 4.1 99

Fig. 5.2: Estimated boundary relation between Facies A and B at Volstruisleegte. 100

Fig. 5.3: Sharp boundary between facies B and C (Boundary between FA1 and FA2). Estimated contact between facies C and D at Volstruisleegte. 102

Fig. 5.4: Erosional boundary between Facies E (FA3) and C (FA2). Irregular sharp boundary between Facies C and D (FA2) at Miller. 102

Fig. 5.5: Sharp irregular surface boundary between Facies E and F at Swaylands. 104

Fig. 5.6: Contact relations between tidal flat facies E and F. Both boundaries are sharp and erosional. 104

Fig. 5.7:	Erosional boundary surface with scours between Srm and Slr at Swaylands.	104
Fig. 5.8:	Small ridges formed by facies J with facies A on the lower edges covered by vegetation at Campherspoort's syncline.	105
Fig. 5.9:	Unconformable contact between facies A and facies J at Campherspoort.	107
Fig. 5.10:	Hypothesized sedimentary environment of Model 1 representing FA1 and FA2.	109
Fig. 5.11:	Hypothesized sedimentary environment of Model 2 representing Stage 1 followed by Stage 2.	111

APPENDIX A

Fig. A1:	Overview of Volstruisleegte with GPS points corresponding to the different lithological units.	129
Fig. A2:	Overview of Miller station indicating GPS point.	130
Fig. A3:	Overview of Swaylands with GPS points.	131
Fig. A4:	Overview of Campherspoort with GPS points corresponding to the different lithological units.	132

APPENDIX C

Fig. C1:	Overview of Sl.	134
Fig. C2:	Matrix (<63 μ) between sand size grains in Dmm.	134
Fig. C3:	Sand - size calcite grain in Dmm.	135
Fig. C4:	Quartz vein (top) cutting through Ffd (bottom).	135
Fig. C5:	Magnetite - quartz - biotite grain in Sm.	136
Fig. C6:	Plutonic rock fragment situated in interstitial material of Dcm.	136
Fig. C7:	Overview of Smc.	137
Fig. C8:	Overview of Ffd with dropstone clasts.	137
Fig. C9:	Calcite rim around rock fragment in Dcm.	138
Fig. C10:	Close up of matrix of Dcm.	138
Fig. C11:	Granitic rock fragment in Sm.	139

Fig. C12:	Close-up of Frc show fine sand grains and matrix with carbon streak.	139
Fig. C13:	Close-up SEM image of folded carbon streak in Frc.	140
Fig. C14:	Large rock fragment surrounded by interstitial material of Dcm.	140
Fig. C.15:	Close-up of SIm with garnet and quartz grain in centre.	140

LIST OF TABLES

	PAGE
CHAPTER TWO	
Table 2.1: General characteristics of the 12 prototype deltas. Modified after Postma (1990).	37
Table 2.2: General guideline for diamictites.	41
CHAPTER FOUR	
Table 4.1: Classification code of facies divisions with key characteristics and location.	63
CHAPTER FIVE	
Table 5.1: Summary of main features of the facies and facies associations.	98
Table 5.2: Correlation between stratigraphic groups and facies associations.	112
APPENDIX A	
Table A1: GPS coordinates of facies divisions, samples and thin sections of each location.	126

APPENDIX B

Table B1: The Udden-Wentworth grain-size classification scale (Boggs, 2006).

143

CHAPTER ONE

INTRODUCTION

1.1 Background

During the late Carboniferous to early Permian two diamictite deposits formed in the Cape – and Main Karoo Basin along the southern margins of South Africa. They are respectively known as the Dwyka diamictite and the Miller diamictite.

The Dwyka diamictite is distributed over an extensive area throughout South Africa which commonly forms the outer margin of the Main Karoo basin. In South Africa, this diamictite is stratigraphically part of the Dwyka Group. The Miller diamictite is only exposed in the eastern part of the Witteberg basin, in the area between Willowmore and Port Elizabeth in the Eastern Cape, South Africa. These key study areas offer a unique opportunity to study both the Dwyka - and Miller diamictite insitu. Due to its limited exposure, this is the only locality in South Africa with both units exposed and readily accessible. Stratigraphically the Miller diamictite is referred to as the Miller Formation which forms part of the Witteberg Group. The study area is situated north east of Willowmore extending east over four locations (farms); Volstruisleegte, Miller, Swaylands and Campherspoort (Figure 1.1).

During the late Palaeozoic period, which started around 275 Ma (Eyles, 1993), the Gondwana continent drifted across the South Pole. According to Crowell and Frakes (1972) the glaciation period during this time was initiated due to this movement when broad continental areas reached near polar positions, causing moist and cold climatic conditions that were enough to support glacial conditions (Figure 1.2).

During the near polar position of southern Africa, and the high latitudinal position in which the Cape Supergroup was deposited during the Carboniferous, the Witteberg Group was most likely influenced by winter storms, favouring cold to temperate climates and glacial conditions (Broquet, 1992). These glacial conditions were possibly recorded by the Kommadagga Subgroup (in which the Miller Formation is present), followed by the deposition of the Karoo Supergroup. Visser (1989) suggested that the shelf facies of the Dwyka Group was deposited under subpolar conditions in a distal marine deposystem, whereas the valley facies was laid down by temperate tidewater glaciers (Visser and Young, 1990).

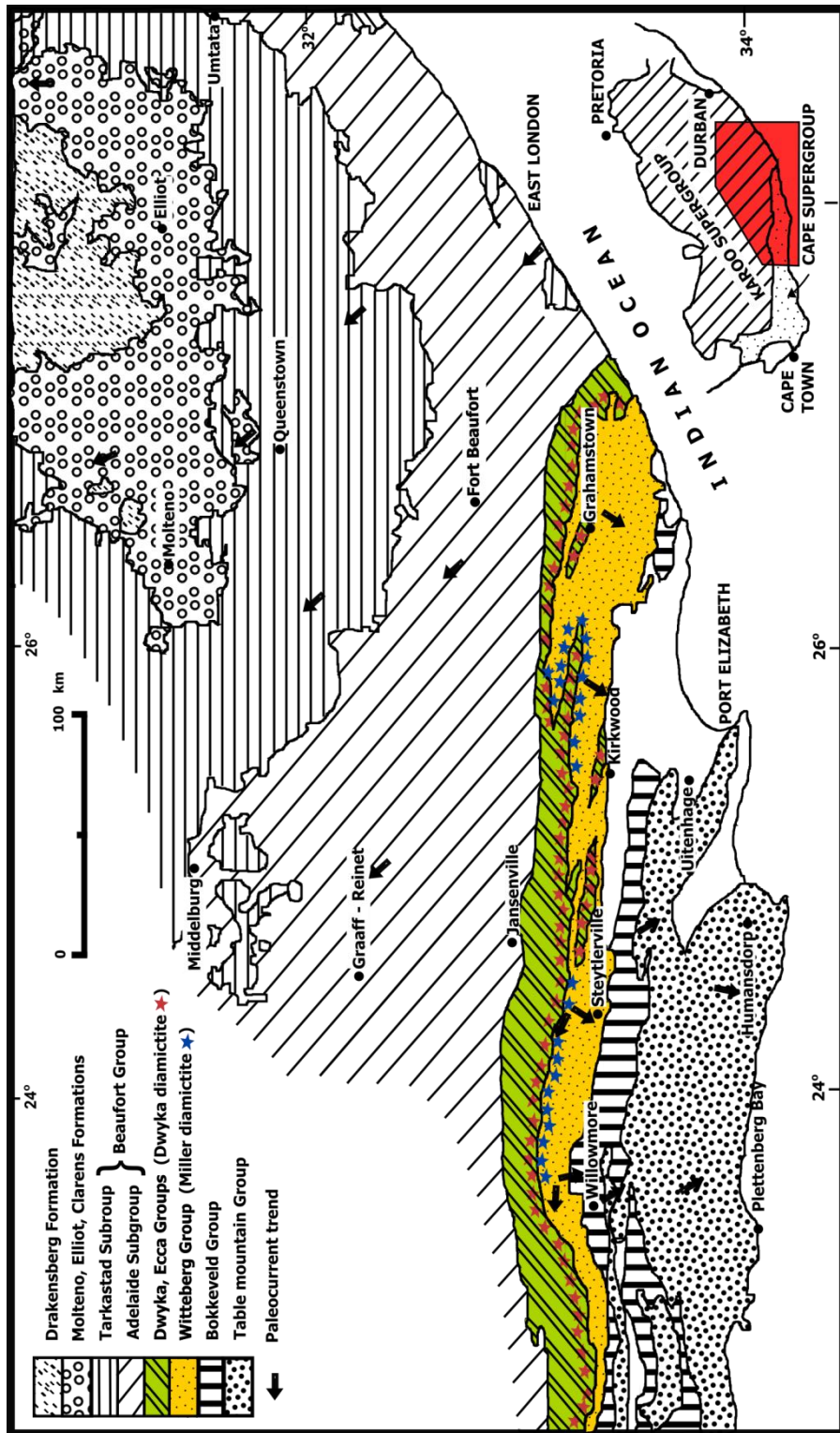


Figure 1.1: Location of the study area northeast of Willowmore indicating the Miller and Dwyka diamicite (not to scale) (Modified after Johnson, 1991).

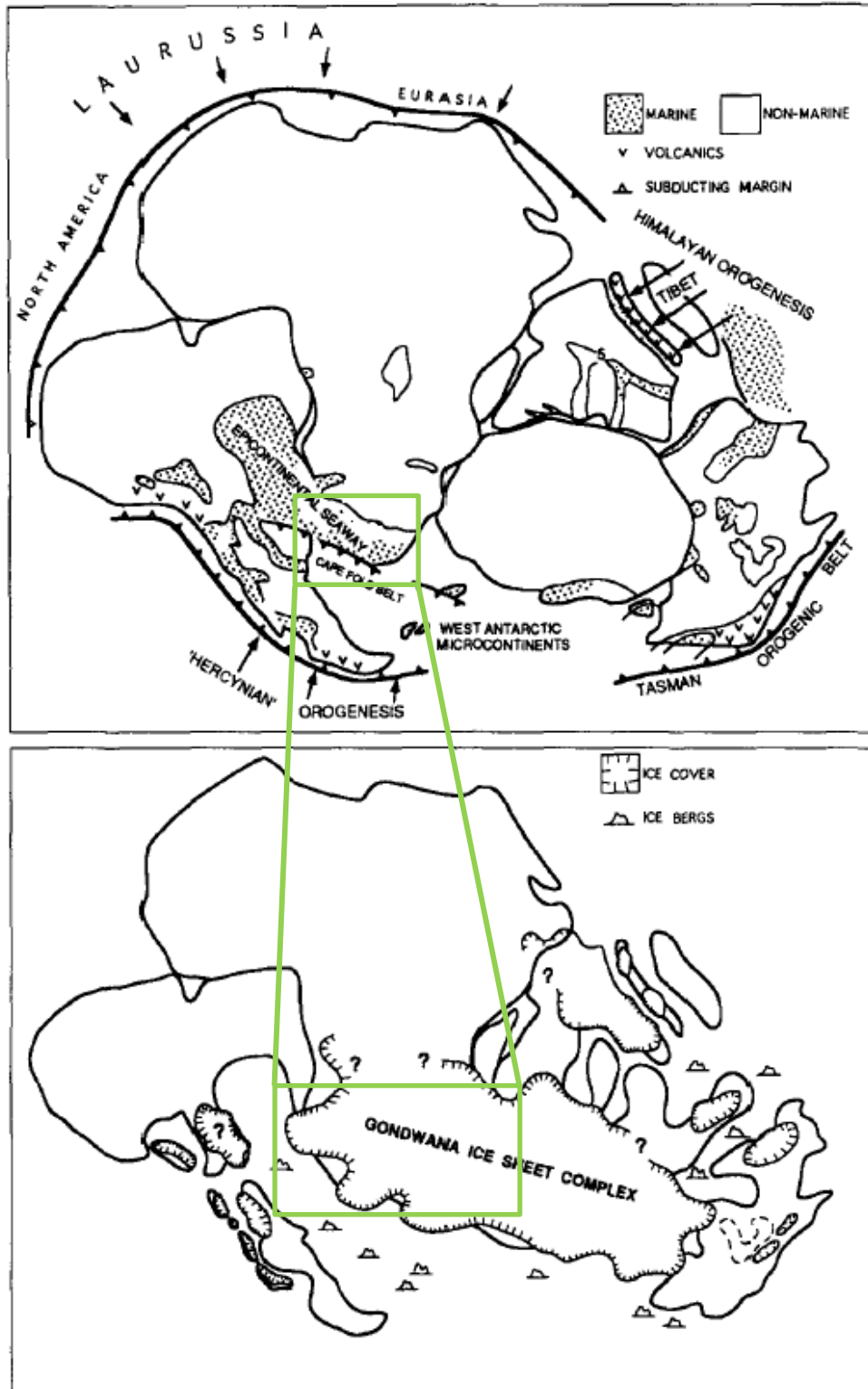


Figure 1.2: Top - Late Palaeozoic glaciated basins; Bottom - maximum extent of glacially influenced marine conditions across Gondwana during Late Palaeozoic glaciations (Modified after Eyles, 1993).

According to Visser (1986, 1991) and Rossouw (1953), these two diamictite deposits represent glacial periods during the formation of the Cape – and Main Karoo Basin. However, in some cases there has been debate about whether both of these diamictite deposits are indeed related to glacial periods, since diamictites are not necessarily of glacial or ice sheet origin (Reimold et al., 1997).

Rossouw (1953, 1970) made no direct attempt to interpret the Miller Formation, and his research was mainly descriptive. The fact that he used the name basal tillite suggests that it was interpreted as a tillite of direct glacial origin. He did not elaborate on the kind of tillite or depositional process it represents. Johnson (1976) agrees with this “interpretation” without any real confirmation. He only states in his paper (Johnson, 1991) that the “discontinuous Miller diamictite Formation is considered to reflect either a minor glacial episode or extensive slumping”, which is stated as two contradicting facies, but can actually represent the same. Crowell (1957) and Bell (1981) interpreted it as a debris flow deposit off the front of a delta, based on its lack of sedimentary structures and poor sorting. Swart (1982) agreed with this view and states that “no evidence for the glacial origin proposed by Rossouw (1953) and Johnson (1976) was found in this study”. Thus the depositional environment of the Miller diamictite is poorly defined.

Swart (1982) provided a detailed description and facies interpretation of the Dwyka diamictite. It is interpreted as a deposit characteristic of glacial marine sediments. For the most southern part of the Main Karoo Basin surrounding the study area, the Dwyka diamictite is interpreted as being deposited beneath/below semi-grounded and rafted ice sheets. This accumulated by subaqueous rain-out (drop stones) from a floating ice sheet (Crowell and Frakes, 1972; Visser et al., 1990; Smith et al., 1993; Catuneanu et al., 1998) and locally reworked by downslope resedimentation. The depositional environment was considered to have been in a gently sloping deep water shelf setting subjected to large scale mass flows, due to the absence of shallow water indicators (Eyles, 1993). In summary; the Dwyka Group (which includes the Dwyka diamictite) represent a glacial environment with deposition from grounded ice in the glaciated highlands to the north (referred to as “valley facies” - alluvial) and floating ice in semi-submerged lowlands to the south (referred to as “platform facies” - marine) (Smith et al., 1993; Catuneanu et al., 1998) (

Figure 1.3).

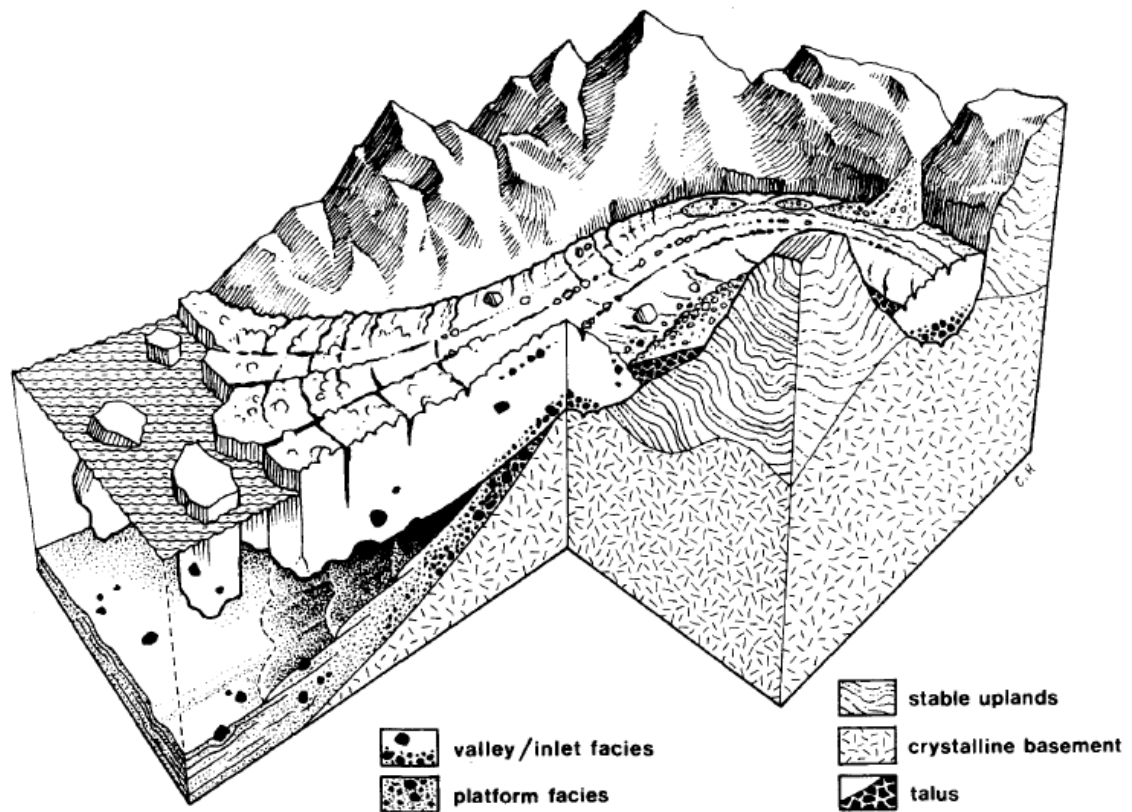


Figure 1.3: Schematic reconstruction of the depositional setting for the valley and platform facies associations of Dwyka diamictites (Smith et al., 1993).

Rossouw (1953, 1970) also suggested that the Miller diamictite (named by Rossouw as “basal tillite”) was wedged apart from the Dwyka diamictite (named by Rossouw as “main tillite”) by a fissile shale band. This statement made by Rossouw does not clarify whether these diamictites were “wedged apart” due to tectonic influences or whether this was an interlayered shale band which was laterally pinching out. His lack of a clarification here alludes to a very implicit assumption that the Miller and Dwyka diamictite may in some manner be related to each other. Although Dunley and Hiller (1979) mentioned that during the hiatus of about 20 to 30 Ma (Visser, 1991; Catuneanu et al., 1998; Tankard et al., 2009), between the closing of the Witteberg Basin and opening of the Main Karoo Basin, the Witteberg Basin continued to receive sedimentation and partially filled in the time gap via the Kommadagga sub-basin. This may suggest that the Miller diamictite (representing the last sedimentation of the Witteberg-basin) could be related to the Dwyka diamictite (representing the opening of the Main Karoo Basin), under the condition that there was no hiatus present between the Kommadagga Subgroup and Dwyka Group.

1.2 Purpose of study

The purpose of this study is to compare the two diamictite deposits by means of facies analysis that will demonstrate the mode of deposition within the sedimentary environment(s) via facies models. This information will also contribute to understanding differences in diamictite deposits from different sedimentary environments. The project aims to:

- Provide a better understanding of the different facies deposited by diamictites in general, and to establish which controls can influence the manner of deposition.
- Identify specific characteristics to distinguish between diamictites from glacial and non-glacial environments.
- Establish whether the Miller diamictite is indeed a diamictite and/or a tillite.
- Establish the depositional environment in which the Miller and Dwyka diamictites were deposited and whether they are part of the same depositional system, and if so, also answer how they are sedimentologically related.

1.3 Methodology

1.3.1 Field work

Four locations (farms) were selected based on previous literature and present day accessibility. These locations were specifically Volstruisleegte, Miller Station, Swaylands and Campherspoort (Fig. 1.4a). Geological maps of 1:50 000 and 1:25 000 were consulted to establish the location of the Dwyka Group as well as the Waaipoort – and Floriskraal Formation at each location.

Traverses were walked from the Waaipoort – or Floriskraal Formation (South) boundary towards the Dwyka Group boundary (North), documenting field observations at each location. Any significant change in the lithology was recorded by a GPS point which allowed the identification of a number of units and their contacts for each traverse (Appendices Table A1, Fig. A1, Fig. A2, Fig. A3 and Fig. A4). For each unit, general detailed field observations were made and recorded and presented as stratigraphic profiles.

1.3.1.1 Stratigraphic profiles

Stratigraphic profiles were made documenting the observations by walking the traverses, from South (Waaipoort boundary) to North (Dwyka boundary), at each of the four locations (Fig 1.4). One profile was made at each location at Volstruisleegte and Campherspoort (Profile 1; Fig. 1.5a and Profile 6; Fig. 1.6a). Two profiles were made at each location at Miller and Swaylands (Profile 2, Profile 3; Fig. 1.5a and Profile 4, Profile 5; Fig. 1.6a). All stratigraphic profiles were taken perpendicular to the strike of the units except at Swaylands (Location 1) and Campherspoort. This was due to the poor quality of outcrops. Geological cross sections of all four locations are displayed in Fig 1.5b,c and Fig 1.6b,c respectively.

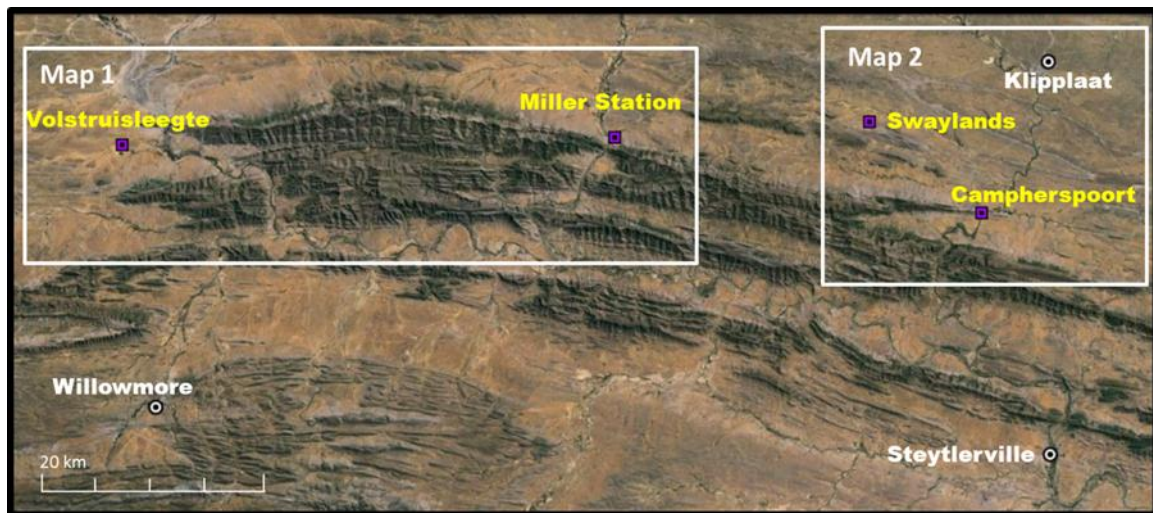


Figure 1.4: Map overview of main locations (Map1 and Map2) visited during fieldwork.

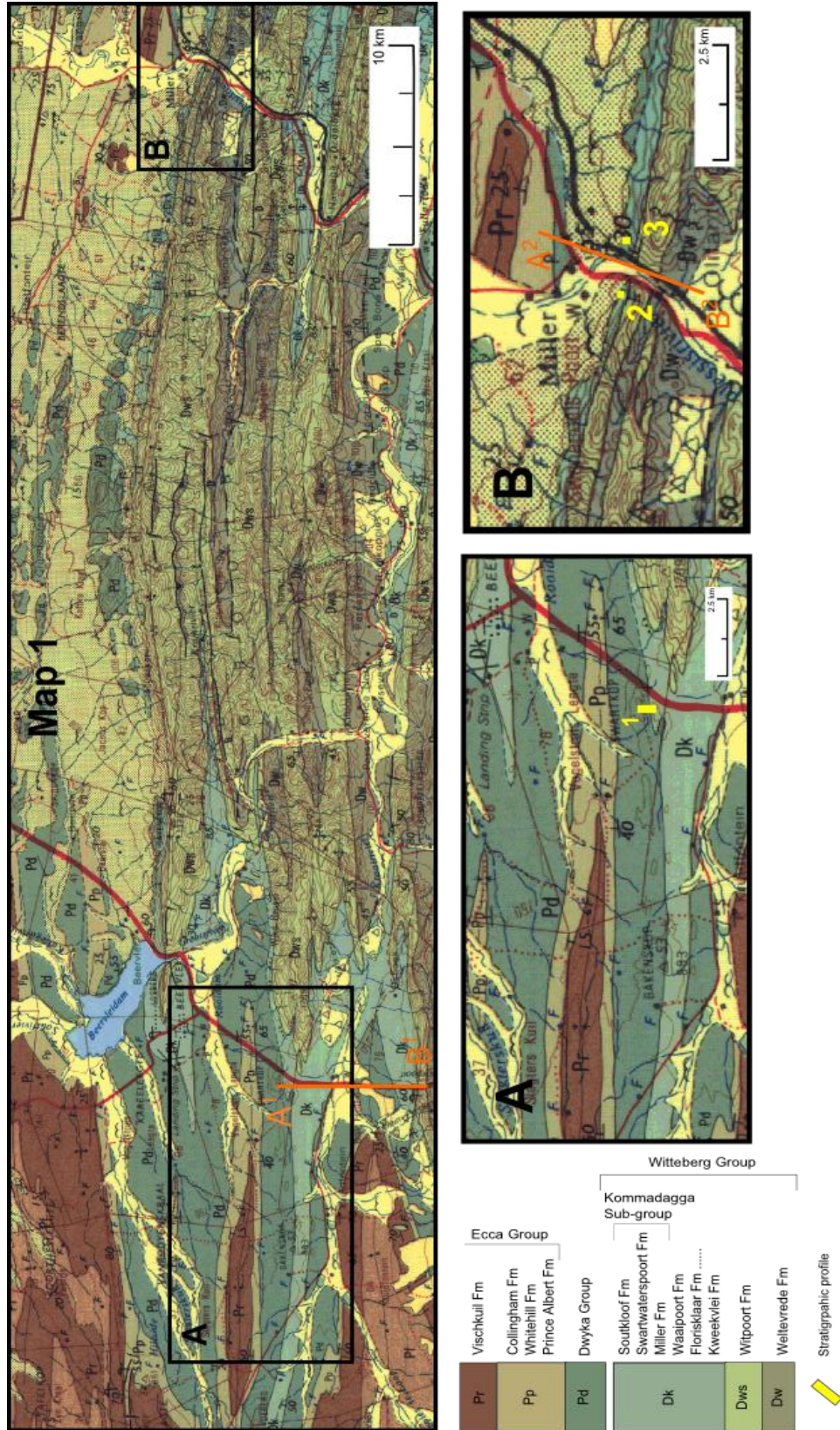


Figure 1.5a: Geological Map 1 indicating stratigraphic profile 1 at Volstruislegte (A) and profiles 2 and 3 at Miller (B).

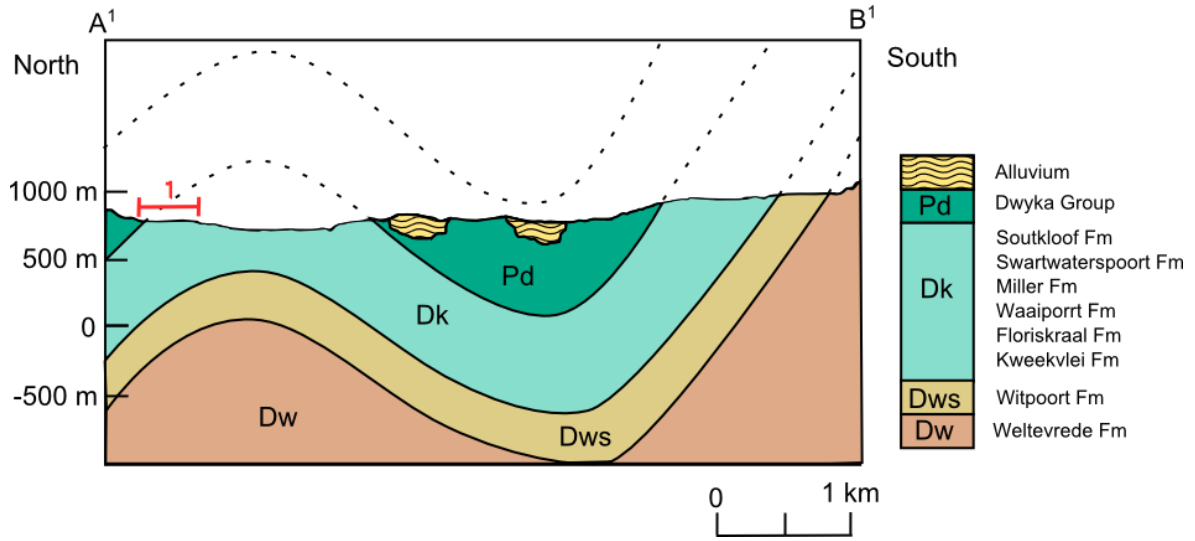


Figure 1.5b: Cross section A¹ – B¹ through study area at Volstruisleegte indicating stratigraphic profile 1 (Geological Map 1; Fig. 1.5a).

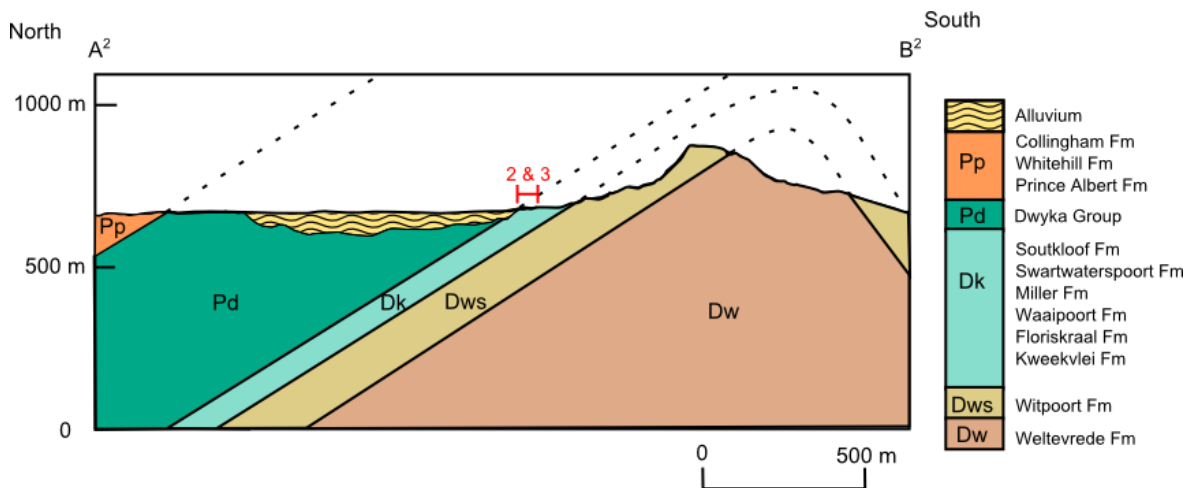


Figure 1.5c: Cross section A² – B² through area surrounding study area at Miller indicating stratigraphic profiles 2 and 3 (Geological Map 1; Fig 1.5a.).

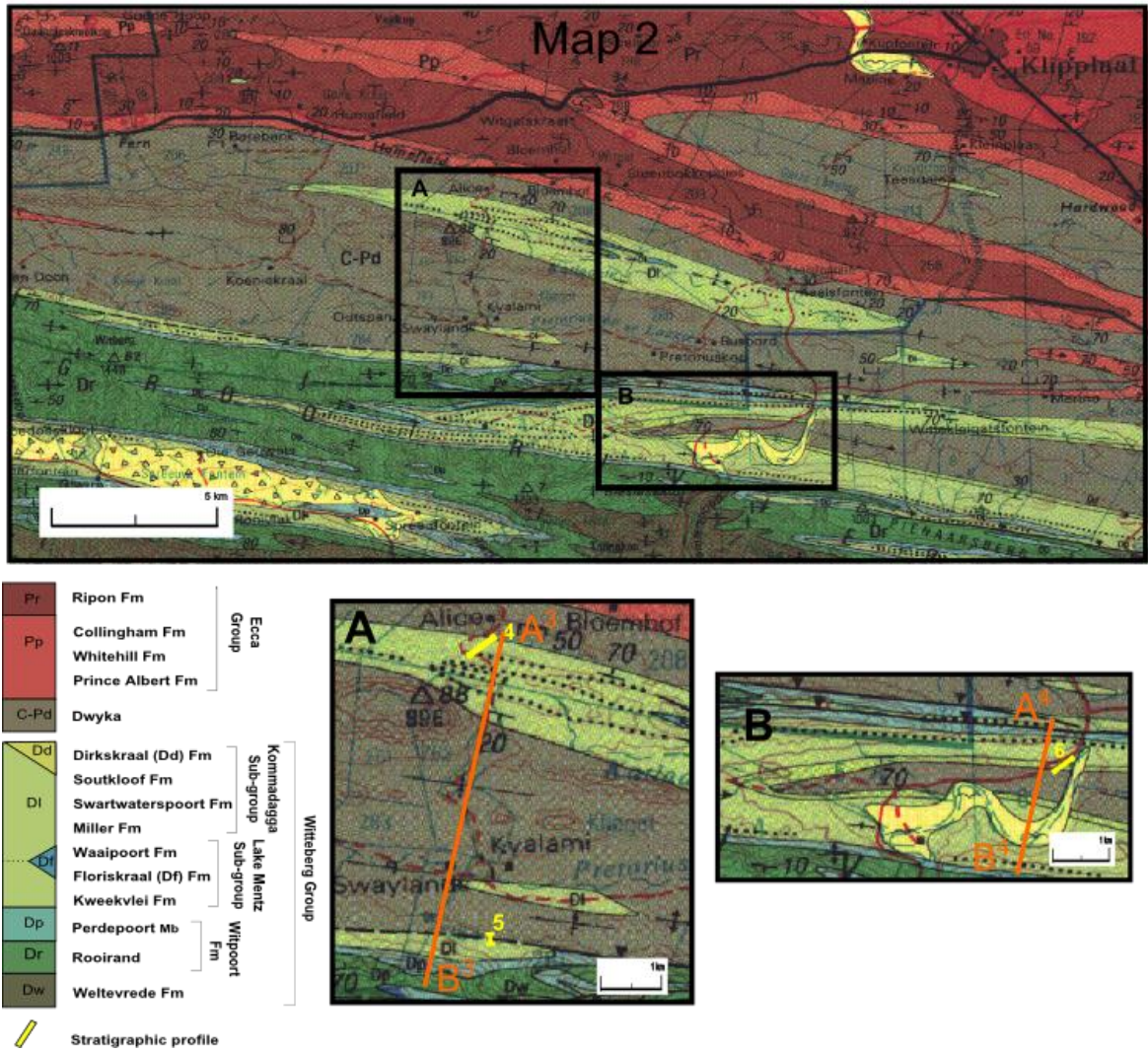


Figure 1.6a: Geological Map 2 indicating stratigraphic profiles 4 and 5 at Swaylands (A) and profile 6 at Campherspoort (B).

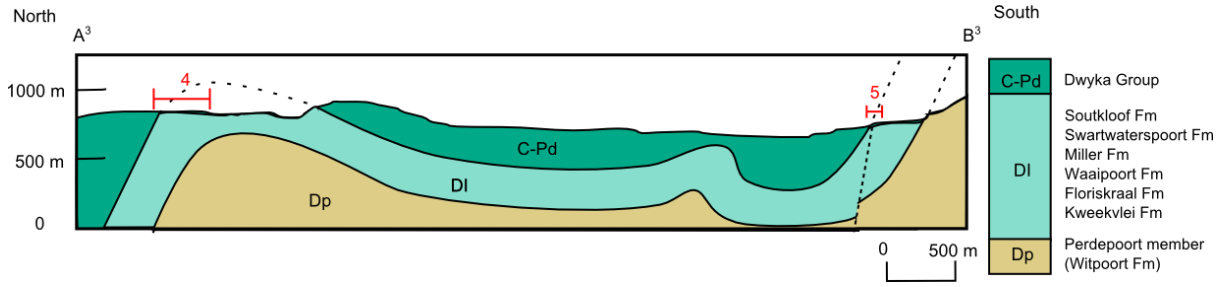


Figure 1.6b: Cross section A³ – B³ through area surrounding study area at Swaylands indicating stratigraphic profile 4 and 5 (Geological Map 2, Fig. 1.6a).

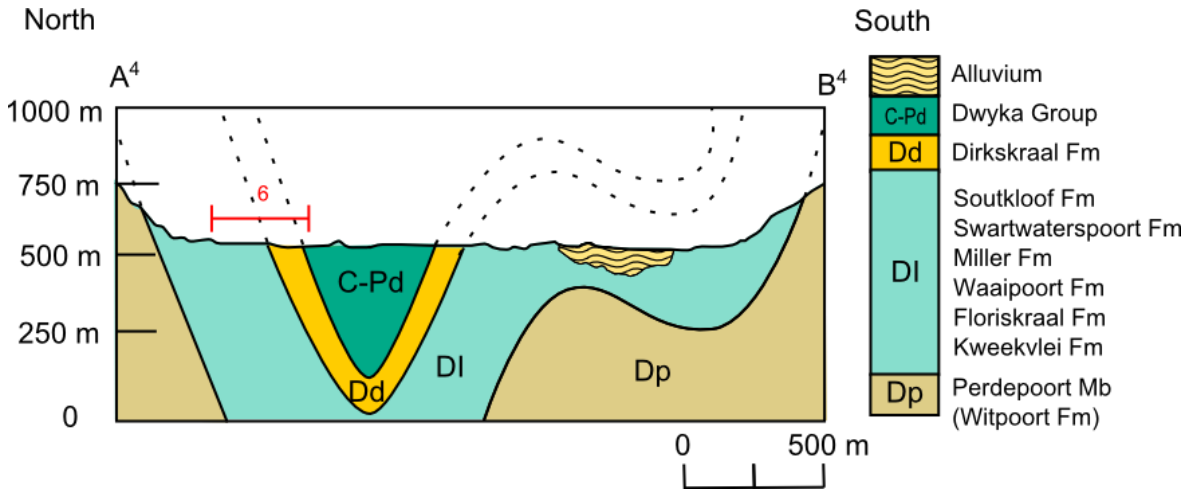


Figure 1.6c: Cross section A⁴ – B⁴ through area surrounding study area at Campherspoort indicating stratigraphic profile 6 (Geological Map 2, Fig 1.6a).

1.3.1.2 Sampling

Representative specimens were collected of each unit. These were described in the traverses and stratigraphic profiles (Table A1). The samples were also described by the use of a hand lens with x5 magnification. Maturity of rock, sedimentary structures, - texture and grain size (according to Udden – Wentworth grain size scale; Table B1), - shape, -roundness, - sphericity and – sorting (Stow, 2006), visible through the hand lens, was recorded.

1.3.2 Laboratory work

1.3.2.1 Petrography

A petrographic study was done on all the units (Table A1) by investigating their texture, sedimentary structure and mineralogy in detail. A standard petrographic microscope was used to describe the total of 37 thin sections (Table A1). From a sedimentological point of view specific attention was given to the following:

- Grain size, sorting, roundness, sphericity, grain contacts, grain to matrix relation, grain orientation/fabric.
- Mineral composition of grains and matrix/cement, proportion of minerals with regards to whole rock, distribution and orientation of minerals, Correlation between composition, size and shape of each mineral, any extra optical properties.
- Sedimentary structures.
- Maturity.
- Recognition of different populations in each unit with regards to difference in texture, sedimentary structures and mineralogy, or combination of all three.
- Classification of rock types by taking account of the above mentioned.

For each (carbon coated) thin section, a scanning electron microscope (SEM) was used to study the specifications listed above at a microscopic level. This was especially useful for samples with a very fine grain size, matrix or cement and to identify any unknown minerals that could not be identified under the petrographic microscope.

1.3.3 Facies analysis

All the information, provided by field descriptions and petrographic analysis, on texture, sedimentary structures, mineralogy and different populations in each unit, was used to establish what mechanisms were responsible for the transport and deposition of the rock unit.

Once the above was established, a facies, assembled by singular or multiple facies codes (modified after Eyles et al. (1983 and Mail (1997)) was assigned to each unit based according to the mechanism involved with transport and deposition. Related facies were grouped together to form facies associations, which in turn developed into a facies model, which describes the sedimentary environment of deposition.

Together with the facies model and other interpretations made from field and laboratory results, the respective project outcomes (previously mentioned) could be reached and satisfy the purpose of the study.

CHAPTER TWO

SEDIMENTARY SYSTEMS

2.1 Classification and definitions of sediments

To be able to determine whether the Miller Formation diamictite was under glacial influence it is necessary to re-evaluate the classification of a diamictite.

The classification of diamictites, and in fact any sediments containing gravel size particles maybe ambiguous. The percentage of gravel-particles to distinguish a diamictite from e.g. sandstone with dispersed clasts or sandy mudstone can vary. Therefore it seems appropriate to consider current classifications and existing terminology to be used in this study.

Conglomerates, including breccias and diamictites, can be referred to as rudaceous rocks as a general class name. Rudaceous rocks consist of more than 30% gravel-size (>2mm) rock pieces in a matrix. Rock pieces can vary from individual minerals to rock fragments of any rock type. The rock fragments can be of igneous, metamorphic or sedimentary composition, depending on the source rocks and depositional conditions. The matrix is made up of sand- or mud-size grains (Boggs, 2006). This description is only useful to distinguish rudaceous rocks from other siliclastic rocks, thus it cannot distinguish between different types of rudaceous rocks such as conglomerates, breccias and diamictites.

Rudaceous rocks can be divided into 3 groups by their composition: (1) Agglomerates (volcaniclastic), (2) Calcirudites (carbonates) (3) Silirudites (silicates), (Selley, 2000). Since agglomerates and calcirudites are rare and unlikely to be associated with this study, the focus will be on silirudites.

Since rudite (or rudaceous rock) is commonly referred to as conglomerate it is important to state that from this point forward the term rudaceous rock/rudite refers to conglomerates, breccias as well as diamictites. All terminology, descriptions and classifications that will be discussed on rudites in the following section are applicable to conglomerates, breccias and diamictites, except where else stated.

There are a wide variety of ways to classify and name terrigenous rudites (siliciclastites) but mostly it is based on texture, composition of clasts and source of clasts. Using these 3 divisions allows extracting sufficient information from the rock to describe and classify it.

2.1.1 Texture

Terrigenous rudites are texturally named and classified by (1) the portion of gravel-size particles with respect to the matrix and (2) the clast shape and orientation. Texture is used to divide rudites into proper conglomerates, breccias and diamictites. For the other classifications (composition and source) they are not distinguished from each other.

The portion of gravel-size particles, or clasts, with respect to the matrix, can be divided into two types, clast-supported or matrix-supported. Clast-supported rudites are when the clasts touch each other and the intervening space generally is filled by a matrix of poorly sorted sand and clay. With matrix-supported rudites the clasts are seldom in contact with one another, but are dispersed through a finer grained matrix. (Selley, 2000). According to Boggs (1992) there is no fixed percentage of matrix to distinguish a clast-supported rudite from a matrix-supported rudite. He states that the only way to determine the fabric support is to view a three-dimensional outcrop. If the clasts touch each other it is clast supported, if they do not, it is matrix supported. He also suggests that clast-supported rudites be referred to as **proper conglomerates** and matrix-supported conglomerates as **diamictites**. Hambrey (1994) stated that a proper conglomerate should contain 50% clast, whereas Friedman (2003) raised it to 80%. Friedman's 80% clast ratio is more or less relevant for a perfectly hexagonal packed proper conglomerate, with uniform sized clasts. However naturally this is very rare. Most proper conglomerates reach a state of clast support with a 50% matrix/50% clast ratio (Treagus, 2002). Thus Hambrey's 50% clast boundary between diamictites and proper conglomerates seems more reasonable. Hambrey also proposed a textural classification to be used for field investigation to distinguish between proper conglomerates and diamictites (Hambrey and Glasser, 2003). This classification is based on the proportions of sand and mud (as matrix) against the proportion of gravel clasts, using a hand lens, or the naked eye (Figure 2.1).

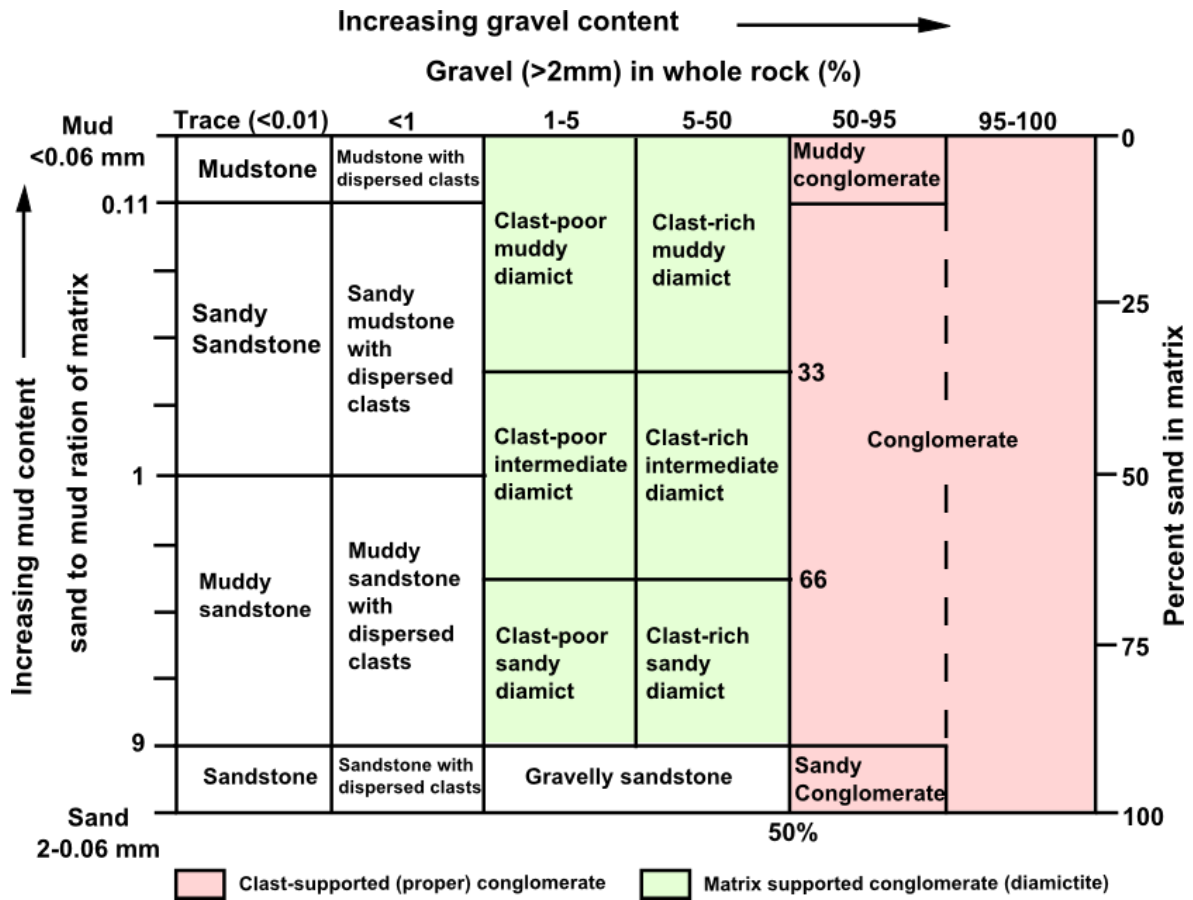


Figure 2.1: Non-genetic classification of poorly sorted sediments with 50% as maximum proportion of gravel in diamict. The term "diamict" embraces both diamicton (unconsolidated) and diamictite (consolidated). "Mud" as used in this context, covers all fine sediments, i.e. mixtures of clay and silt. Modified after Hambrey (1994).

Clast shape and orientation are key aspects used to understand processes involved in transporting the material and depositing gravel and can also be used to texturally classify rudites.

In this section clast shape will be used for textural classification. Clast-supported conglomerates that are mostly well sorted and consist of rounded to sub-rounded clasts in a matrix are proper conglomerates. If the clasts of a proper conglomerate are angular in shape it is called a **Breccia** (Boggs, 1992). Diamictites (matrix-supported conglomerates) are mostly non-sorted or poorly sorted with clasts ranging in different sizes and shapes (Boggs, 2006).

Combining the classifications of Hambrey and Boggs leaves little room for uncertainty in classifying conglomerates and offers a good guideline for field investigations. Therefore in this study the combination of these two classifications will be used to describe the texture of rudites. Using the classifications of Hambrey and Boggs a silirudite can be divided into proper conglomerates, breccias and diamictites according to texture. In essence, a **proper conglomerate** can be defined as a moderate to well sorted rock that consists of rounded to sub-rounded clasts in a matrix, where the clasts take up >50% of whole rock. A **breccia** can be defined as a moderate to well sorted rock that consist of angular clasts in a matrix, where the clasts take up >50% of whole rock. **Diamictite** is a non-sorted or poorly sorted rock that consist of a wide range of clasts that take up >1% but <50% of the whole rock, in a fine grained matrix.

As the term diamictite is defined above, it is a non-genetic term that can be used regardless of depositional environment, whether glacial, proglacial, periglacial, non-glacial, terrestrial or marine (Frakes, 1987). This term, which tends to cause confusion in literature, is often used for poorly sorted glacial sediments. Only if a diamictite deposit can be proven to have been deposited directly by a glacier, may it be referred to as the genetic term Tillite. As defined by Menzies (2003), a tillite is a consolidated sedimentary rock formed by the lithification of glacial till. In turn a till is sediment that has been transported and is subsequently deposited by or from glacier ice, with little or no sorting by water. To prevent this possible miss-interpretation of a genetic connotation to the term diamictite, Hambrey and Glasser (2003) made an important statement "For an objective study of sedimentary facies, a non-genetic classification of poorly sorted sediments is required before process related terms such as a "till" are to be used". This will be the

golden rule in this study as it should be for any study of diamictite and any other sedimentary facies.

2.1.2 Composition

The composition of rudites can be divided into two types (1) composition of clasts and (2) composition of matrix.

The clast composition can vary extensively since any rock type, igneous, metamorphic or sedimentary rock may be present in a conglomerate, depending on source rocks. (Boggs, 2006). According to the composition of the clasts, rudites can be divided into two types, polymictic or oligomictic. Polymictic rudites consist of clasts that have a diverse composition of more than one rock type. Oligomictic rudites consist of clasts of only one rock type (Boggs, 1992; Selley, 2000; Friedman, 2003)

The matrix of rudites is the relatively fine grained (>2mm, i.e. sand and finer) material that fills the interstitial spaces between the clasts. Any kind of mineral or small rock fragments (lithic fragments) can be present as the matrix (Boggs, 1992). The matrix commonly consists of various clay minerals and fine micas and/or silt-or sand-size quartz, feldspars, rock fragments and heavy minerals. The matrix can be cemented with quartz, calcite, iron oxides, clay or other cements (barite, anhydrite and zeolite) (Boggs, 2006).

2.1.3 Source

The source of the clasts can also be divided into extraformational or intraformational. Clasts that originated outside of the depositional basin make extraformational rudites and clasts that originated within the depositional basin make intraformational rudites (Boggs, 1992, 2006; Selley, 2000).

2.1.4 Summary

Proper conglomerates, breccias and diamictites are all included in the term rudaceous rocks, or rudites. They are distinguished from each other by textural differences, but can also be classified as a group under the term rudites. This group, termed rudites, can also be divided into different groups according to composition and source.

With detailed descriptions of field observations and petrographic studies of rock samples, the summary diagram (Figure 2.2) and Hambrey's textural classification (Figure 2.1) can be used to describe and classify rudites. It is also appropriate to use this as a starting point to further classify rudites according to their depositional environment.

2.2 Sedimentary processes

Once a rock record has been classified with regards to its texture and composition, it needs to be fitted into a series of sedimentary conditions to determine how it was formed and deposited. This is done first by finding the appropriate physical mechanisms or processes that are responsible for the rock record. Secondly, the physical process should be linked to specific environments which provide the appropriate conditions. Since one type of process can occur in more than one environment (and vice versa) it would seem that there could be endless possibilities. Therefore it is important to select a few appropriate sedimentary processes and environments that would be of interest to the specific rock record (in this case diamictites). By using pre-existing knowledge on the subject the processes and environments can be linked together to establish which the interpreter can use to make an accurate and "realistic" interpretation.

With regard to diamictites' formation and deposition, gravity flow processes (specifically debris flows), glacial and deltaic environmental systems will be the focus. All relevant information will be combined in an effort to produce a guideline which will assist in the interpretation and facies analysis of the two diamictite deposits in this case study.

2.2.1 Gravity flow processes

2.2.1.1 Debris flow

Debris flows can be defined as a rapid mass movement of highly concentrated mixtures of sediment and water commonly composed of poorly sorted grains, soil and organic matter. This gravity driven flow flows like a non-Newtonian liquid yet can stop on sloping surfaces and form lobate deposits that can range in composition from relatively fine-grained silty

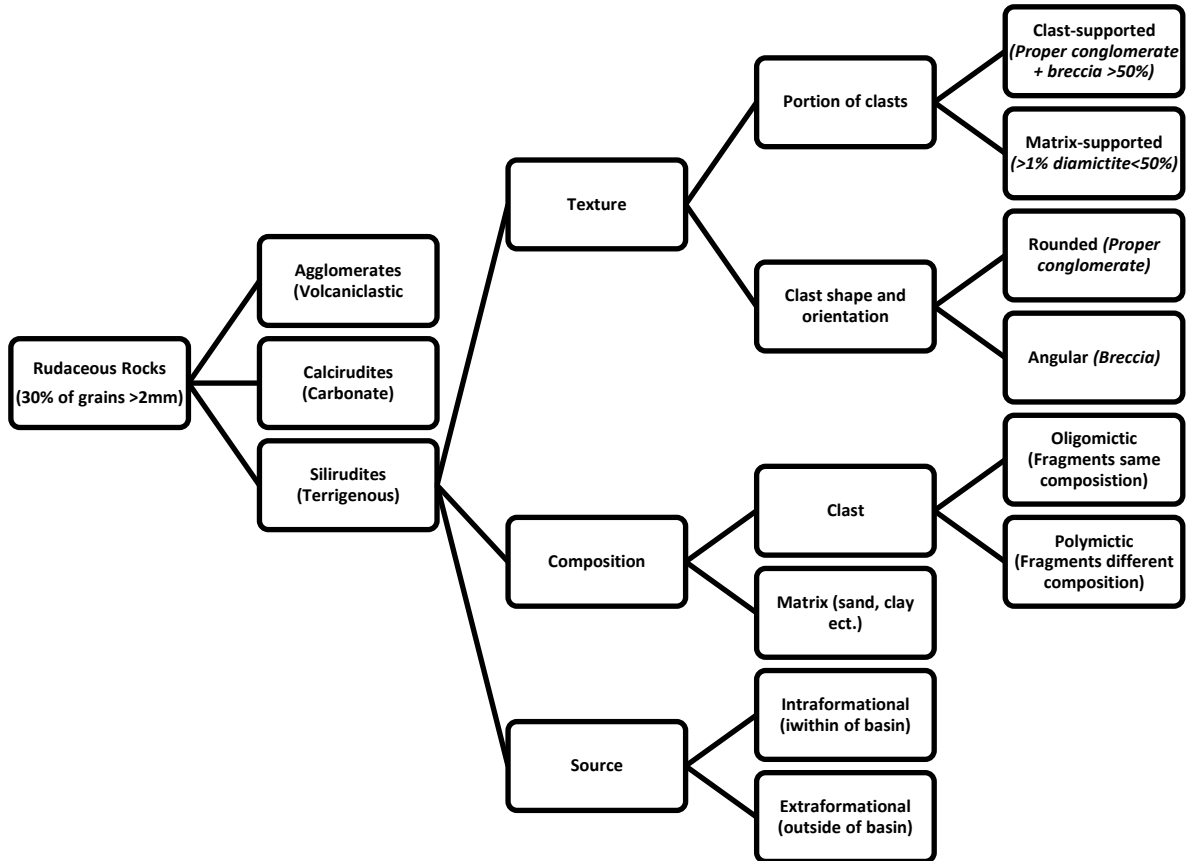


Figure 2.2: Summary of the possible classifications of Rudaceous rocks (conglomerates) with the main focus on terrigenous conglomerates.

clay-rich slurry to coarse-grained cobble boulders in a muddy to sandy matrix. Debris flow includes mudflow (debris flow containing mostly sand, silt and clay), lahar (volcanic debris flow), and till flow (debris flow from active or stagnant ice) (Major, 1997; Major, 2003). This is a combination of definitions that can be used to summarise the most important characteristics of a debris flow in the manner in which it moves and the kind of deposits it forms.

Debris flows occur in a wide range of sedimentary environments, in both subaerial and subaqueous settings (Boggs, 2006). A slope is needed in all situations though. Debris flow forms when a mass of sediment is mobilized and transformed into a slurry-like flow that is triggered by terrestrial rainfall, rapid snowmelt or earth quakes in a subaerial setting. In a subaqueous setting it is triggered by a combination of rapid sedimentation, gas release and storm wave loading. It produces turbidity currents and transport sand from continental slopes to abyssal plains (Major, 2003; Figure 2.3).

When a debris flow terminates, it forms a lobate deposit with a steep and blunt terminal snout, coarse-grained steep sided lateral levees and surface features (e.g. protruding clasts, ropy surface patterns (Major, 1997; Mulder and Alexander, 2001; Major, 2003). The deposits are mostly massive in structure (i.e. massive/structureless bedding), with a mixture of sediments ranging in size from clay, silt, sand to cobbles and boulders supported by a poorly sorted matrix. They can also be poorly graded and if grading is present it can be either fining up or coarsening up (Major, 1997; Selley, 2000; Boggs, 2006). Due to the massive and poorly sorted textures it is common to conclude that the debris flow deposit resulted from a single *en masse* emplacement (Mulder and Alexander, 2001). Opposed to a single *en masse* emplacement flume experiments as well as under natural circumstances indicates that debris flows deposited by incremental accretion also produce homogeneous, massively textured, poorly sorted, matrix supported deposits (Major, 1997). Thus it is not possible to determine from the deposit whether a debris flow was deposited *en masse* or through multiple surges. The deposits may have a few signs of internal structures because of plug flow and *en masse* deposition, traces of shear fabric may occur near the flow base, margins and also within the flow surging (Major, 1997). Coarse particles may be concentrated in particular horizons or given a directional fabric as a result of pulsed shearing within the flow body (Leigh and Hartley, 1992).

Grain-size sorting and orientation vary within different margins of the deposit body. The clast orientation is found to be parallel to the slope direction. It has been found to have

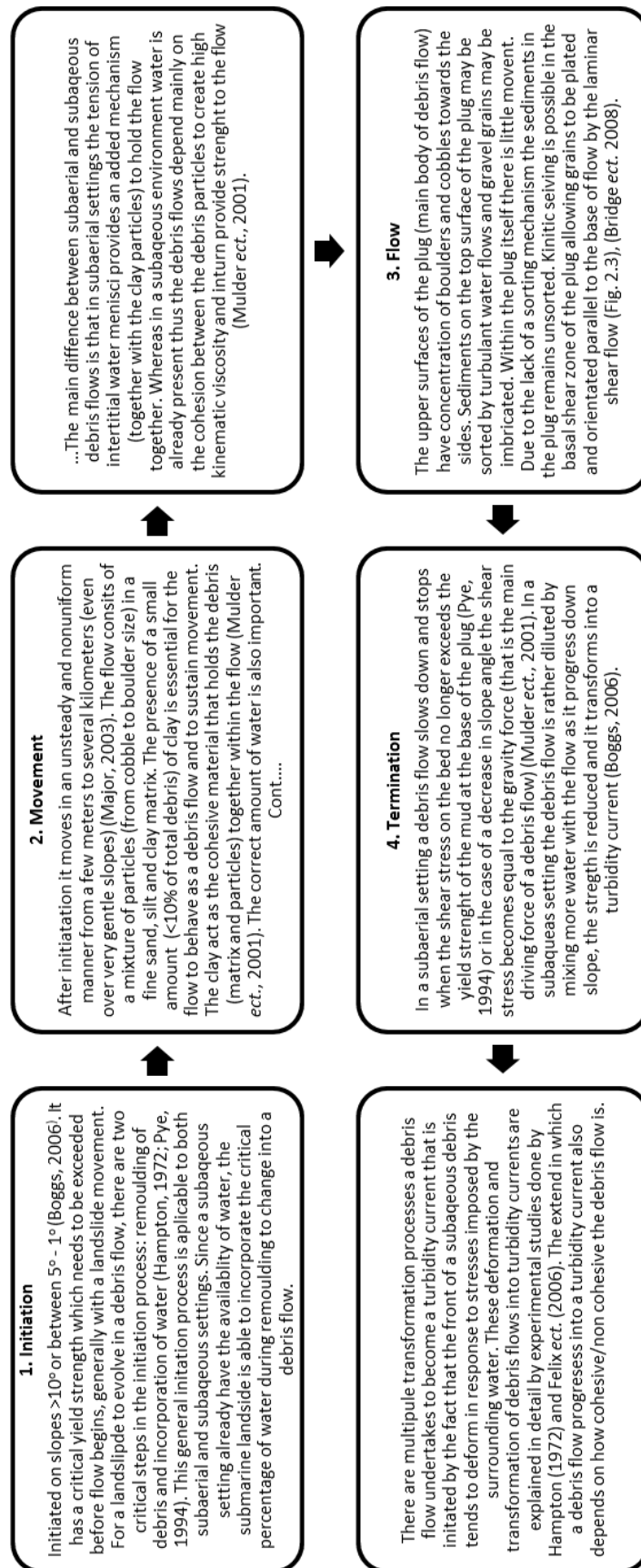


Figure 2.3: Development of a debris flow in subaerial and subaqueous settings.

occasionally oblique and transverse orientations, particularly in the lateral levees and lobes. The clast fabric can show imbrication especially in the lobe deposits that is parallel and normal to the flow direction. (The clasts are mostly inclined parallel to the local slope surface in the levee and channel deposits). The best developed imbrication is found in the frontal lobes, where the rapid deceleration causes internal thrusting, and on the transitions from steeper to gentler slopes (Bertan et al., 1997). The base of the deposit is normally sharp and erosional and overlain by fine-grained sediments with some scattered coarser grains (Figure 2.4B), (Bridge and Demicco, 2008). This is relevant to both subaerial and subaqueous settings, although the clast orientation is usually better developed in subaqueous settings with more defined imbrication (Boggs, 1992).

The amount of coherent (clay) material also influences the deposition and what depositional structures to expect. Marr et al. (2001) conducted experiments on coherent and non-coherent debris flows to establish the difference in depositional structures. They concluded that the features of a debris flow deposit were directly related to flow coherence (amount of clayish material). Weakly to moderate coherent flows produced significant turbidity currents. These deposits showed coarse-tail grading, water-escape structures and thin turbidites downslope of the deposit (Figure 2.5B). Strongly coherent flows generated only minor subsidiary turbidity currents. These deposits were structureless and ungraded and showed major slope-response changes in thickness, tension cracks, compression ridges, water-escape structures and detached slide blocks (Figure 2.5A). Although these experiments were conducted under a subaqueous setting, it is possible to consider similar behaviour and deposit structures in a subaerial setting.

2.3 Relevant environmental systems for diamictites

2.3.1 Glacial systems

The glacial system can be divided into two environmental settings, (1) the areas that are in **direct contact with glacial ice**, and (2) depositional environments **around the margins of the glacier (indirect)**.

The areas that are in **direct contact with glacier ice** can be divided into the basal or subglacial zone (contact with the bed rock), supraglacial zone (upper surface of glacier), ice-contact zone (margins of the glacier), and englacial zone (interior within the glacier)

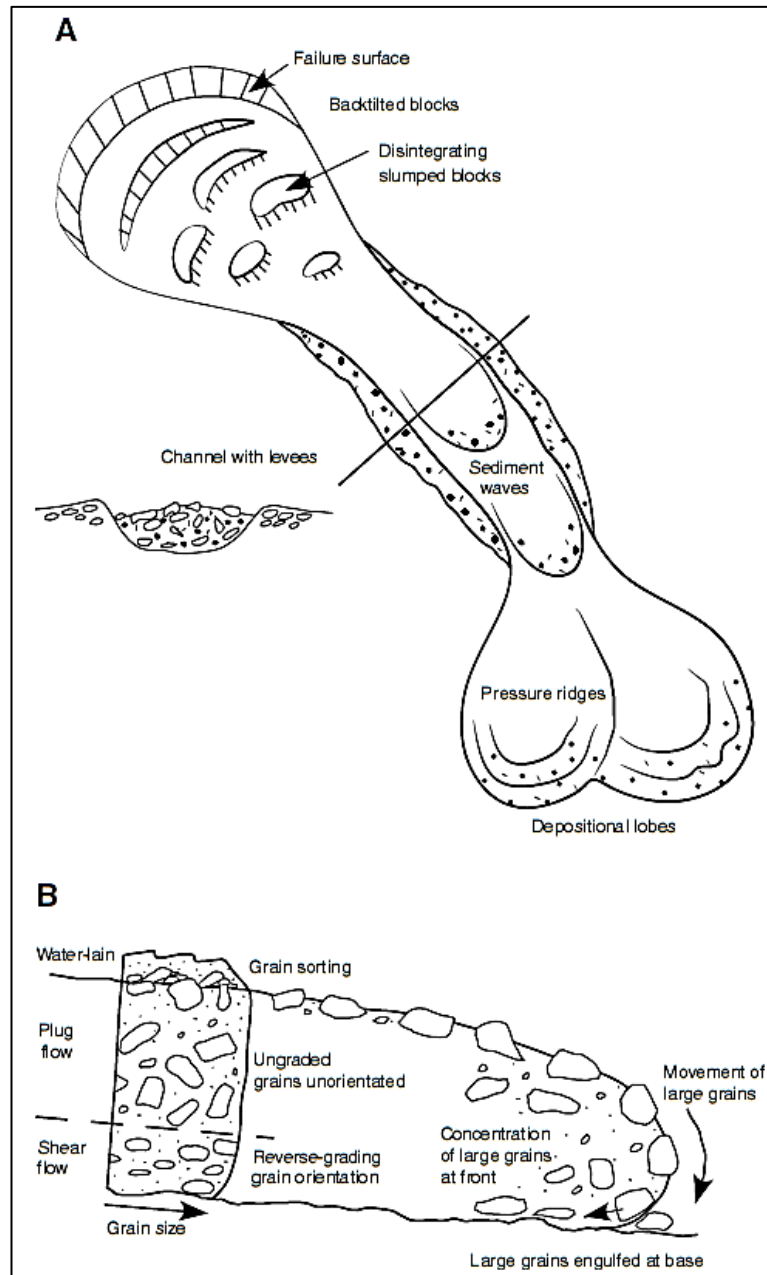


Figure 2.4: (A) Geometrical features of a debris flow, with distorted scale. (B) Sorting mechanisms and deposits of a debris flow (Bridge and Demicco, 2008).

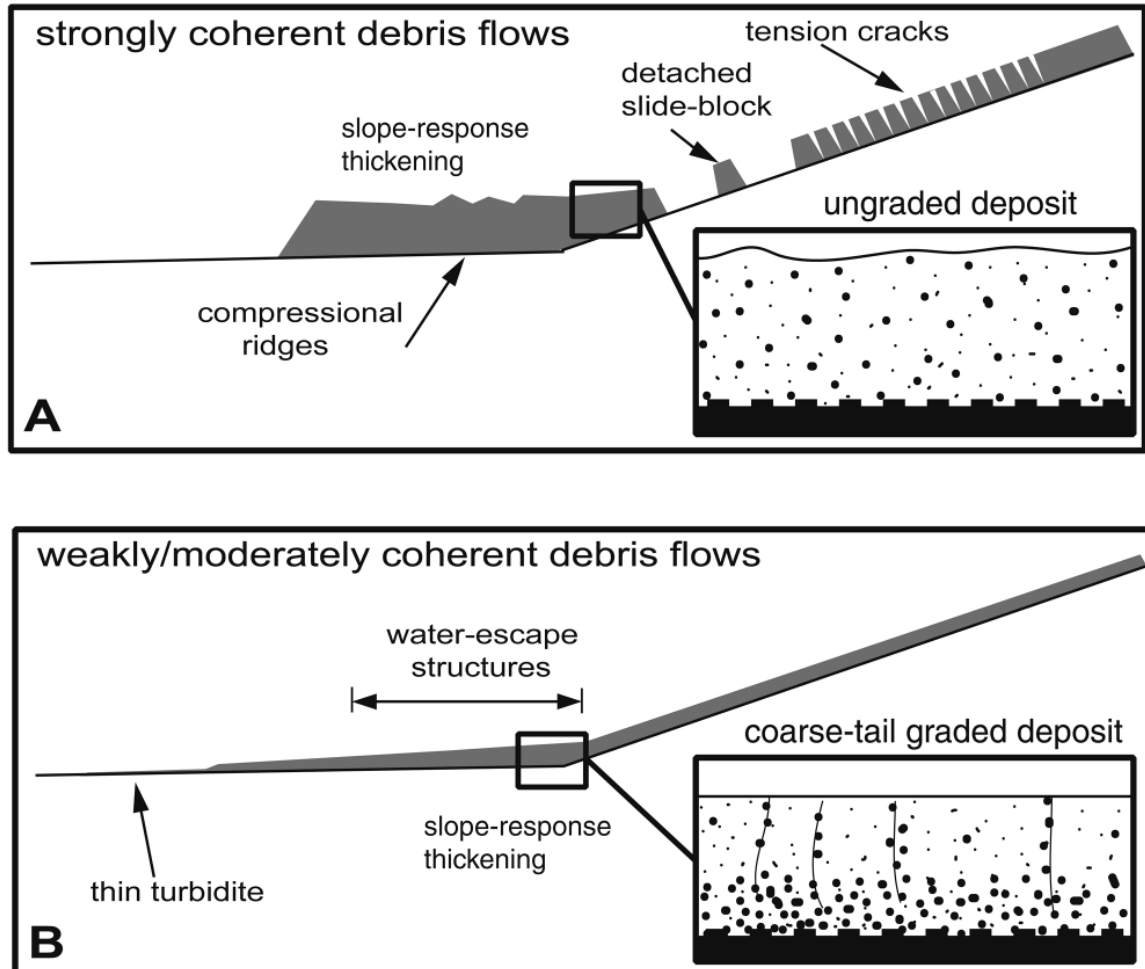


Figure 2.5: Depositional structures of (A) strongly coherent debris flows and (B) moderate and weak coherent gravity flows (Marr et al., 2001).

(Boggs, 2006). Sediments are transported and concentrated along the ice contact and subglacial zones due to abrasion and plucking, and sediment rich melt water that is trapped as the melt water freezes to the base of the ice. Sediments also occur in the supraglacial zone, and are derived from rock-falls, landslides and sediment gravity flows.

The englacial zone is supplied with sediments that are washed down crevasses, transported by melt water streams within the glacier, and buried as snow accumulates above the snow line. Thrust planes at the glacier snout, produced by faster moving ice, carry subglacial and englacial sediments to high positions on the ice front where it can melt out (Bridge and Demicco, 2008).

The sediment load carried by the glacier is deposited due to frictional drag on the sediment within basal ice, and by melting of sediment-laden ice at the base and front of a glacier, to form glacial moraines. Glacial moraines are depositional environments under and next to the ice. They can be divided into ground moraines and end moraines. Ground moraines are deposited at the base of a glacier and consist of subglacial traction till (Figure 2.6). The upper surface of a ground moraine contains distinct landforms such as drumlins, flutes and rogen. End moraines form irregular ridges along the margin of a glacier depositing interconnected mounds of till (melt-out/ablation), debris flow -, and meltwater deposits. End moraines can be divided into lateral, median and terminal moraines. Lateral moraines form from concentrations of debris carried along the edges of the glacier where the ice is in contact with the valley wall through ice streams. The lateral moraines can be easily confused with medial moraines which form at the boundary of two adjacent valley glaciers (Boggs, 2006). Terminal moraines can form due to the deposition of a large concentration of sediment in stagnant ice. End moraine deposits commonly overlie ground moraine deposits (Bridge and Demicco, 2008).

Sediment is also transported by melt water streams that flow under, within, and on top of the ice. Deposition occurs where they decelerate in space and when subglacial streams emerge at the front of the ice. These deposits subglacial streams form ridges called eskers. Meltwater stream deposits along the lateral margins of a glacier form Kame terraces. Meltwater stream deposits are similar to river channel deposits, although if sediment is deposited next to or on top of ice and the ice melts, soft sediment deformation structures form. They are likely to be associated with till and lacustrine deposits.

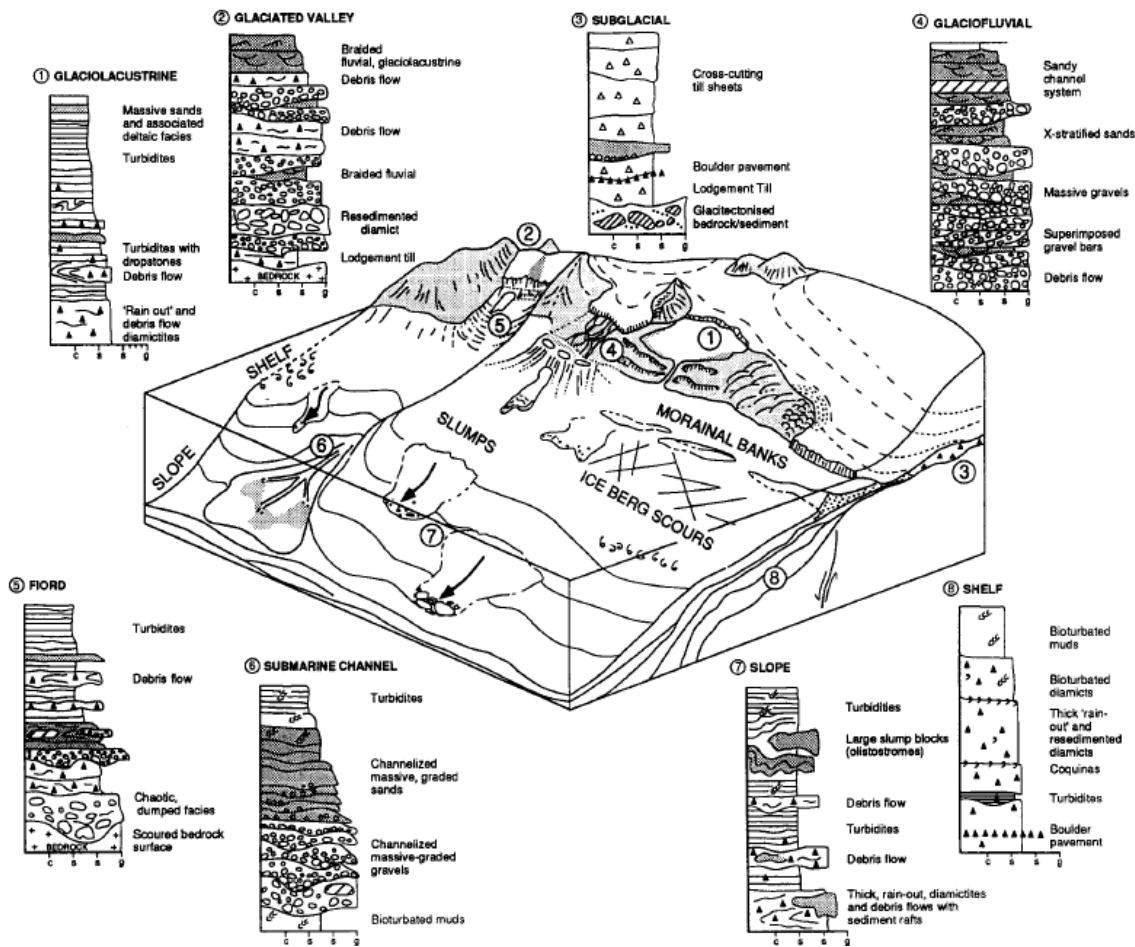


Figure 2.6: Glacio terrestrial and glaciomarine depositional systems with associated facies (Eyles, 1993).

The depositional environments **around the margins of the glacier** are influenced by melting ice from the glacier, but are not in direct contact with the ice. These environments include proglacial – and periglacial environments. Proglacial environments are just beyond the ice margins, which include glaciofluvial, glaciolacustrine and glaciomarine settings. The area beyond the proglacial environment is the periglacial environment.

Glaciofluvial (Figure 2.6) setting is associated with outwash plains or fans that are river dominated areas downstream of ice margins. Outwash plain deposits are typically stratified sands and gravels that are similar to braided river deposits. The deposits typically form downstream of terminal moraines and become finer-grained downstream. Glacial advance and retreat may result in outwash-plain deposits on top of till.

Glaciomarine (Figure 2.6) settings can be either proximal or distal to the grounded ice margin. The proximal zone extends 1km from the ice front, followed by an intermediate (1-100 km) and distal zone (>100km).

In the proximal zone, sediments are deposited directly from the grounded ice margin (where the glacier connects with open water) by meltwater via channels or tunnels into subaqueous fans. Additional sediment deposition by melting of ice rafts also occur. Thus sediments that are deposited in this proximal environment are dominantly fan gravels, sands, diamictites, muds and tills. In this subaqueous environment ground moraines and end moraines form beneath the grounded ice margin thus depositing subglacial traction till and melt-out till. This subglacial and melt-out till is similar to those discussed previously in a terrestrial environment. Submarine fans and deltas are formed due to subglacial meltwater stream sediments from the grounded ice margin. Sediments such as coarse cobbles and gravels with cross stratified sands are deposited. The slopes of submarine fans, deltas and moraines can be reworked by downslope sedimentary gravity flows which form subaqueous flow tills, debris flow deposits and turbidites. Reworking of sediments is also caused by traction current activity and ice rafting which deposit coarse grained diamictites with a muddy sand matrix across the fans. Floating icebergs that break off from the grounded ice, generally deposit melt-out diamictites which form due to individual rock fragments that fall from the melting icebergs (dropstones) into underlying marine sediments such as muds and sands. These deposits are also commonly known as "rain out" diamict. The degree of stratification in melt-out diamictites can vary from

unstratified to well-stratified, depending on how much the marine sediment has been reworked and resedimented pre/post "rain out".

In the distal zone glaciers are not in direct contact with marine waters thus it is dominated by non-glacial marine processes. Glacial sediments are supplied by floating icebergs which deposit sediments in the same manner as discussed in the proximal zone on the continental shelf. The deposits are unstratified diamictites with a fine matrix. These unstratified deposits can be reworked by waves, wind-shear currents and tides forming stratified deposits. In deeper water the debris fallout from the floating icebergs may be retransported via turbidity currents (Eyles et al., 1985; Boggs, 2006; Bridge and Demicco, 2008).

Glaciolacustrine (Figure 2.6) settings are associated with high energy ice-contact lakes that are characterised by large and rapid influxes of poorly sorted sediment or non-ice-contact lakes where the glacier plays a more distant role. In an environment where the ice is in contact with the lake, it undergoes more or less the same processes as described in glaciomarine environments. The sedimentation rates, in a lacustrine environment where the glacier plays a distant role, are more reduced and depositional processes are driven by seasonal meltwater discharges (Eyles, 1993). Sediment transport and deposition are controlled by seasonal variation in water temperatures, thermal layering and suspended sediment concentration.

All of these different glacial environments, whether in close contact with ice or around the margins, represent specific facies associations common to the glacial environment, but show a variation on the "normal" due to glacial influence. The diamict deposits seem to be quite unique and specific to some glacial environments thus these till and diamict deposits mentioned above will be discussed in more detail.

As mentioned in the previous chapter, a till is a unconsolidated diamictite that was deposited by a glacier (direct contact), thus providing the genetically derived term, Tillite, for consolidated sediment.

Till can be divided into 3 main types according to their location around the ice body, (1) Subglacial till, (2) Melt-out till (around margins), (3) Flow till (on top of glacier).

There are three distinctive types of subglacial till – subglacial traction till, subglacial melt-out till and glactectonite. *Subglacial traction till* (Figure 2.7) is sediment deposited from the base of a glacier by frictional drag on sediment within the basal ice, and by pressure

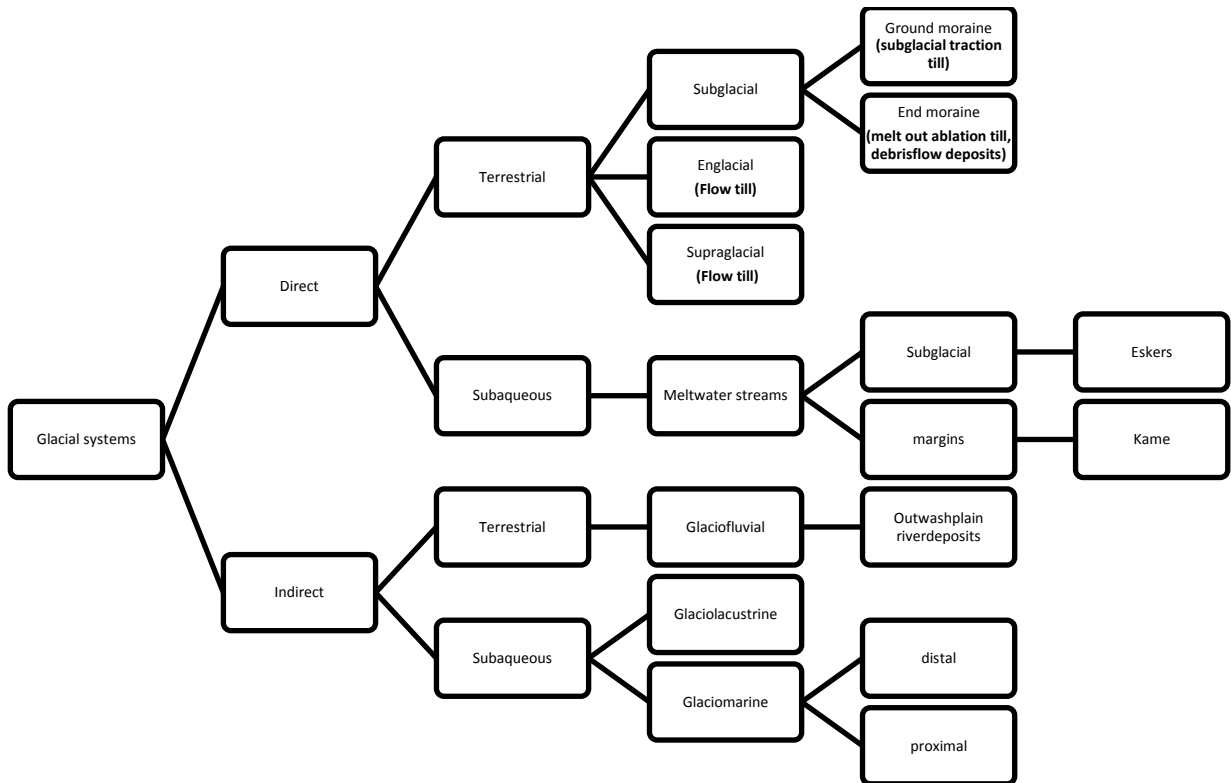


Figure 2.7: Summary of different glacial environments, indicating in which till deposits form.

melting of sediment-laden basal ice. It is deposited below the ice as a wide-spread, sheet-like hummocky blanket composed of overlapping and stacked lenticular bodies with erosional bases. It typically rests on a regional erosion surface. The deposit can be meters to tens of meters thick and tends to have a low porosity, is massive, unsorted, structureless, but may show some sorted, stratified layers. It also includes sediment fills of cavities on the bed (Bridge and Demicco, 2008).

Subglacial traction till includes lodgement till and deformation till as described by Eyles (1993). Lodgement tills characteristically contain glacially-shaped clasts. The clasts characteristically have a flat-iron or bullet-like appearance and are a unique trademark of clasts that have experienced transport and lodgement at an ice base. The clasts are commonly parallel to the ice-flow direction and little or no imbrication is present (Boggs, 1992). Deformation tills are deposited en masse by shear stresses applied by glacier movement over unconsolidated sediments, resulting in remoulding and mechanical mixing of sediment or bedrock particles below the ice base (Eyles, 1993).

Subglacial melt-out till defines a sediment that is released by melting or sublimation of stagnant or slowly moving sediment-rich ice, and is not subsequently remobilized or deformed. *Glacitectonite* is defined as rock or sediment that has been deformed by subglacial shearing but retains some of the structure of the parent material. It is recognized by its folds, faults, shearing and abundant crushed and sheared sediment grains (Bridge and Demicco, 2008).

Melt-out (ablation till) (Figure 2.7) is deposited at the margins of a glacier which includes subglacial melt-out till. It is likely to be preserved as restricted lenses within complexly-structured moraine landforms recording the wasting of stagnant ice margins (Eyles, 1993). It is commonly meters thick and not deformed. It can show random grain fabric and it can also have layering consisting of silt, sand and clay with scattered cobbles and boulders. These layered melt-out tills originate from layered sediment-laden basal ice and the layers are preserved if the ice is confined as it melts. Sediment escape structures and clastic dykes can be present due to high pore-water pressures in the melt-out tills (Bridge and Demicco, 2008).

Flow tills (Figure 2.7) are debris flow deposits that form due to gravity flow of pre-existing tills (especially waterlogged melt-out tills), or by gravity flow from the material carried on top of the glacier down the steep front of the glacier (Bridge and Demicco, 2008).

2.3.2 Deltaic systems

In a combined definition of Boggs (2006) and Nemec (1990), a delta can be defined as any deposit, subaerial or subaqueous, built by a terrestrial feeder system, alluvial and fluvial, that builds out into a standing body of water, either a lake or sea. There are a few classification schemes for deltas based on individual concepts, for example the feeder system (Holmes, 1965), thickness distribution patterns (Coleman & Wright, 1975), tectono-physiographic coastal settings (Ethridge & Wescott, 1984) and delta-front regimes (Galloway, 1975). These classifications are more generic orientated and do not contribute to universal rock record descriptions of deltas. Postma (1990) came forth with a classification that is based on the differences in alluvial feeder systems, basin depth, river mouth processes and diffusion processes by wave, tide and gravity. Combining these differences Postma established twelve prototype deltas (Fig 2.8), which aids in the comparison of modern and ancient deltas, making it very useful for facies analysis and associating with rock records. This will be the preferred classification used for Deltaic systems in this study.

All deltas have a subaerial and subaqueous component. The subaerial component is referred to as the delta plain (upper- and lower plain) and the subaqueous component is subdivided into delta front, delta slope (if the basin is deep enough) and prodelta (Figure 2.9).

The subaerial component is referred to as the **delta plain**. In general the delta plain is an area of variable slope gradient affected mainly by the type of feeder - and distributary system, and to a lesser extent by tidal currents and wave currents. In this sense they are similar to normal alluvial floodplains, yet with a radial pattern out from a point source (the apex). This subaerial component is often divided into upper delta plain, which lies largely above the high tide level and lower delta plain, lying between the low tide mark and the upper limit of the tidal influence. **The upper delta plain** exists above the area of significant tidal or marine influences. It is the continuation of an alluvial valley and is dominated by fluvial processes. Sedimentation is controlled by the type of feeder – and distributary system, which may vary between a very steep to shallow gradient (Type A – D feeders in Fig 2.8). The **Lower delta plain** lies within the realm of fluvial-marine interaction and extends landward from the low-tide mark to the limit of tidal influence, thus it is exposed during low tide but is covered by water during high tide.

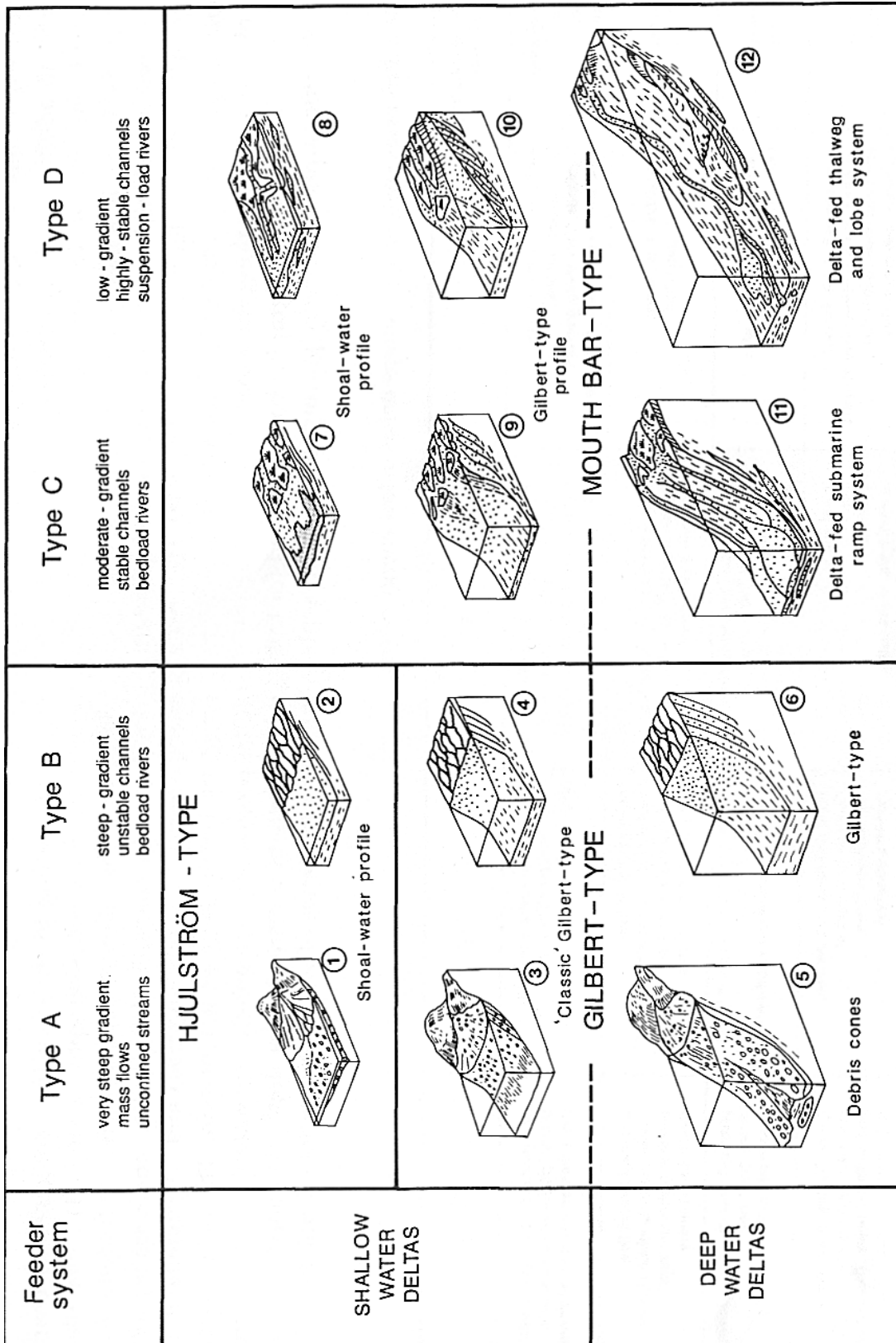


Figure 2.8: Twelve prototype deltas, distinguished on the basis of a unique combination of four different type of feeder/distributary system and two ranges of basin depth. It also takes into account the variations due to inertia-friction and buoyancy-dominated river discharge (Postma, 1990)

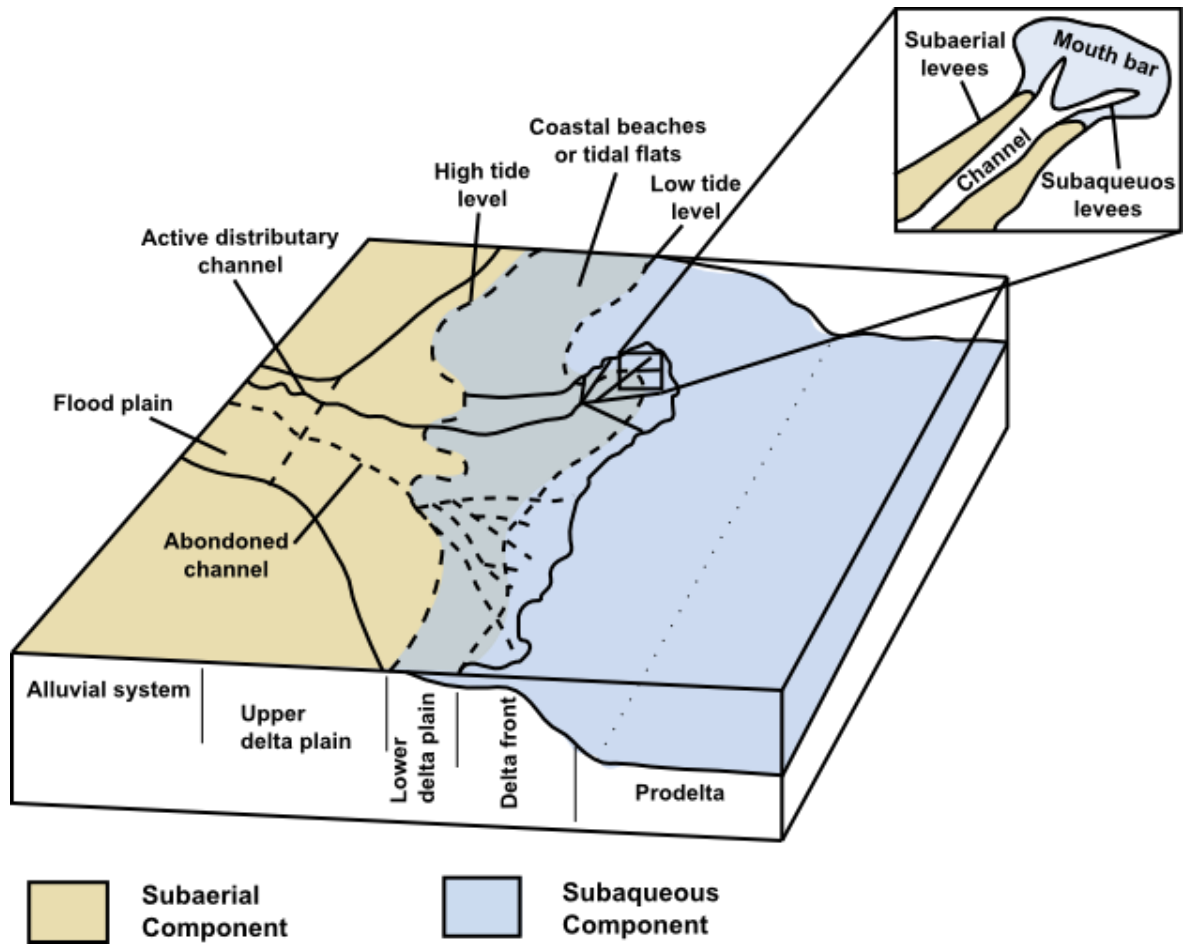


Figure 2.9: Geometry of a delta. Modified after Boggs (2006) and Bridge and Demicco (2008)

The subaqueous component is the part of the delta lying below the low-tide water level extending seaward and contains relatively open aquatic fauna. The uppermost part of the subaqueous component is commonly called the **delta front**. The **delta front** forms a rim around the delta plain, where the feeder system is active, by depositing sediments via channels and mouth bars. This depositional area may be exposed directly to wave- and tide action where channels enter open water. It is most commonly characterised by a seaward fining of sediments, sands and coarser clastics being deposited near the river mouths and finer grained sediment dispersed seaward from downslope mass-movement processes, or from suspension in water columns. Bed load is deposited immediately as the flow is decelerated, whereas suspended sediment is added to the delta front mostly beyond the zone of bed load deposition. As the flow decreases finer grains settle progressively further from the river mouth, depending on the effects of nearshore wave, wind-shear and tidal currents.

The **prodelta or prodelta slope** is the remaining seaward part of the subaqueous component. It may extend seaward for distances of a few kilometres to tens of kilometres, and the prodelta may extend to water depths as much as 200-300m (Colella and Prior, 1981; Boggs, 2006; Bridge and Demicco, 2008).

Table 2.1 provides a very useful summary of different facies found in different types of deltas in a specific geometrical region. The principal depositional environments in the upper delta plain include braided-channel and meandering-channel deposits, lacustrine delta fill and floodplain deposits. Therefore the sediments deposited are predominantly fluvial sands, gravels and muds.

Braided channel deposits are characterised by sand bodies that display high lateral continuity, but are rather thin (< 30m). Deposits show multiple fining-upward cycles in sand bodies which are defined by a scoured base and overlying sets of large-scale cross bedding. In general they have a high ratio of coarse sediments, such as gravel and sand. Sedimentary structures include ripple bedding, cross bedding, horizontal lamination and scour and fill structures. Plant remains, root burrows and fresh water fossils are common.

Meandering channel deposits are associated with active channels, abandoned channels and over bank deposits and therefore have a much higher ratio of fine sediments than in braided channel deposits. Characteristically meandering-channel deposits are sand bodies that consist of sand units which are often separated by thin clay and silt layers and have a scoured base. Above the basal unit is normally a massive, thick sand unit displaying

Table 2.1: General characteristics of the 12 prototype deltas. Modified after Postma (1990)

Code	Feeder (distributary) system												Sedimentary structure	Depositional processes/facies				
	A				B				C						D			
	Shallow-water delta		Deep-water delta		Shallow-water delta		Deep-water delta		Shallow-water delta		Deep-water delta				Shallow-water delta		Deep-water delta	
C	Shoal-water type delta	Gilbert-type delta	Deep-water delta		Shoal-water type delta	Gilbert-type delta	Deep-water delta		Shallow-water type delta	Gilbert-type delta	Deep-water delta		Shallow-water type delta	Gilbert-type delta	Deep-water delta	Plants and mud films	Swamp deposits	
Fb																Homogeneous commonly bioturbated muds	Suspension settling and density currents	
Fcf																Massive, with fresh water molluscs	Backswamp pond deposits	
Fcf																Massive, with fresh water molluscs	Backswamp pond deposits	
Fl																Fine lamination, very small ripples	1. Overbank or vaning floor 2. Density currents	
Fm																Massive, desiccation cracks	Overbank or drape deposits	
Fr																Rootlets	Seat-earth	
Fsc																Laminated to massive	Backswamp deposits	
Gg																Graded and massive cross-strata	Shelf processes	
Gh																Horizontally stratified gravel	Traction carpets driven by stream flow (comparable to sheet flow) or high density turbulent flow	
Gm																Massive clast-supported gravel	Longitudinal bars, lag deposits, sieve	
Gmm																Massive matrix-supported gravel	Cohesive debris flow	
Gms																Massive clast-supported gravel	Cohesionless debris flow	
Gp																Planar crossbeds	Traction	
Gt																Trough crossbeds	Traction	
P																Pedogenic structures	Soil	
Se																Crude crossbedding	Scour fills	
Sg																Graded and massive cross-strata	Shelf processes	
Sh																Horizontal lamination	Planar bed flow (lower and upper flow)	
Shl																Horizontally layered sand	Traction carpets	
Sm																Massive (structureless) sand, commonly with water-escape structures	Rapid suspension fall-out	
Sp																Solitary or grouped planar crossbeds	Linguleid, transverse bars, sand waves (lower flow regime)	
Sr																Ripple marks of all types	Ripples (lower flow regime)	
Ss																Broad shallow scours	Scour fills	
St																Solitary or grouped trough crossbeds	Dunes (lower flow regime)	
Ta-e																Bouma sequence	Turbidite	

lateral accretion and thin laminations of organic debris. The uppermost unit of the point bar often consists of silt and sand beds of a few centimetres thick displaying ripple laminations alternating with silty-clay and clay beds. Faunal remains are generally absent, but plant remains are sometimes common (plant and mud films).

Quiet-water deposition, reducing conditions, abundance of burrowing organisms and occasional wave and current action are characteristic of Lacustrine delta fill environments. Deposits within the lake bottoms consist of dark grey to black organic rich clays containing scattered silt/sand lenses (lenticular bedding). Diversion of a stream channel into one of the lake basins causes an increase in sedimentation rate. Because of the infilling process, sedimentation rates increase within the lake sequence and both grain size and thickness of laminations increase vertically upward leading to progradation of the system. Common types of sedimentary structures include parallel and lenticular laminations, intense bioturbation and distorted primary structures. Microfaunal remains are usually abundant within lacustrine deposits (Colella and Prior, 1981).

The lower delta plain includes the active distributary system of the delta as well as abandoned distributary-fill deposits. Distributary channels are numerous, but passive environments between channels make up the largest percentage of the lower delta plain. These environments include actively migrating tidal channels, natural levees, interdistributary bays, bay fills, marshes and swamps (Boggs, 2006). The general vertical sequence of bay-fill deposits is a coarsening-upward sequence with shallow brackish water clays and organic debris forming the lower part, and well sorted clastics forming the upper sand body. The lower part of the distributary-mouth bar (Fig 2.9) itself is characterised by the type of jet (channel) and sediments transported along the jet. Finer sediments settle on the mouth bar away from the river mouth forming a coarsening upward vertical succession. Common sedimentary structures are a wide variety of cross stratification, ranging from ripple lamination, through cross bedding to lateral accretion. Capping the bay-fill sequence is essentially an interdistributary bay or a marsh deposit, which consists of highly burrowed silts and silty clays.

There is no orderly plan in the infilling process of abandoned distributary channels since it is an extremely complex process. In general the channel fills entirely with fine grained, poorly sorted sand and silt containing organic debris, logs and clays. Near the base of the infilled channel sand bodies with erratics and contorted clay layers, as well as slump type, distorted bedding and clay infills are common. In the centre part silts and silty clays are

deposited which display thin silty and sandy layers that intercalate with highly burrowed clays. The uppermost part of the fill consists primarily of organic-rich clays that generally show intense root burrowing. Occasionally thin seams of shell debris and silt-infilled animal burrows can be detected (Colella and Prior, 1981).

Deposition on the delta front and on the basin floor (the prodelta region) is episodic. Delta front deposits, also referred to as distal bar deposits, are associated with distinct floods, migration of bedforms such as ripples, dunes and bars, and discrete sediment gravity flows. It primarily consists of laminated silts and clays containing numerous thin-graded and cross-laminated sand-silt layers. Lower parts of the delta front show small burrows and shell remains, generally scattered throughout the deposit that often result in partial destruction of parallel and lenticular lineations. Higher up in the delta front deposits, a wide variety of structures such as small-scale cross laminae starved current ripples, small scour and fill and graded sand units can be found. In general the amount of clays and silty clays begin to diminish within the section thus causing coarsening upwards in sequence due to progradation. Prodelta deposits are associated with flood-related variation in suspended-sediment load and with turbidity currents. A slump on a delta front may turn into a debris flow or mudflow and then into a turbidity current (as discussed in the earlier section on Gravity flow processes). Most common deposits found in prodelta deposits are parallel clay lamination, thin graded silt and silty clay parallel lamination, bioturbation and slump structures. Microfaunal remains generally indicate marine deposition and diversity of species is generally quite high, indicating an open, inner to outer shelf depositional environment (Colella and Prior, 1981; Bridge and Demicco, 2008).

2.4 Linking sedimentary processes with environments

By combining the above information on gravity flow processes with glacial and deltaic environments, it is possible to establish what the general characteristics are for all diamictite deposits. It can be used to identify key aspects for field identification to distinguish between diamictites that were deposited in possible subaerial, subaqueous, glacial or non-glacial environments. Although this guideline can be ambiguous and overlapping, it needs to be stressed that it is a very important and good starting point to find their facies relationships. An organisational guideline is provided in Figure 2.10 and

Table 2.2.

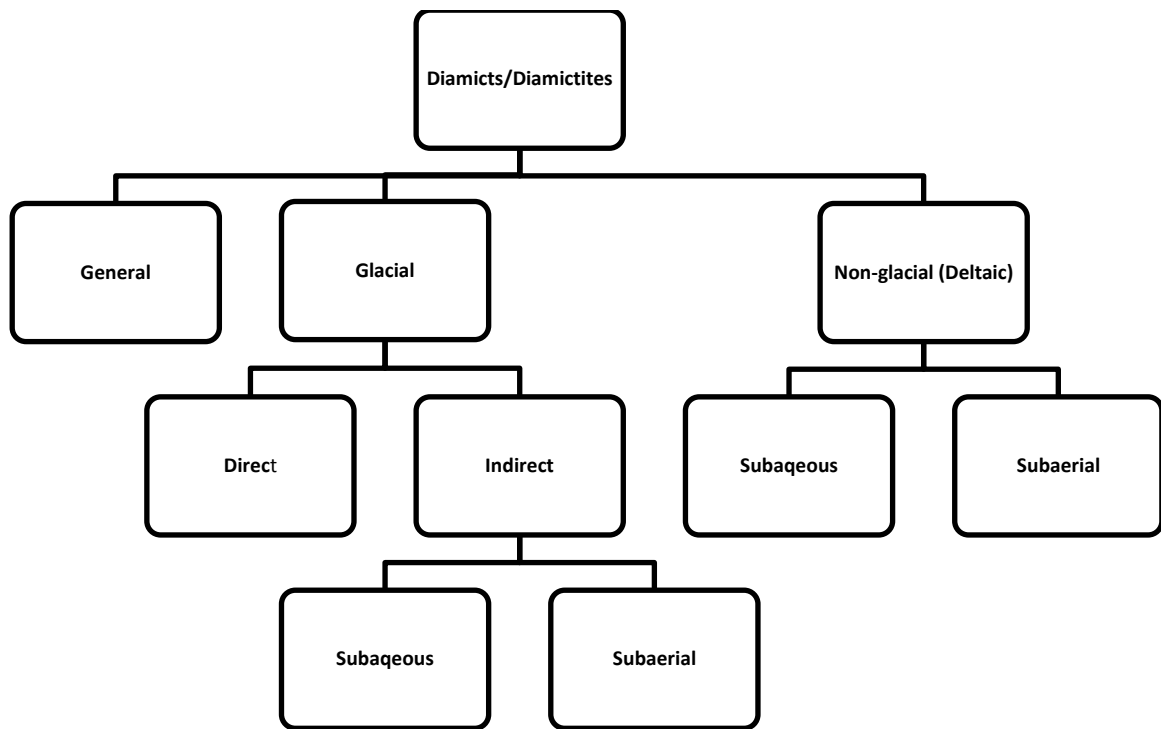


Figure 2.10: Schematic representation of diamictite guideline.

Table 2.2: General guideline for diamictites.

General		
All diamictites have pebble to boulder size clasts which is situated in a matrix that consist of sand, silt and clay particles (which can vary in proportions respectively). Texturally it is massive, structureless and poorly sorted		
Non – glacial (Deltaic)		
Diamictites deposited by debris flows always contains clay (it is a necessity) as part of the matrix. Due to its lobate form the deposits tends to be thinner and less extensive than tillites and glacial marine diamictites. Deposits are mostly massive in texture. The base of the deposit is normally sharp and erosional and overlain by fine-grained sediments with some scattered coarser grain. Clast shape not deformed. Facets may be common; may be massive or show contoured bedding surfaces. (Same characteristics for indirect glacial marine environments)		
Subaqueous	Subaerial	
Weakly to moderate coherent debris flow deposits show coarse-tail grading, water-escape structures. Strongly coherent debris flow deposits are structureless and ungraded and show major slope-response changes in thickness, tensions cracks, compression ridges, water-escape structures and detached slide blocks. Presence of marine/freshwater fossils	Diamictites that make up the plug of the debris flow deposit is usually unsorted and associated with coarse grained steep sided lateral levees and surface features. Shear fabric in debris flow deposits may occur near the flow base margins. The clasts are mostly inclined parallel to the local slope surface in the levee and channel deposits. Presence of plant fragments.	
Glacial		
Clasts – range in size up to a few meters; range in lithologies reflecting terrain over which ice flowed; Range in shape from very angular to rounded. Mineral composition is immature. Facets are common		
Direct	Indirect	
Clasts more rounded than subaqueous (indirect) diamictites due to basal transport. Individual units are only a few meters thick and extensive (not as much as glacial marine). Subglacial lodgement till deposit lenticular bodies with erosional bases. Basal tills are typically overlain by pebbly laminates and by shallow water marine deposits (<200m depth). Mostly massive, though stratification can occur in some tills especially ablation and flow tills; Basal tills likely to have strong fabric in which the long axis of pebbles are aligned parallel to flow; Subglacial traction tills may show some sorted, stratified layers. It also includes sediment fills of cavities on the lee sides of obstacles on the bed; Lodgement tills characteristically contain glacially-shaped clasts. These clasts have a flat-iron or bullet-like appearance and are a unique trademark of clasts that have experienced transport and lodgement at an ice base. The clasts are commonly parallel to the ice-flow direction and little or no imbrication is present; It is commonly meters thick and not deformed. Can show random grain fabric and it can also have layering consisting of silt, sand and clay with scattered cobbles and boulders. Melt-out tills can show sediment escape structures and clastic dykes. Extremely poor sorting and general lack of stratification. Abrasion surfaces – Grooved striated and polished surfaces, friction cracks and chatter marks.	Subaqueous	Subaerial
	Maybe slightly sorted with vertical grain size variation within unit. Clast and sand grains tend to be more angular than those that occur in direct glacial contact. Individual units may be tens to hundreds of meters thick, with gradual boundaries. Massive to finely laminated. Laminae are not graded and may be lenticular. Stratification should occur (better sorted and stratified than direct glacial diamictites). Two or more directions are common. Clast fabric is mostly random. Elongated pebbles may lie with long axis perpendicular to bedding surfaces if matrix was soft at deposition. Presence of marine fossils and general poorer sorting and stratification than normal marine deposits. Display extreme variation in clast type, reflecting various sources. Presence of dropstones, which may deform sedimentary structures such as laminae when dropped into soft sediment. Associated with in situ fossils. Associated with rhythmites and resedimented deposits (subaqueous gravity flows)	Tends to better sorted and stratified than direct glacial diamictites. Have the same characteristics as subaerial non-glacial diamictites, but with a glacial influence (mostly this can't be seen in the field and needs to be further examined through laboratory analysis)

2.5 Facies analysis

2.5.1 Meaning of Facies analysis

The term "facies" is described by Ghibaudo (1992) as "a bed or a group of beds showing lithological, geometric and sedimentological characters which are different from adjacent beds. A facies is considered to be the product of a specific depositional mechanism or several related mechanisms acting at the same time".

By combining the facies analysis done on specific successions in a study area a facies model is constructed to display the historical environmental system the rock record displays. Posamentier and Walker, (2006) defines the concept of facies modelling by stating "it involves a synthesis of information from ancient and recent depositional environments, in an effort to understand the nature, scale, heterogeneity, and controlling physical processes of the elements represented in each environment. The object is to identify the salient features of recent sediments and ancient rocks, such that these features can be identified, combined, and distilled into models that characterise that particular environment. Once a model is available, however simple and basic, it can be used to further our understanding of natural systems"

When making facies associations for facies models it is important to make a realistic model, which shows uncertainties, rather than an idealistic model where the facies analysis is modified to suite the model. As Posamentier and Walker (2006) states "however simple and basic, it can be used to further our understanding of natural systems"; this is not possible if the model is "idealistic" and not "realistic" since the facies associations are modified to suit the needs of the model. To further our understanding of sedimentary environments there must be a truthful relationship between the features in the facies analysis and the data/observations it is based on.

CHAPTER THREE

REGIONAL AND LOCAL GEOLOGY

3.1 Plate tectonics of Cape – and Main Karoo Basin

The Cape Basin represents a divergent margin basin with passive rifting seen as the preferred mechanism for divergence in which southern Gondwana was extended, and allowed for the sedimentation of the Cape Supergroup (Figure 3.1). Early rifting occurred along the newly developed basin margin in response to subsidence, this is currently interpreted as the mechanism for emplacement of the Table Mountain Group. This was followed by episodic transgression and regression, which resulted in the sedimentation of the Bokkeveld - and Witteberg Groups. Sediments were emplaced under deep burial under conditions of load diagenesis which allowed for the lithification of the Cape Supergroup sediments (Shone and Booth, 2005).

Around 278 Ma (270 million years after the deposition of the first Cape Supergroup sediments, the rifting was followed by compaction in southern Gondwana due to the subduction of the palaeo-pacific plate underneath the Gondwana plate (Catuneanu et al., 1998) (Figure 3.1). This resulted in the deformation of the Cape Supergroup and development of the Cape Fold Belt (CFB) which ended around 230 Ma. The CFB was generated through compression, collision and terrain accretion which resulted in deformation of the Cape Supergroup and lower part of the Karoo Supergroup via thrusting and folding (Catuneanu et al., 1998; Shone and Booth, 2005).

The Karoo retroarc foreland basin to the north of the CFB is a direct result of the CFB. The Karoo retroarc foreland basin developed in response to the supralithospheric loading generated as a result of crustal shortening and thickening in the CFB (Johnson, 1991; Catuneanu et al., 1998; Shone and Booth, 2005).

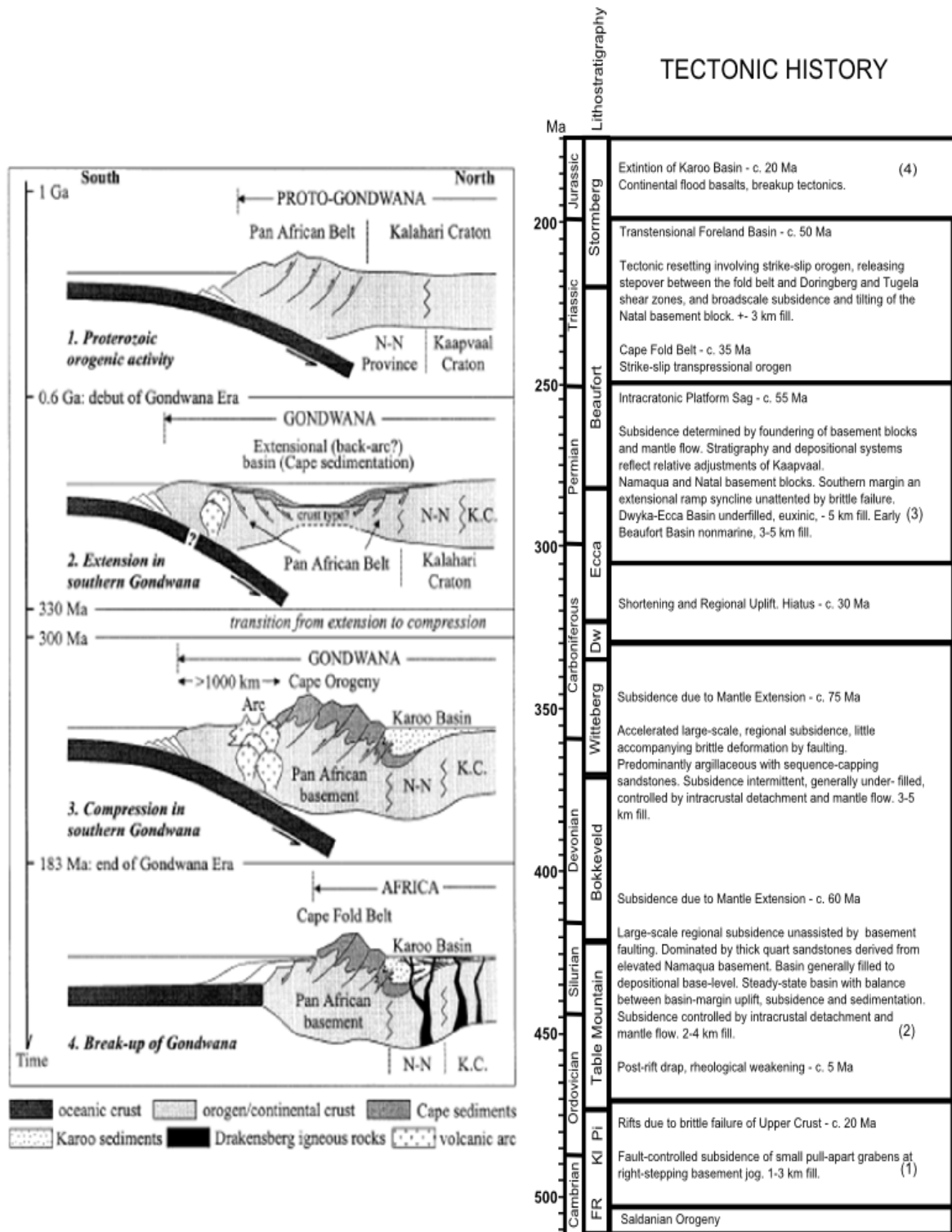


Figure 3.1: Crustal evolution of southern Africa. N-N = Namaqua-Natal; K.C. = Kaapvaal Craton (Shone and Booth, 2005) with a description of the tectonic history (Modified after Tankard et al., 2009).

3.2 Paleogeography

3.2.1 Basins

The focus of this section will be on the opening of the Witteberg Basin, which is part of the main Cape Basin and includes the smaller Kommadagga sub-basin, to the opening of the Main Karoo Basin and infilling of the Dwyka deposits (Figure 3.2). The basinal history of the Cape - and Main Karoo basin, which are both extremely large basins with a long paleogeographic history of about 300 Ma years, is beyond the scope of this study and will not be discussed in detail.

3.2.1.1 Witteberg Basin and Kommadagga sub-basin

The Witteberg Basin recorded the final stages of infilling of the Cape Basin which involved a number of transgressive and regressive pulses (Swart, 1982; Fourie et al., 2011). Since the deposition of these final stages occurred before the major tectonic and climatic changes associated with the final amalgamation of Pangea and the initiation of the Cape Fold belt and Main Karoo Basin (Broquet, 1992), the basin represented a quiet, stable shelf environment (Bell, 1981). According to Du Toit (1921) the basin had low relief with low ranges towards the north-east. The flatter parts of the region were not high above sea-level, with to the south a large part of it below water (most likely marine).

The Cape Basin axis, along which maximum subsidence and sediment accumulation took place, was oriented roughly east-west and located towards the southern basin margin, but it seems to have shifted northwards with time (Johnson, 1991) (Figure 3.2). This is most likely why sedimentation of the Witteberg Basin seems to have been confined to an area north-easterly of the basin. Evidence for the depositional settings within the Witteberg Basin has been interpreted to be a wave-storm shallow marine setting, with associated deposits preserving distal delta to freshwater lagoon conditions (Dunley and Hiller, 1979; Broquet, 1992; Shone and Booth, 2005).

The Witteberg succession is in general between 1100 to 2200 m (Broquet, 1992), but reaching a thickness of up to 2600 m in the Eastern Cape (Shone and Booth, 2005). It is compiled of almost equal proportions of interbedded sandstone and mudstone showing lateral continuity (except where truncated by thrusting). The thickness of the group

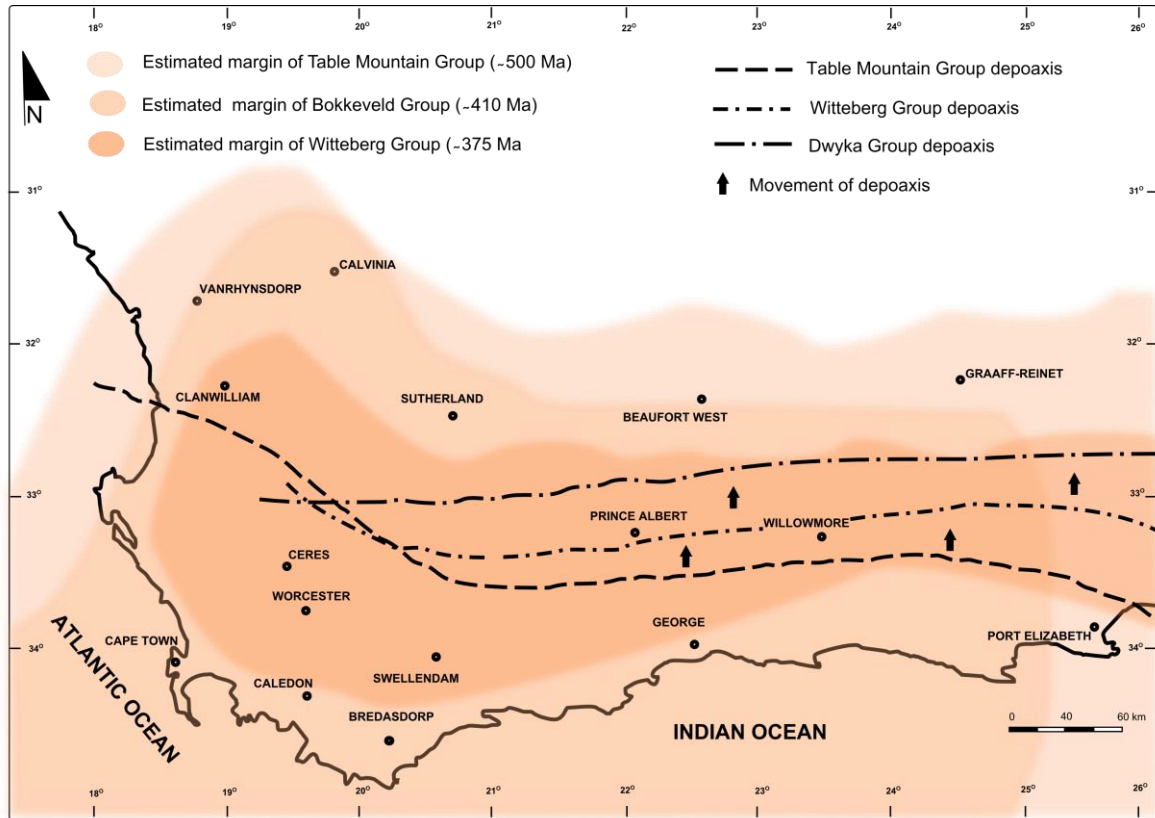


Figure 3.2: The Cape basin indicating the estimated boundaries from the opening (Table Mountain Group) of the basin towards the closing (Witteberg Group), as well as the northwards movement of the depoaxis during this period. (Modified after Dunley and Hiller, 1979).

increases rapidly from north to south and west to east (Fourie et al., 2011). Most of the Witteberg sandstones are quartz arenites or subfeldspathic arenites. The most common sedimentary structures are trough – and planar cross bedding, wave ripples, hummocky cross stratification and low-angle cross stratification. Wavy –, flaser – and lenticular bedding characterise many of the thinly-intercalated mudstone/sandstone units. Paleocurrent directions determined for the Witteberg are mainly towards the south, southeast and southwest (Shone and Booth, 2005; Fourie et al., 2011). Fossils include Spirophyton, lycopod stems and rare, small invertebrates (Bell, 1981).

The last and closing stage of the Witteberg Basin is represented by the Kommadagga sub-basin which is marked as the final regressive phase. After this regression the Cape Basin was nearly completely closed and sedimentation ceased (Swart, 1982). Two separate troughs existed in the Witteberg Basin (Swart, 1982) which confined the Kommadagga sub-basin to an area east of 23°E of the Witteberg Basin only (Figure 3.3). Sedimentation in the Kommadagga sub-basin which deposited diamictites, sandstones and mudstones, started around 360 Ma. Characteristically sedimentary structures are the same as already described in the Witteberg Basin. There is a lack of body fossils in the Kommadagga succession which is due to the fact that these deposits may have formed in a narrow basin with restricted circulation and as a result salinities were too high for the development of abundant life (Swart, 1982).

After sedimentation there was a period of pre-Dwyka erosion of the upper units in the Kommadagga succession which is evident in the disconformable and unconformable contact between the Kommadagga and overlying Karoo succession. It is thereby suggested that there was a hiatus between the sedimentation of the Cape and Karoo Supergroup, even in the areas where the Dwyka diamictite appears to rest conformably (to the west of the basin) on underlying strata (Dunley and Hiller, 1979). This hiatus represents a time gap of about 20 to 30 Ma (Visser, 1991; Catuneanu et al., 1998; Tankard et al., 2009). According to Dunley and Hiller (1979) the Witteberg Basin continued to subside and receive sedimentation in the eastern side of the basin via the Kommadagga sub-basin. Thus it fills part of this time gap, but it is unlikely that the Kommadagga sedimentation represents the whole period involved.

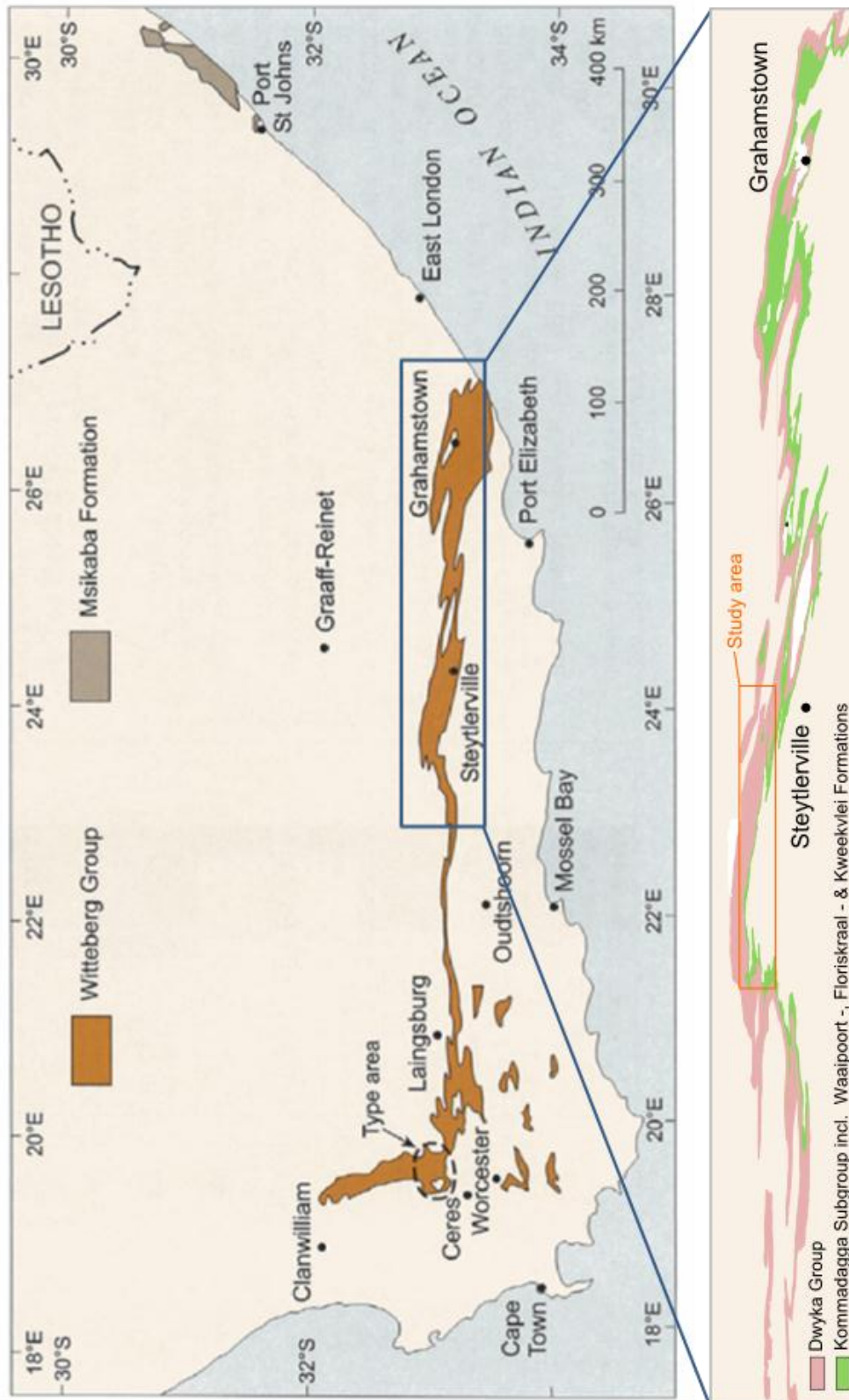


Figure 3.3: Distribution of Witteberg Group. Marked area indicates the region which the Kommadagga Subgroup is confined to (Modified after SACS, 1980).

3.2.1.2 Main Karoo Basin

Probably during the 30 Ma hiatus there was some uplift and glacial erosion on fjord-like margins of the highlands, prior to the start of deposition in the Main Karoo Basin (Visser, 1991). The Main Karoo Basin was initiated by the Dwyka depositional basin which consisted of a broad foreland basin downwarped on its southern margin, under the load of the Southern Highland tectonic arc, and faulted on its northern margin (south of the intracratonic Kalahari Basin). The basin may have been closed eastwards on the Antarctic margin of Gondwana but opened westwards where it extended north as a broad epicontinental seaway between South America and southern Africa (Figure 3.4) (Eyles, 1993).

It was also at the same time when the southern part of Gondwana drifted over the south pole. This resulted in a continental ice sheet over the highlands and floating ice on the lowland platform (Figure 3.5) (Smith et al., 1993). This ice sheet lay north of the Main Karoo Basin and extended southwards to the near south coast of Africa. This extensive ice sheet had several lobes or units, namely Namaland, Griqualand West, Transvaal and Natal (Du Toit, 1921), which carried debris into its centres respectively (Figure 3.6). The Transvaal ice sheet centred over the shield area of southern Africa which merged with the Natal sheet further east and southeast. In the west was the Namaland lobe which transported ice into the Main Karoo Basin from the west and northwest. The western margin was poorly established and the eastern margin was overlapped by the Botswana (Griqualand West) and Transvaal lobe (Crowell and Frakes, 1972; Isbell, 2008). The ice sheets were generally moving in a southerly or pole-ward direction (Du Toit, 1921; Dunley and Hiller, 1979; Bell, 1981).

The Dwyka sedimentation which occurred in a number of tectonically or climatically controlled pulses, was initiated around 300 Ma (Catuneanu et al., 1998). The advance and retreat of the ice sheet(s) is recorded in the sediments and can be recognised by the presence of various pro-glacial features interbedded within the main diamictite (Swart, 1982). The Dwyka sediments were deposited in the northern highlands (proximal facies) by ground ice on a stable craton and in the south (distal/shelf facies) by floating ice in the Cape Basin (Dunley and Hiller, 1979). This is why in the northern parts of the Main Karoo Basin the Dwyka sediments lie directly upon glaciated pavements eroded across various

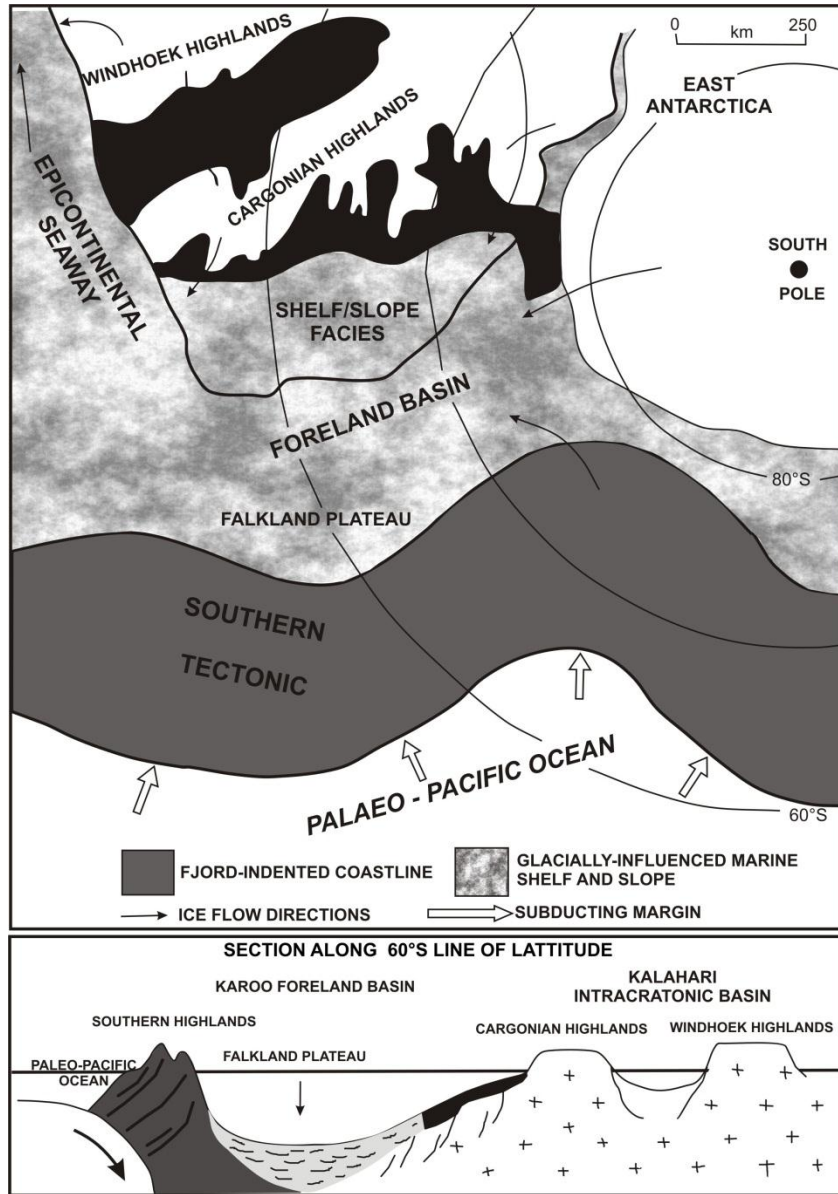
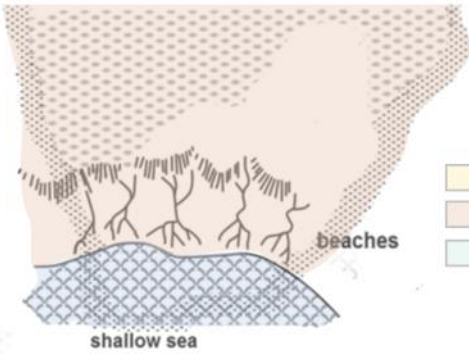
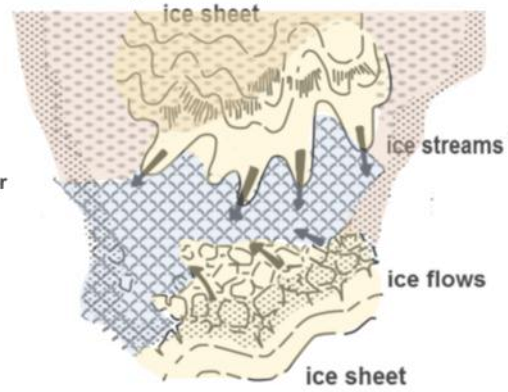


Figure 3.4: Paleogeographic (top) and paleotectonic (bottom) setting of Late Palaeozoic Dwyka Group (Eyles, 1993).

Witteberg Group (pre-Karoo)
shallow sea-beach-deltaic deposits



Dwyka Group
glacial deposits



Ice cover
Land
Water

Figure 3.5: Sedimentary environments of pre-Karoo and Main Karoo Basin (Modified after Smith et al., 1993).

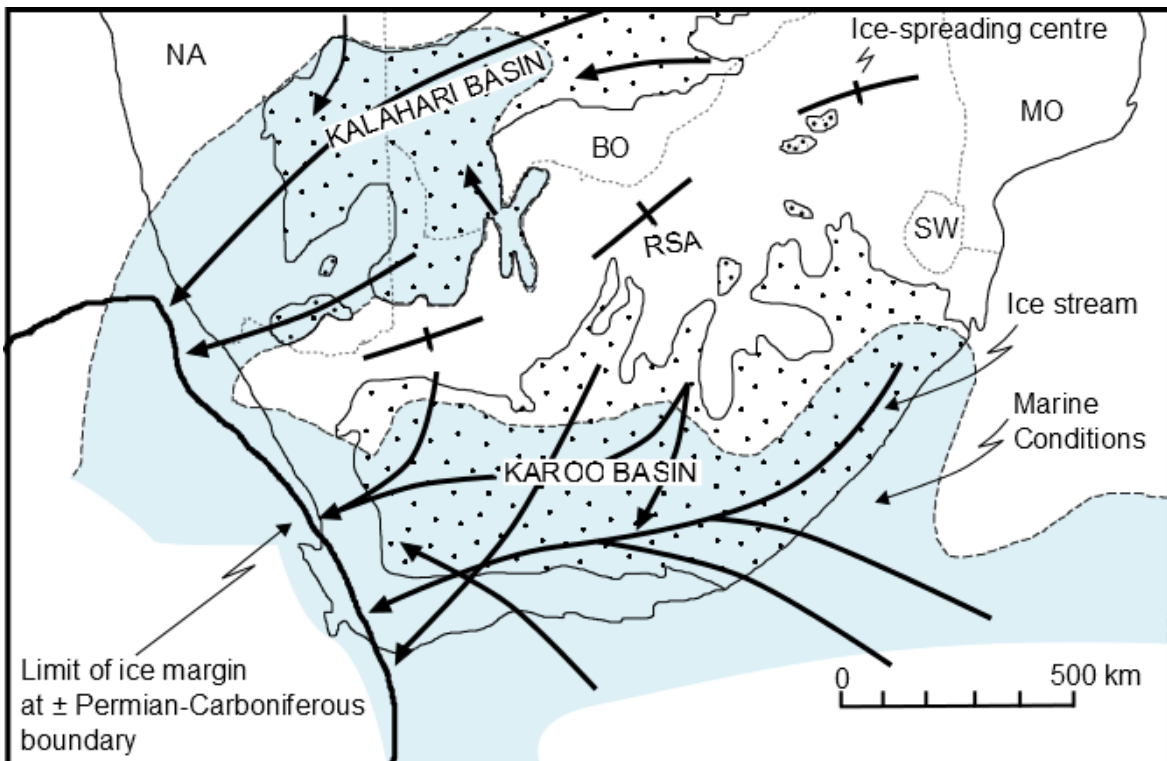


Figure 3.6: Flow direction of ice sheets during the Dwyka glaciation. Also show limits of marine conditions and extent of the Gondwana Ice sheet at about the Carboniferous-Permian boundary (Visser, 1997).

older formations and to the south of latitude 32°, the glacial sediments lay conformably and in some parts unconformably on strata of the Witteberg sediments (Bell, 1981).

According to Catuneanu et al. (1998) the difference between the proximal and distal Dwyka deposits, as well as the overall pattern of southwards ice movement, suggest that the surface profile during the Dwyka time was dipping toward the south. This may explain the diachronous age of the top of the Dwyka Group, younger in the north relative to the south. This is possibly due to the continental glaciation lasting longer in the north (at higher altitude in the highlands) than in the south, where the marine environment would have led to the rapid melting of the floating ice during the climate warming in the Early Permian (Figure 3.5 & Fig. 3.7).

3.3 Facies analysis of local geology

In this section the characteristics of the Kommadagga Subgroup and Dwyka Group (Figure 3.8) will be discussed based on previous attempts of facies analysis. This will be used as a framework and discussed in a later chapter with the newly reviewed features and facies analysis obtained from this study. With the combined efforts of previous and present work an updated and "realistic" facies model will be attempted.

3.3.1 Kommadagga Subgroup

The Kommadagga Subgroup is confined to an area east of 23°E of the Cape Basin (Figure 3.3). To date only a handful of studies have contributed to our understanding of the Kommadagga Subgroup (Rossouw, 1953, 1970; Loock, 1967; Johnson, 1976, 1991 and Swart, 1982). In this literature it is either described in detail, but with no interpretation, or vice versa. In Rossouw (1953, 1970) the Kommadagga Subgroup is described under the old terminology where it was seen as part of the Dwyka series (Figure 3.9). In the older stratigraphic nomenclature the Miller Formation was known as the Basal tillite, Soutkloof Formation as the fissile shale band, Dirskraal Formation as the greenish sandstone and the Dwyka Formation as the main tillite, which all formed part of the Dwyka Tillite Stage, now known as the Dwyka Group (Figure 3.9).

The basal unit of the Kommadagga Subgroup is the Miller Formation. In the western part of the Kommadagga basin, near Willowmore, the Miller Formation, as described by Rossouw (1953, 1970), is a darkish rock, somewhat argillaceous, generally containing

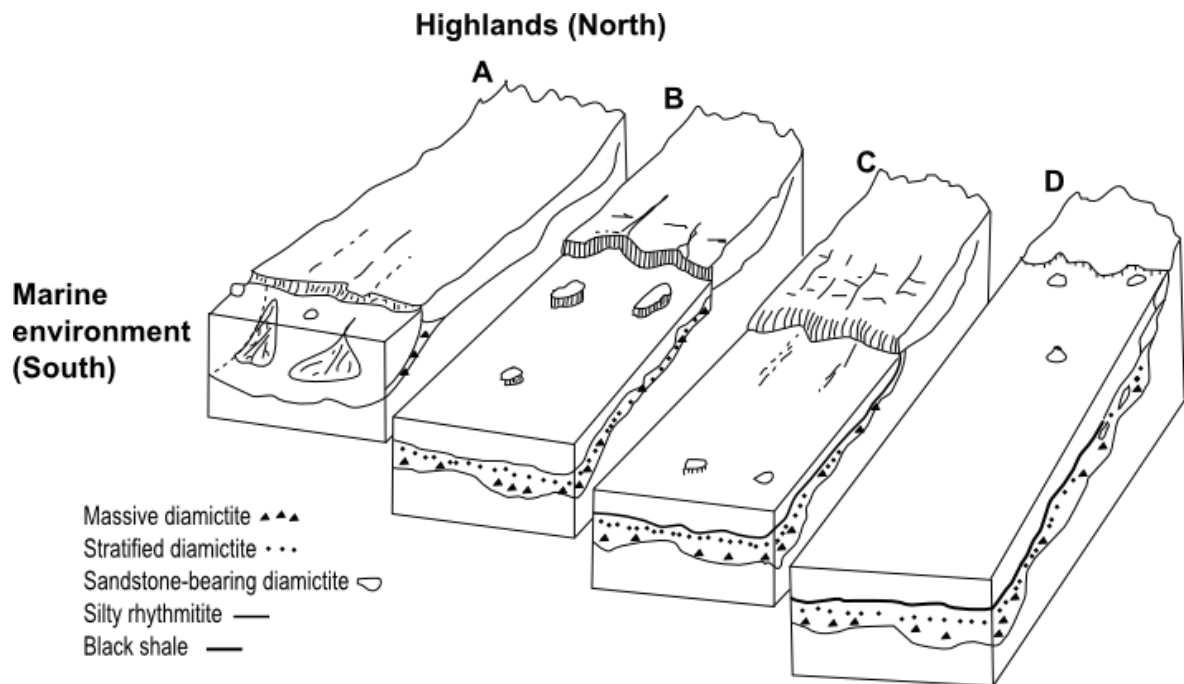


Figure 3.7: Schematic diagram of the deglaciation sequence in the Main Karoo Basin (A-D). A – Maximum extent of ice sheet over Main Karoo Basin from north to south (Cambrian-Permian); B – Collapsing of ice margin allowing iceberg rafting in south. Active glaciation in north; C & D – Retreating phase of ice margin due to changes in climate with ice only restricted to the highlands in the north (Modified after Visser, 1997).

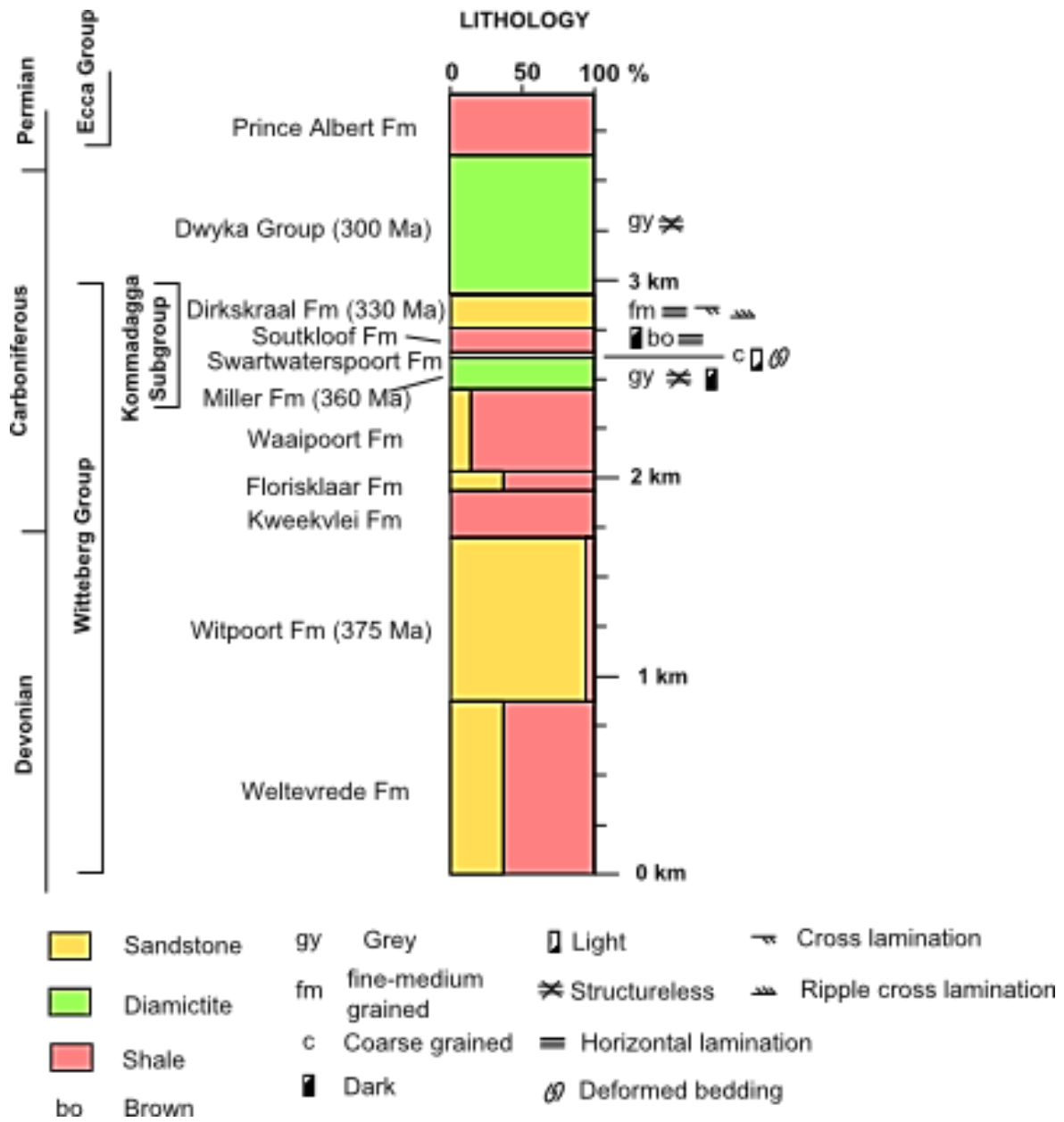


Figure 3.8: Stratigraphic column summarising lithology of Dwyka Group and Kommadagga Subgroup (Modified after Johnson (1991), Booth and Shone (2002), Johnson et al., (2006)).

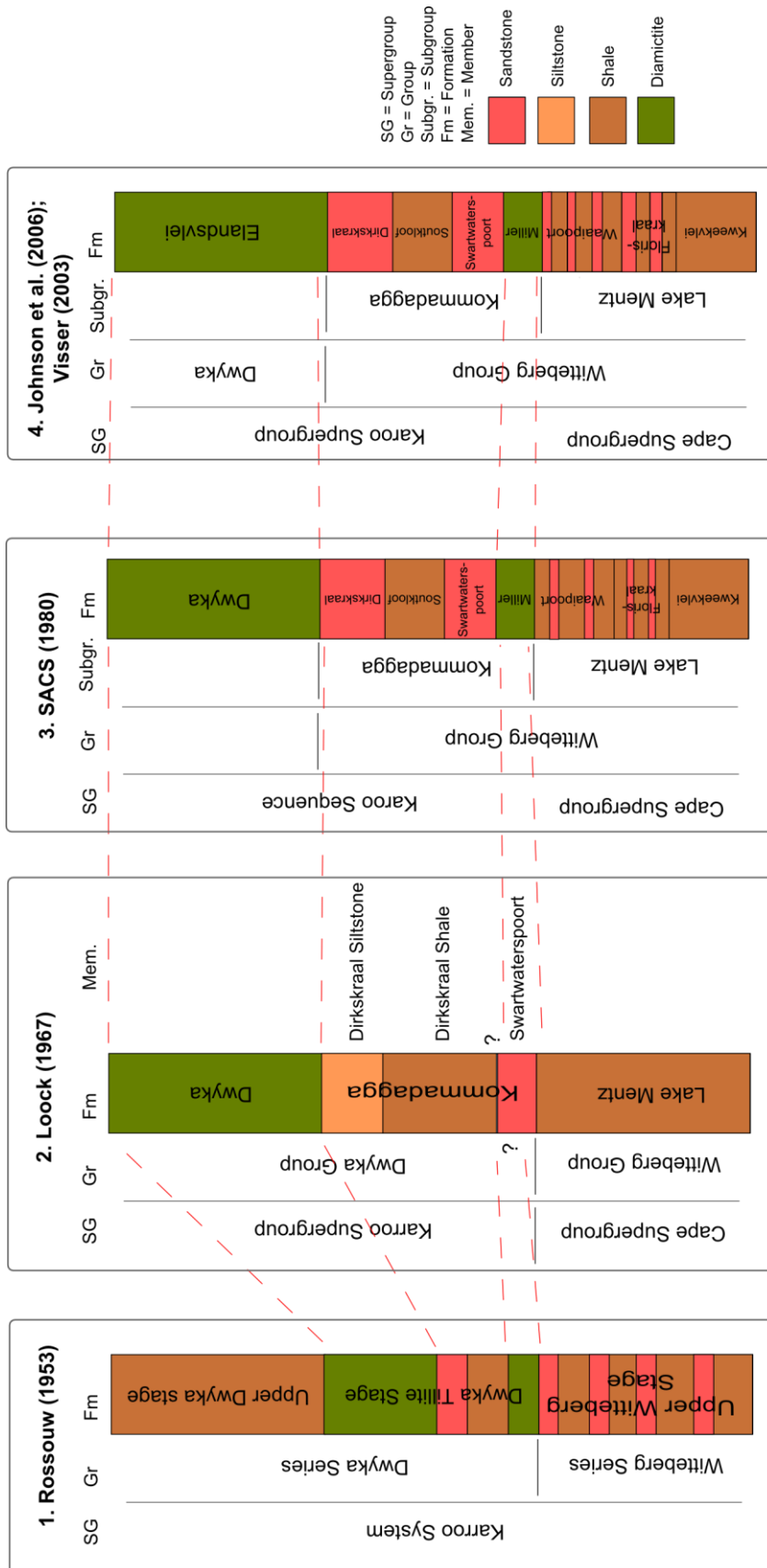


Figure 3.9: Stratigraphic nomenclature changes of the Witteberg Group and Dwyka Group from 1953 to present (not to scale).

clasts measuring about 15 mm in diameter. Further east at Miller station, the Miller formation is composed of pebbles of quartz and quartzite, 7.6 cm in diameter. It has a dark colour, is quite arenaceous, carries lenses of grit and sandstone, and contains elongated boulders up to 0.9 m in length. Rounded inclusions of quartzite, conglomerate, nodular diamictite and brown sandstone are present. Inclusions of the last-named seem to be derived from the brown sandstone in the uppermost Witteberg immediately underlying the Miller Formation. The diamictite more often than not contains plicated and lenticular bodies of white quartzite. It weathers to a characteristic chocolate brown colour. On the eastern side of the basin, near Kommadagga and Saltaire Station, Swart (1982) describes the Miller Formation as a fine to medium grained diamictite with occasional pebbles up to 2cm in long dimension. Unweathered sections present dark blue but it weathers to a dull brown colour. No sedimentary structures were found despite careful examination of fresh and weathered outcrops. It is possible that the dark colour of the rock obscures any sedimentary structures that are present. The diamictite is very poorly sorted, with a grain size ranging between ~ 2 cm - 0.1mm, with a continuous gradation in size between these two extremes. Grains exhibit high degrees of rounding, indicating a certain degree of textural maturity, although poor sorting contradicts this. This unit lacks both bioturbation, and body fossils, however a single plant fragment (possibly of *Archaeosigillaria*) was found at Kommadagga kop. The outcrop of this unit is commonly discontinuous along strike with a high degree of variability to the total thickness. It is the thinnest at Campherspoort (few meters) and Kommadagga Kop to a maximum thickness of 92 meter at Kruidfontein (Rossouw, 1935; Johnson, 1991).

The Miller Formation is overlain by the Swartwaterspoort Formation. Rossouw (1953, 1970) never explicitly described the Swartwaterspoort Formation, but only mentioned sandstone units that are interbedded with the basal tillite (Miller Formation) which possibly refer to the Swartwaterspoort Formation. According to Swart (1982) these sandstone units are discontinuous in the eastern part of the basin where it is easily recognised by its coarse grain size, clean white weathering nature, presence of iron oxide staining and slump structures. A 0.1cm to 3cm thick horizontal lamination, defined by iron oxide staining, is common in the Swartwaterspoort with soft deformation structures as the only sedimentary structure commonly observed. No fossils have been found. Swart (1982) is the only author who gives an observed thickness for this unit, which is 5m. He interpreted this sandstone unit as representing a reworking of the Miller Formation due to

its close spatial and mineralogical relationship with regards to each other. Johnson (1976) also interpreted it as a beach deposit which represents the reworking of glacial outwash of the Miller Formation.

The following formation overlying the Swartwaterspoort Formation is the Soutkloof Formation. Rossouw (1970) describes it as dark fissile shale which is often banded. Whereas Swart (1982) describes it as a consists of light coloured shales which are poorly exposed throughout the Kommadagga area (and the rest of the basin) due to its vulnerability to weathering and erosion. It shows very thin horizontal lamination (often <1 mm). It is possible that other sedimentary structures such as bioturbation do exist, but have been obscured by weathering. Intermittent carbonate layers with a maximum thickness of 6 cm occur interbedded with the shale. These carbonate layers consist dominantly of calcite with some minor clays. In hand specimen the characteristic features of these carbonate bands are their brown-grey colour and the presence of cone-in-cone structures, which are covered by a clay layer. They form during the early process of diagenesis by precipitation of calcite (Franks, 1969). No fossils have been found in this unit. The maximum thickness of this unit in the Kommadagga area is 127 m and its minimum thickness is 12m at Volstruisleegte.

The uppermost unit of the Kommadagga Subgroup and Witteberg Group, overlying the Soutkloof Formation, is the Dirkskraal Formation. It is characterised by fine grained sandstone with the presence of mottling and a ripple lamination. The lamination is defined by layers of dark organic material, but is laterally discontinuous, nor does there appear to be a preferred orientation to these structures. Horizontal lamination is also found, being only 1mm-2mm thick. The sandstones may occasionally appear massive, but when they are followed along strike units which initially appear massive, they actually have a well-developed ripple or horizontal lamination. A distinguishing feature of the formation is the widespread mottling found within it. Some mottles may be flattened parallel to the lamination. The fact that the lamination is not disturbed by the mottling would suggest a syn-depositional origin for the mottles, but no textural differences can be seen between mottles and host rock. Scour surfaces associated with channelling are common and these may be found with mud flake conglomerates. These channels may be quite large, they can be 1m –1,5m in depth and 3m – 4m in width. Trough cross bedding is occasionally present and load casting is found where sand overlies finer grained material. Concretions

with a maximum diameter of 20 cm are found but are not common. No fossil material was found within these concretions. Unidentified plant fragments have also been found in this formation. Near Kommadagga area the Dirkskraal Formation has a maximum thickness of 100m (Swart, 1982). Rossouw (1970) has a similar representation of this sandstone formation.

Both Loock (1967) and Johnson (1976) interpreted the Soutkloof - and Dirkskraal Formation as proglacial sediments deposited in a marine environment, which possibly fit their theory that the Miller Formation is a tillite. Swart (1982) and Johnson (1991) on the other hand suggest that it represents a coarsening upward sequence, characteristic of a delta, with the Dirkskraal Formation representing delta front deposits and the Soutkloof formation the pro-delta muds. This supports Bell (1981) and Swart's (1982) interpretation that the Miller Formation could be a diamictite deposited by a debris flow off the slope of a delta.

The only interpretation made on the Kommadagga Subgroup was made by Swart (1982) who interpreted it as a prograding delta complex. The other authors did not combine their descriptions and interpretations of the Kommadagga basin as a whole into a representative facies idea/model.

3.3.2 Dwyka Group

The Dwyka Group consists of up to 1000m (Crowell and Frakes, 1972) of massive and stratified diamictite as well as mudstone and sandstone bodies. The colour of a fresh sample of the diamictite is dark grey and weathers to a brownish colour. Most of the scattered pebbles/clasts, derived from its Precambrian basin floor towards the north, are granites, gneisses, metavolcanic rocks, quartzites, dolomites and cherts. Clasts derived from the Cape System, incorporated in the southern and western border of the Main Karoo Basin, are predominantly quartzitic and granitic.

Depending on location throughout the Main Karoo Basin, the Dwyka Group shows distinct lithological differences (Crowell and Frakes, 1972) between the northern (valley) and southern (shelf/platform) facies. The northern facies, which is known as the Mbizane Formation (Figure 3.10), has a thickness of about 700m, representing deposition in major valleys which consists of massive stratified diamictites and mudstones with subordinate

sandstone and conglomerates (Visser and Young, 1990), debris flow diamictites. Thus the valley facies represented fjords in the highlands (Eyles, 1993) where subglacial tills formed due to grounding and debris-laden ice (Crowell and Frakes, 1972; Visser and Young, 1990). The southern facies, known as the Elandsvlei Formation (Figure 3.10), is older and thicker (up to 800 m) than the Northern facies. The deposits consist mainly of massive clast-poor diamictites of up to a 100 m thick with large sandstone rafts and mudstones.

The diamictite of interest is part of the Elandsvlei Formation in the Dwyka Group that lies disconformably over the Precambrian basement in the north and paraconformably to unconformably over the Cape Basin in the south and southwest (Johnson, 1991; Broquet, 1992; Visser et al., 1990).

In the study area Swart (1982) describes the Elandsvlei Formation as a dark blue diamictite which weathers to a dull brown colour. The thickness was measured to 850 meters south of Kommadagga Kop. The diamictite is very poorly sorted with a range in grain size from less than 1mm to blocks of granite 1,2m in diameter. Clasts, which may be angular to well rounded, show a wide range in composition with granites, garnet-hornblende gneisses, sandstones, quartzites, cherts, conglomerates, green amygdaloidal lavas, milky quartz and epidote-clinzoisite bearing gneisses. There is also a substantial proportion of matrix in which clasts generally "float". Sedimentary structures within the main diamictite are absent, but shales and sandstones interbedded with the diamictite may show some structures. The shales are very finely laminated and dropstones may be present, but are not common. No fossils have been observed in this formation.

3.4 Provenance

The provenance for the Cape Supergroup sediments, thus including the Witteberg Group, is suggested to be to the north and west of the Cape Basin (Johnson, 1991; Broquet, 1992) which were brought into the basin via a widespread fluvial system into an epicontinental sea open to the ocean in the south (Broquet, 1992). Detrital zircon age dating done by Fourie et al. (2011) confirmed the dominant source area to be the Mesoproterozoic Namaqua-Natal Metamorphic Belt. For the Kommadagga Subgroup

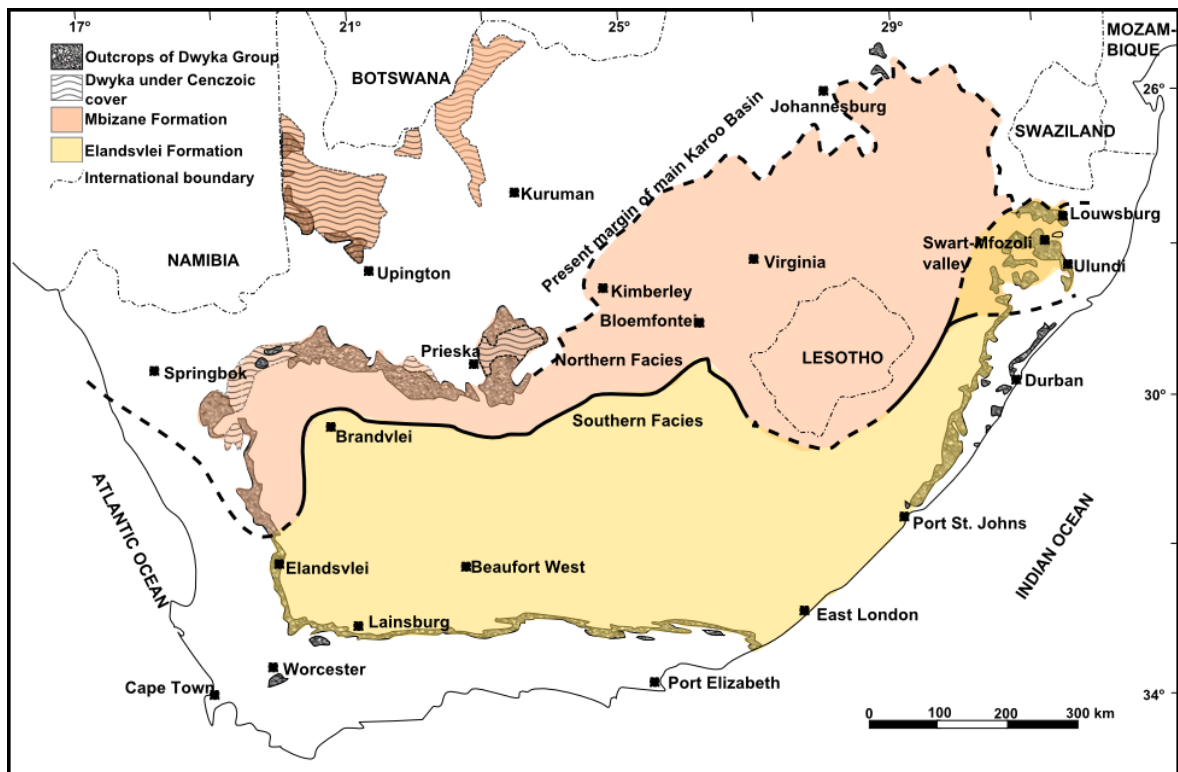


Figure 3.10: Distribution of Elandsvlei - and Mbizane Formations of Dwyka Group (Visser and Young, 1990).

Johnson (1967) and Swart (1982) proposed a metamorphic-igneous-sedimentary terrain as a source area for this deposit although there are limited paleocurrent indicators.

CHAPTER FOUR

DESCRIPTIONS OF FACIES

4.1 Introduction

Facies are distinguished only on a descriptive basis taking into consideration any unique characteristics and sedimentary structures of unit/s (facies divisions). Some facies consist of a single facies division, where others include a range of divisions (modified from Benvenuti (2003)). The facies divisions are grouped together or singularly represent a particular depositional event which was produced by a particular sedimentary process to deposit a particular facies. Individual facies are identified based on morphological and textural characteristics, which are then grouped into associations as these can be genetically related.

In this chapter all facies of the contact within the Kommadagga Subgroup and Dwyka Group found over the four locations, Volstruisleegte, Miller, Swaylands and Campherspoort (Fig. 1.4a) will be described and interpreted by what sedimentary process was involved during deposition. The classification code of the facies divisions (Table 4.1) was carried out using a modified version of Eyles et al. (1983) and Maill (1997). Figure 4.1 show the stratigraphic profiles at all four locations with corresponding facies divisions and facies. Positions of profiles can be seen in Fig 1.5 and Fig 1.6

4.2 Facies A

4.2.1 Description

Facies A comprises of two facies divisions: A clast-rich muddy diamictite (Dcm) and a medium to coarse grained sandstone (Sm). Facies A is found at all four locations, Volstruisleegte, Miller, Swaylands and Campherspoort.

Within Facies A, Dcm is a clast-rich muddy diamictite which forms the brownish dark grey hills, which can immediately be identified by its unique tombstone weathering. It is dark grey in colour and weathers to a lighter greenish brown to dark brown (Fig. 4.2). Outcrop width is uncertain, but is definitely extensive. No clear bed boundaries can be identified and actually seems absent. Geometry of outcrop is parallel and continuous. There are no visible

Table 4.1: Classification code of facies divisions with key characteristics and location.

Facies divisions	Description	Location
Diamictite		
Dcm	massive, clast rich muddy diamictite	Volstruisleegte, Miller, Swaylands, Campherspoort
Dmm	massive, clast poor sandy diamictite	Volstruisleegte, Miller
Sandstone		
Sl	lower plane bed laminated, gravelly sandstone	Volstruisleegte, Miller
Slm	lower plane bed laminated to massive, fine sandstone	Campherspoort
Slr	lower plane bed laminated, rippled, medium sandstone	Swaylands
Sm	massive, medium to coarse sandstone with dispersed clasts.	Volstruisleegte, Miller
Smc	massive, muddy sandstone with occasional carbon streaks	Miller
Smq	massive, quartzitic, coarse sandstone	Swaylands
Srm	massive, rippled, fine to gravelly sandstone	Swaylands
Mudstone		
Fdp	deformed, silt, clay mudstone with carbonate bands	Swaylands
Ffb	fissile, silt, clay mudstone with bioturbation	Campherspoort
Ffd	fissile, silt clay mudstone with dropstones	Volstruisleegte, Miller
Flp	layered, silt, clay mudstone with carbonate bands	Campherspoort
Fm	massive, silt mudstone	Swaylands
Frc	ripple cross laminated, fine sand, silt, clay mudstone with occasional carbon streaks	Miller, Swaylands
Frt	ripple cross laminated, silt, clay mudstone with trace fossils	Campherspoort
Grain size		
g	gravel	
vcs	very coarse sand	
cs	coarse sand	
ms	medium sand	
fs	fine sand	
vfs	very fine sand	
sl	silt	
cl	clay	

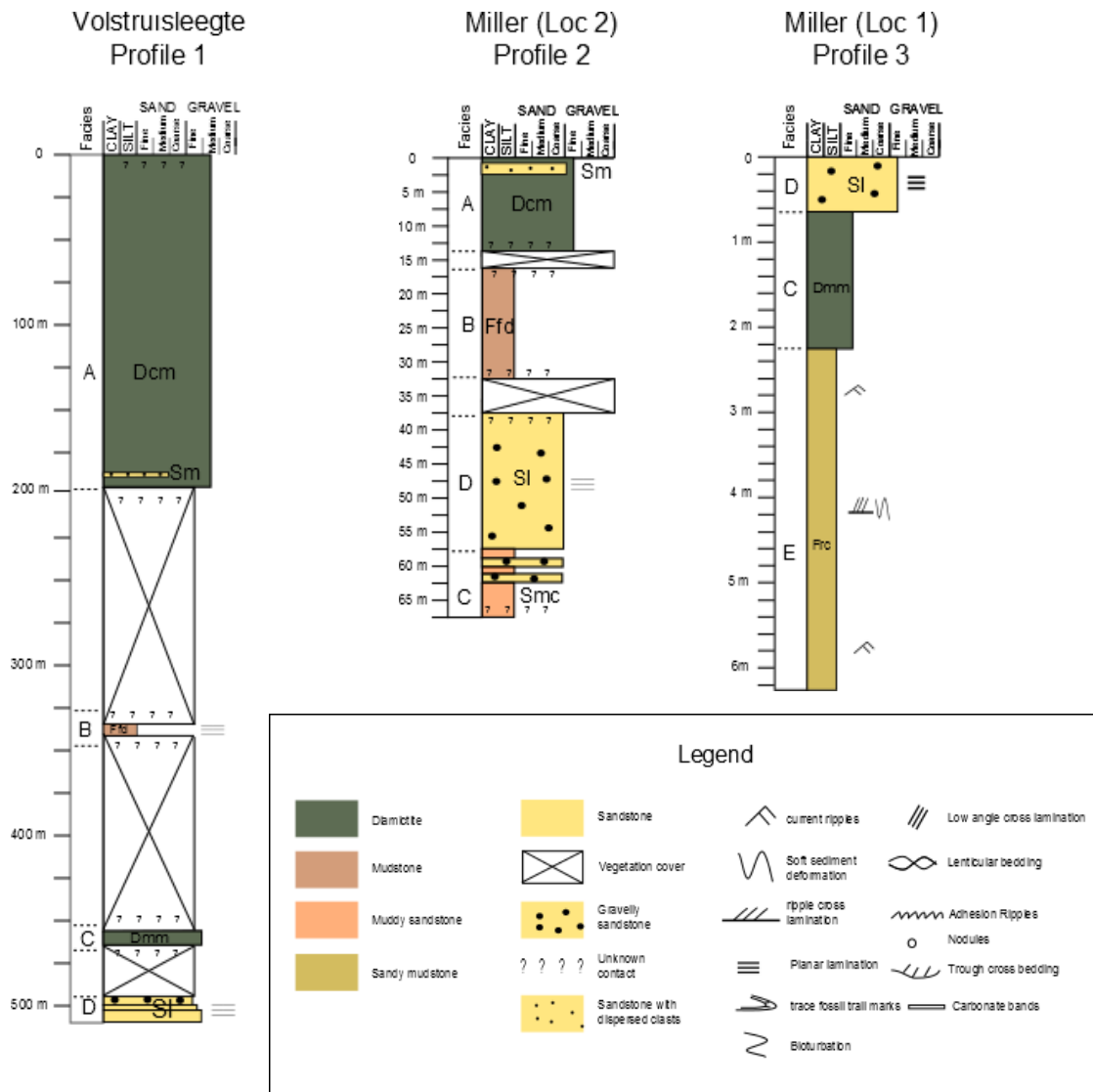


Figure 4.1a: Stratigraphic profiles 1, 2 and 3.

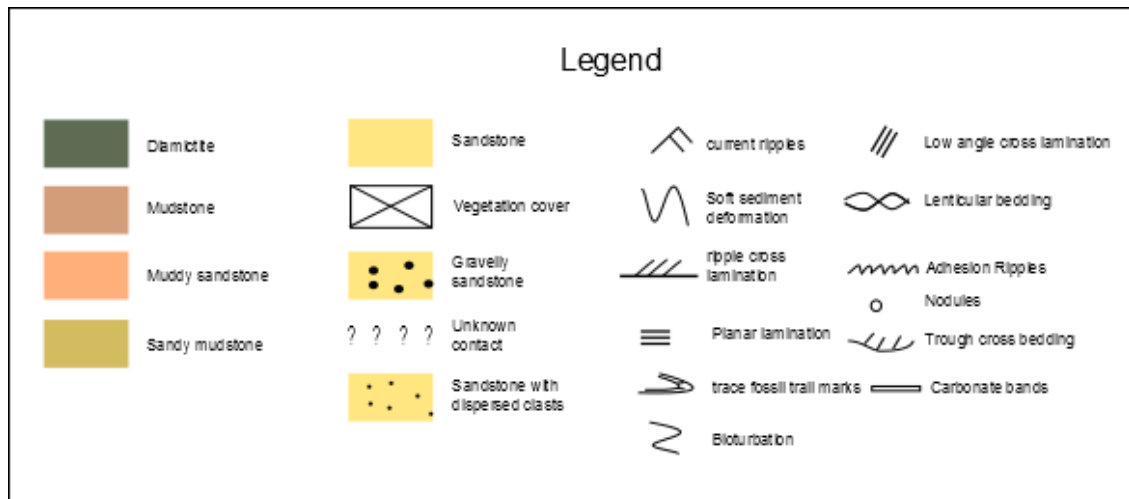
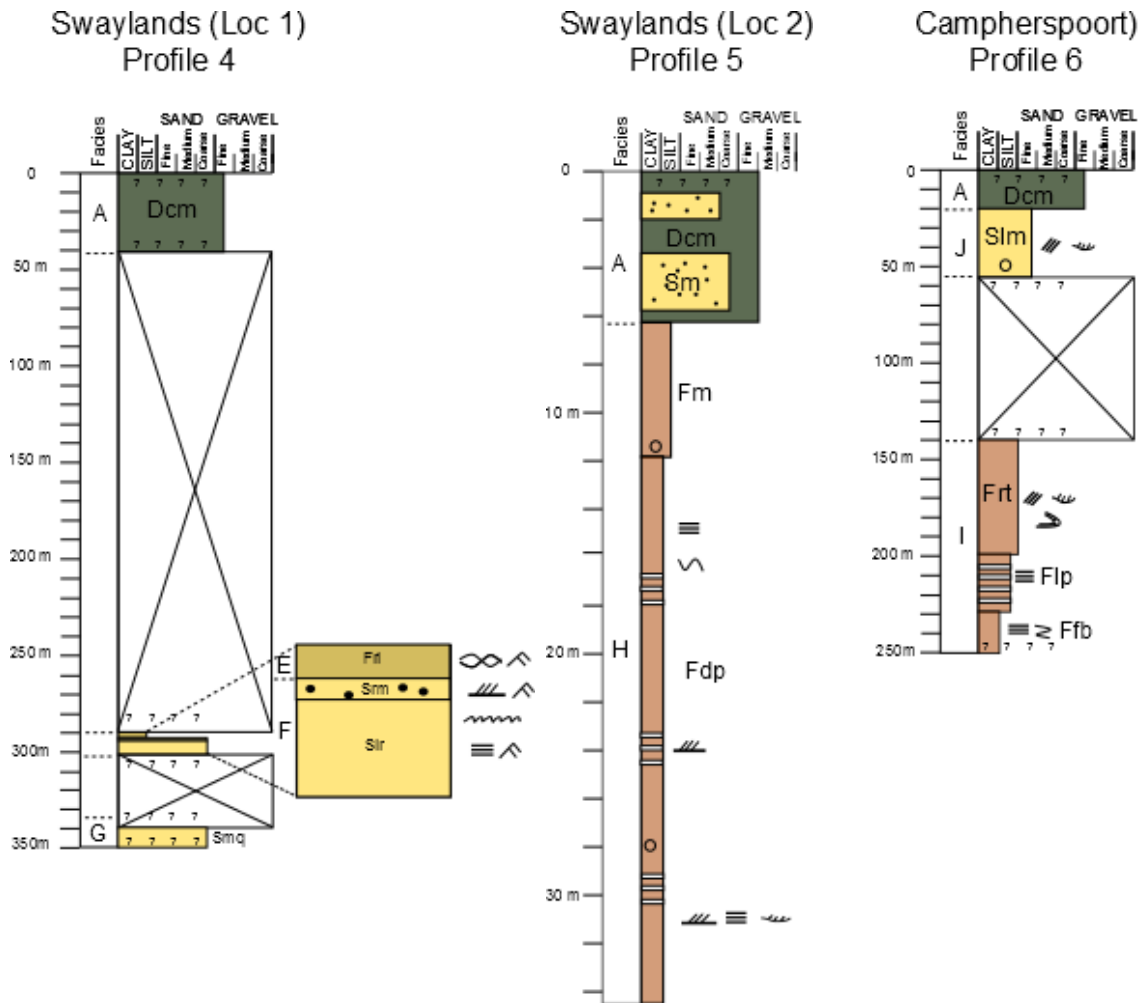


Figure 4.1b: Stratigraphic profile 4, 5 and 6.



Figure 4.2: Texture of Dcm, a diamictite, indicating random sized clasts in a matrix. A – Weathered rock; B – Fresh rock.

sedimentary structures. The matrix is of a silty to fine sand nature with granules to small cobble sized clast (up to 1.5 cm) randomly situated within the matrix (35% g; 13% cs + ms; 34% fs; 49% sl + cl) and is very poorly sorted. The clasts in the diamictite are very prominent. Clast size ranges from small cobbles to small pebbles. There are no visible facets or scratch marks on the clasts. Grain shape vary between rounded and angular, were the smaller grains are more angular than the larger grains (coarse sand to pebble size). The pebble/cobble-size clasts are composed of individual polycrystalline quartz and feldspar grains, and rock fragments originating from sedimentary and plutonic rocks (Fig. 4.3). The granule size clasts are composed of granitic -, chert -, quartzitic – and schist rock fragments. A portion of the rock fragments are surrounded with a rim composed of precipitated calcite. The interstitial material (<2mm) consists of monocrystalline quartz, k-feldspar, calcite, including matrix (<30 μ) of biotite, muscovite, chlorite and heavy minerals (apatite, sphene, garnet and hematite). All minerals are randomly orientated and distributed throughout the rock. Most of the grains larger than medium sand show structures of interstitial material wrapping/bending, caused by foliation (cleavage) of matrix, around the larger grains (Fig. 4.3). Facies division Sm is structureless white sandstone which weathers to a yellowish colour. Sm forms outcrops of 1m-2m wide which is parallel, but discontinuous in geometry (discontinuous lenses). Bed thickness is between 50cm – 60 cm with sharp boundaries. Sm beds are underlain and overlain by facies division Dcm. Structural features includes slickenside structures on the bedding planes, possibly due to folding or structural deformation, as well as quartz veins cutting in different directions through beds (Fig 4.4). It is medium to coarse grained (<1% g; 45% cs; 52% ms+fs; 2% sl + cl) which is poor to moderately sorted, with dispersed gravel size clasts. The grain shape is angular to subrounded with concavo-convex contacts between grains. There is no significant grain orientation or fabric. The mineral composition consist of about 95% quartz (mostly monocrystalline), <1% rock fragments, which make up the gravel to sand size grains, 1% k-feldspar, 3% biotite and 1% heavy minerals such as zircon, rutile, hematite and garnet (Fig. 4.5). The quartz show wavy, straight and undulosed extinction with occasional zircon inclusions as well as overgrowth and pressure solution. The matrix (<30 μ), which is about 2% of the whole rock, is composed of quartz, biotite, a few zircons and rutile.

No fossils are present in this facies. No paleocurrent indicators are present.

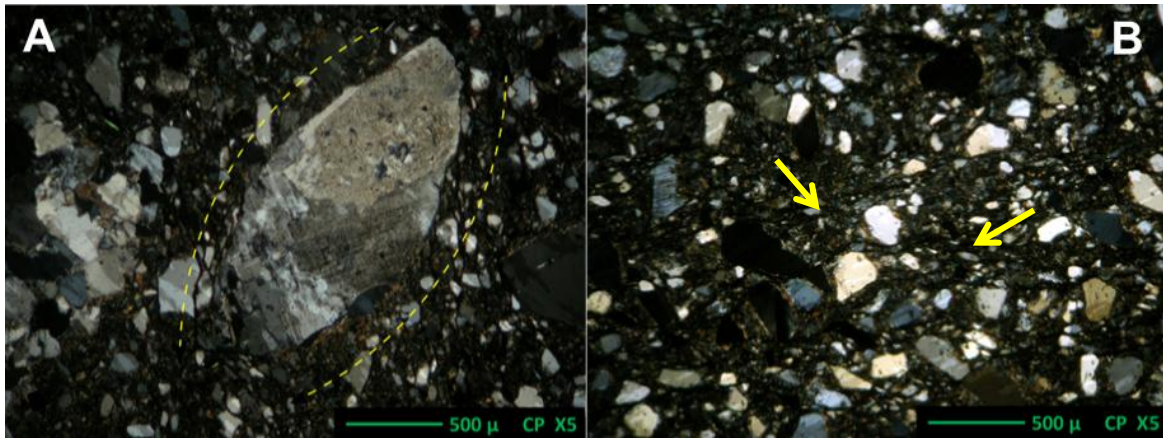


Figure 4.3: A - Plutonic rock fragment with interstitial material wrapping around clast. B - Overall view of clast-rich diamictite, Dcm, showing cleavage seams (arrows).



Figure 4.4: Outcrop of Sm at Miller showing veins and slickenside features on bedding.

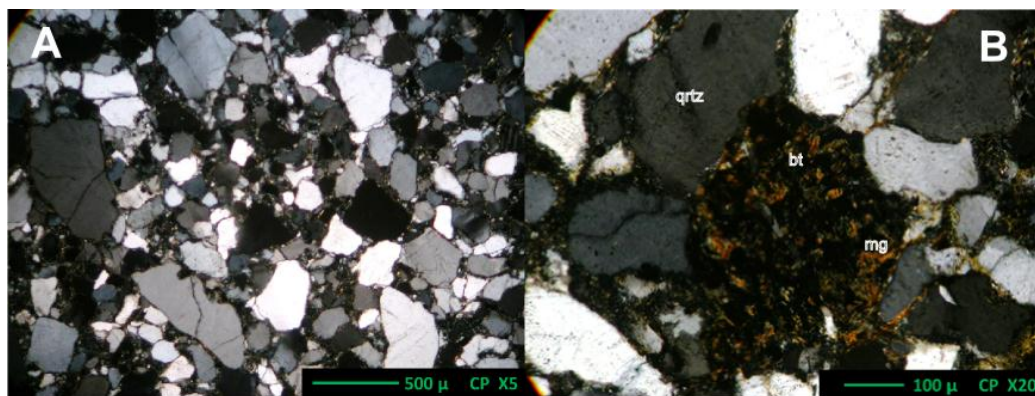


Figure 4.5: A - Overview of Sm indicating coarse to medium sized grains which have point and concavo convex contact relation with each other. B - Schist rock fragment

4.2.2 Interpretation

The massive structure of the diamict, clay-rich matrix and randomly orientated and shaped clasts of various sizes represents a cohesive debris flow deposit (Mulder and Alexander, 2001), although the larger oversized clasts, composed of a variety of rock fragments, can be interpreted as dropstones. This suggests deposition by subaqueous gravity flow in a glacially influenced environment. Unfortunately the wavy dark-cleavage seams, formed due to tectonic deformation by pressure solution, overwrite sedimentological evidence of dropstone structures (bending of under lying laminae and draping of overlying laminae (Chakraborty and Ghosh, 2008)). The alternative of en-masse deposition of a debris flow cannot be ruled out as a result of this.

The massive structure, poorly sorted and random orientation of grains indicates a rapid traction transport of sand sediment. Evidence of deposition via channel system is supported by the isolated, discontinuous lenses of sand bodies, as well as the underlying and overlying subaqueous gravity flow deposits (Dcm). The random dispersed clasts of rock fragments from Dcm is interpreted to represent sandy channel-fills, which likely may have slightly been reworked by the adjacent gravity flow deposits (Dcm). Late stages of post-deposition tectonic deformation are represented by the slickenside features and quartz veins filled fractures.

4.3 Facies B

4.3.1 Description

Facies B is represented by a fissile mudstone (Ffd) found at Volstruisleegte and Miller. The mudstone is a dark greenish brown colour which weathers to a grey colour. It shows strong cleavage (fissility due to parallel orientation of bedding) and quartz veins parallel to strike (Fig 4.6). The visible outcrop of the facies ranges in width from 7m to 21m, being parallel and continuous. Sedimentary structures show thinly laminated beds which are mostly indistinguishable from cleavage. Viewed by the naked eye, the beds are either horizontal or cross laminated, but under a microscopic view they show horizontal and/or wavy lamination, which are defined by alternating layers of silt and clay size grains (Fig 4.7). The mudstone consist of 45 % silt and 55 % clay size grains. The grains are well sorted, subrounded to angular and elongated. A few sand size grains, which are blocky to angular in shape, with



Figure 4.6: Ffd, fissile mudstone.

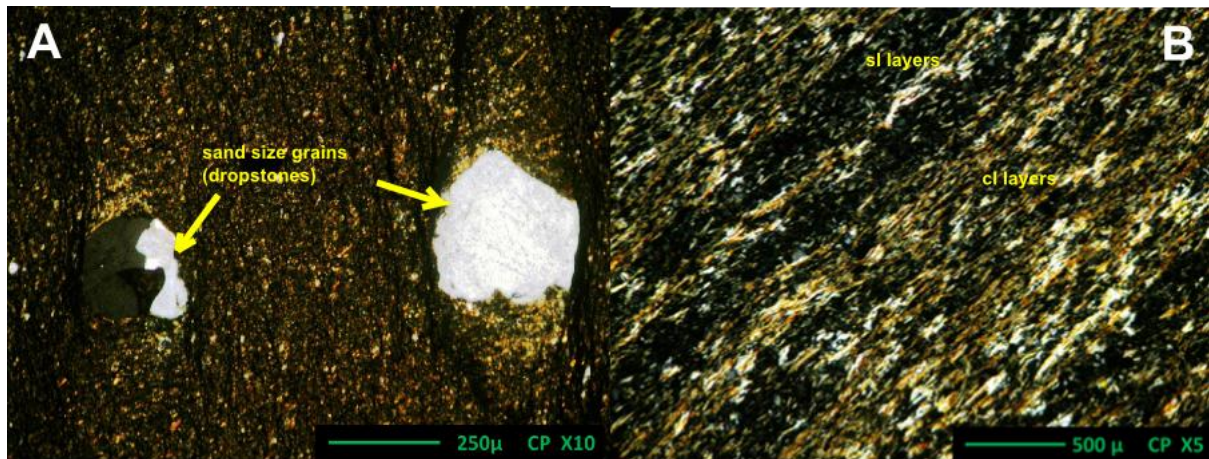


Figure 4.7: A – Lamination in Ffd wrapping around larger sand size grains. B - Lamination between silt (dark layers) and clay (light layers).

lamination wrapping around grains (Fig 4.7), are present (<1%). All elongated grains are orientated with their long axis parallel to lamination. All of the silt size grains are monocrystalline quartz. The clay size grains consist of 35 % biotite, 19% illite and 1% rutile. No fossils are present in this facies. No paleocurrent indicators are present.

4.3.2 Interpretation

The alternating silt and clay layers in Facies B suggest episodic sedimentation where each lamina is separated by time from adjacent ones. The horizontal lamination represents sedimentation from suspension in relatively quiet water, where bottom currents are weak. Higher bottom current velocities result in the formation of wavy/discontinuous lamination. Mud was thus deposited in a quiet subaqueous environment with partial bottom currents action (Potter et al., 1980). The sand size "clasts", showing strong dropstone structures, make a strong correlation with overlying facies A. This suggests that Facies B was deposited in a distal subaqueous marine environment.

4.4 Facies C

4.4.1 Description

Facies C comprises of a clast poor diamictite (Dmm) and a muddy sandstone (Smc). Smc is very similar to Dmm, however it lacks the adequate percentage of gravel sized grains to be classified as a diamictite (Fig. 2.1) and the mineral composition is different. Facies C is found at Volstruisleegte and Miller, although Smc is only visible at Miller.

Dmm is a dark grey/black clast poor sandy diamictite which weathers to a dark brown colour. At Volstruisleegte the outcrop width could not be determined due to poor outcrop exposure and rich vegetation. Small bits of outcrops that are visible show some joints perpendicular and parallel to strike. Because no visible bedding can be seen and it is impossible to determine bed boundaries and geometry the assumption is that it is parallel and continuous. At Miller the outcrop is 1.6 m and can clearly be identified by its strong cleavage. The unit is composed of poorly sorted silt to coarse sand size grains with white quartzite granules (1 mm) and small pebbles (2mm – 6mm) clearly visible in the outcrops (3% g, 3% cs, 15% ms, 40% fs, 20% sl, 19% cl) (Fig 4.8). There is no visible indication of any sedimentary structures and all the grains are very well mixed showing no specific



Figure 4.8: An outcrop of Dmm. Note small white clasts

orientation and random distribution. The grains are subrounded to angular and are also matrix supported with point contacts between grains. The mineral composition consist of 52% monocrystalline quartz, 40% calcite, 1% feldspar (plagioclase), 2% rock fragments, 4% biotite and 1% heavy mineral such as apatite, monazite and rutile (Fig 4.9). Calcite varies between coarse sand to silt size grains and is present as individual grains forming part of the matrix as well as minerals which is part of rock fragments. The rock fragments consist of quartzite and igneous fragments consisting of quartz, feldspar, biotite and calcite.

Smc is a dark grey muddy sandstone which weathers into a dark greyish brown colour. Most of the outcrop is covered with vegetation which makes it difficult to see any structural aspects and define outcrop width (possible about 6m – 8m or more). The bed thickness varies between 50 cm or smaller. Beds are parallel, but there is no certainty if it is continuous. No sedimentary structures are visible. In this poorly sorted unit of silt and sand grains there are occasional white quartz granules of 1mm which is easily spotted with the naked eye (5% ms; 55% fs; 25% sl; 15% cl). Grain shape is angular to subrounded and elongated. Fabric is defined by elongated matrix size grains (<30 μ) orientated with their long axis parallel to each other. All sand size grains are monocrystalline quartz with no inclusion which is randomly distributed throughout the matrix. The matrix (30% of whole rock) is composed of biotite, chlorite, smectite and some heavy minerals such as apatite and rutile. There are a few larger (fine sand) sized chlorite grains which are the result of chlorite growing in rock due to the breakdown of fine grained matrix during low grade metamorphism (Fig 4.10). Small discontinuous organic carbon streaks are present parallel to fabric and as well as a few small calcite veins, which are perpendicular to fabric (Fig 4.10).

No fossils are present in this facies. No paleocurrent indicators are present.

4.4.2 Interpretation

Dmm show similar characteristics as Dcm, although the matrix consist of more sand and fewer gravel-sized clasts. Even though the sand content is much higher, the clay content still exceeds the necessary amount for Dmm to represents a coherent debris flow deposit (Mulder et al., 2001). The debris flow is more weakly/moderate coherent than Dcm, from which limits the debris carrying ability of Dmm to smaller and fewer size clasts (Marr et al., 2001). Deposition was most likely rapid and en-masse. There is no clear structural evidence which a distinction can be made between a subaerial or subaqueous debris flow.

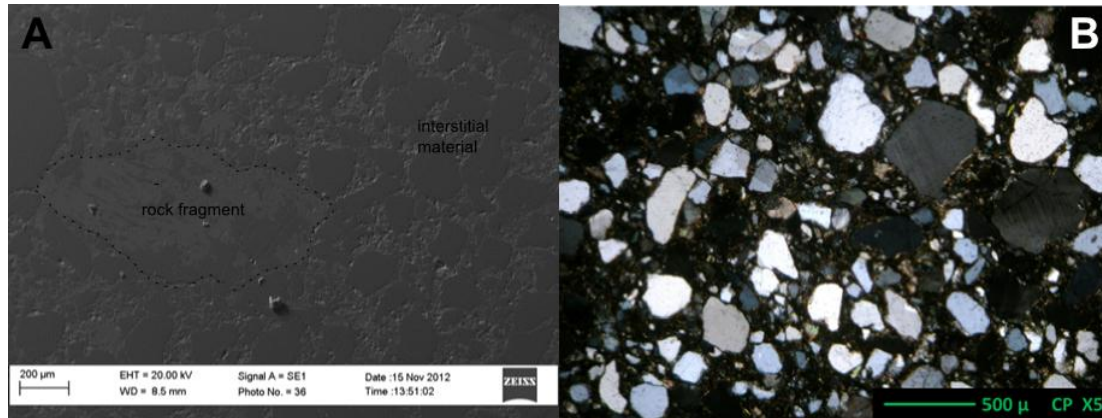


Figure 4.9: A - SEM image of igneous rock fragment in interstitial material. B - Overview of Dmm.

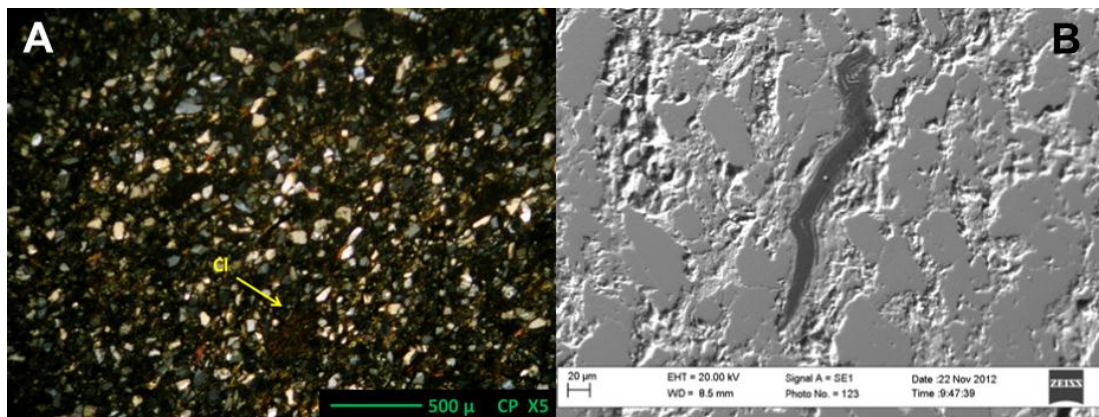


Figure 4.10: A - Overview of Smc with chlorite (cl) grains. B – SEM image of folded carbon streaks in Smc.

The mineralogy suggests a subaqueous environment due to the presence of calcite in the muddy matrix. The precipitation/cementation of calcite in the matrix is strongly associated with the circulation of seawater in shallow marine sediments or shallow depth meteoric waters (Carozzi, 1993).

Smc was transported and deposited in a similar manner as Dmm, although flow was non cohesive, hence the ability to carry only a few granules. The carbon bands suggest the compaction/diagenesis of organic matter.

The sediments of Facies C were transported via a subaqueous debris flow due to slope failure in shallow marine waters. As the debris flow progressed down slope it was diluted to a more non-cohesive flow depositing suspended sediments related to the debris flow deposits.

4.5 Facies D

4.5.1 Description

Facies D is represented by a gravelly sandstone (SI) which can be found at Volstruisleegte and Miller. It is generally light brown in colour weathering to dark brown, with an exception at Volstruisleegte where it has a more whitish appearance with pink weathering patterns. The outcrop varies between 15 - 20 m, except at Miller where only 68 cm is visible. The bed thickness is between 4 - 36 cm and is parallel and discontinuous, with sharp and distinctive bed boundaries. Structurally lateral low angle open folds with slickenside structures are present. Lineation/grooves on the bedding planes which are parallel to the folding axis, caused by deformation, are also visible (Fig 4.11). It is continuous to discontinuous along strike and varies from 3cm - 15cm apart to very small wavy lineations, which is occasionally perpendicular to larger lineations. Smaller structural features include small veinlets and joints, which are mostly perpendicular to strike. Sedimentary structures show lower plane bed lamination which is defined by the variation in colour of lighter and darker layers and varies in grain size, where the darker material is of a finer texture. They are spaced between a few millimetres to centimetres apart. The lamination is made visible due to brown iron oxide stained bands and white coloured bands (Fig 4.12). There are granular to pebble size clasts (1mm - 1cm) scattered over and inside the bedding planes (Fig 4.13). The pebbles show some vague lineation where they are concentrated in bands parallel to the lamination,

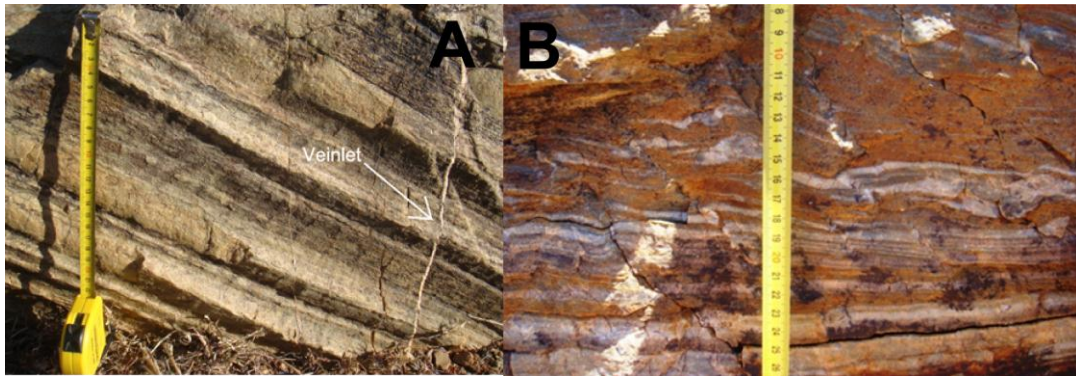


Figure 4.11: A - Grooves on bedding planes of Sl. B - Folding banded layers of quartzitic unit Sl.



Figure 4.12: Low angle planar lamination in Sl. Note the alternating white quartzitic and brown (iron oxide stained) bands defining the lamination.

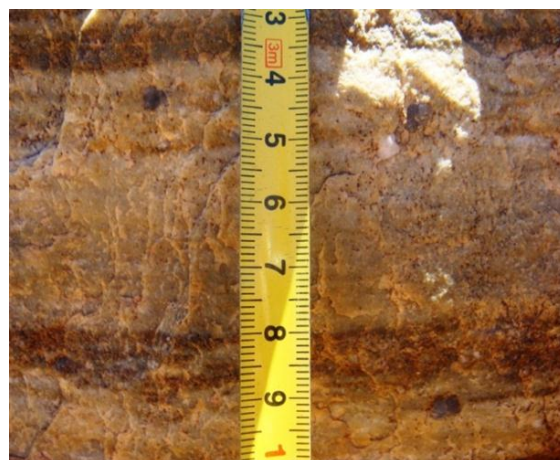


Figure 4.13: Pebbles in bedding.

but seem mostly randomly orientated. The sandstone has a mean grains size between medium and coarse sand (1%g; 5% vcs; 63% cs; 37% ms; 16% fs; 4 % sl +cl). The grains are angular to subrounded and very well sorted. All grains are randomly orientated (no fabric) and are grain supported (concavo-convex grain contacts). Mineral composition is composed of 97% quartz (monocrystalline and rarely polycrystalline), which show straight, wavy and undulosed extinction, rutile inclusions, as well as 1% lithic and chert rock fragments (Fig 4.14). The matrix (<30 μ) consist of quartz, biotite and very small amounts of zircon, garnet, apatite, rutile and chromite. Horizontal lamination is defined by similar sized quartz grains orientated parallel to lamination, as well as finer matrix sized grains (quartz, biotite and clay). The lithic rock fragments (very coarse sand to pebble size) are randomly distributed and orientated (Fig 4.14).

4.5.2 Interpretation

The distinctive layering, lineations, grooves and folding formed from unconsolidated sediment deformation prior to lithification. This sediment deformation could be related to glacial interaction with underlying sediments. Bell (1981) suggested that the deformation may have occurred when the sediments became frozen to the base of overlying ice sheet and deformed together with the ice. The same deformational features are also supported by gravitational slumping (Woodcock, 1976; Bell, 1982). This is the result of subaqueous slope failure caused by melt water from grounded glacier and it may also trigger debris flows.

The facies was deposited via hyperconcentrated density flows (Mulder, 2001) due to its poor sorting, random orientation of grains and angular to rounded shape. Although this type of density flow is non-cohesive it has the ability to support minor larger gravel sized clast due to the strong grain-to-grain collision. Hyperconcentrated density flows are closely associated with debris flows (Facies C). The discontinuous yet parallel geometry, thinning of beds and interbedded debris flow deposits is expected in a subaqueous slope environment where slope failure has occurred.

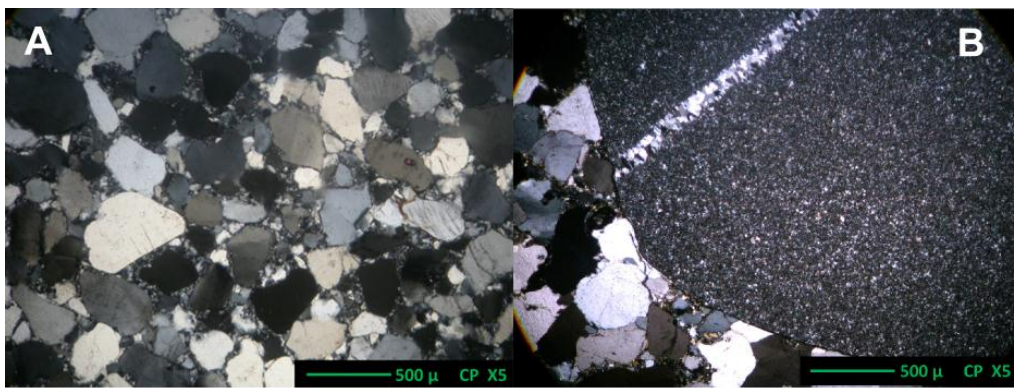


Figure 4.14: A – Overview of sandstone Sl. B - Lithic rock fragment in Sl.

4.6 Facies E

4.6.1 Description

Facies E consist of fine sand to silty rippled mudstone (Frc) which is only present at Mille and Swaylands. It makes an outcrop of 4m and can be identified by its greenish dark grey colour which weathers to a greenish light grey. The bed thickness seems to be about 2cm – 5cm, which show strong cleavage presenting outcrop to be very “flaky” (Fig 4.15). No structural features are visible. Sedimentary structures include ripple cross lamination in beds and ripple marks on the bedding planes (Fig 4.16). The ripple cross lamination is emphasized by lamination alternating between dark (fine sand) and light coloured (silt/clay) material with a thickness of 1mm-2mm. The lamination is wavy and non-parallel, but in some places it is wavy/lenticular and discontinuous, suggesting that the lamination was disrupted or deformed (possibly due to soft sediment deformation). Slightly folded and deformed organic carbon streaks are present in silt and clay layers (Fig 4.17). Lenticular lamination is also visible due to lenses of fine sand being surrounded by silt and clay, and only clay layers (Fig 4.18.). No certainty of paleocurrent since ripple marks is not clearly defined and seems to overflow each other (interference ripples). It consists mostly of very fine grained sand (30% fs; 40% sl; 30% cl) which vary from subangular to subrounded in shape. All sand and a portion of silt size grains consist of monocrystalline quartz with no inclusions and straight extinction. The rest of silt size grains are composed of k-feldspar. The matrix (<30 μ), which is 40% of whole rock, consist of 5% biotite, 15 % smectite and <1% rutile. Lamination is defined by variation in grain size. All fine silt and clay size material forms the fabric which is orientated parallel with the lamination.

4.6.2 Interpretation

The ripple cross lamination and lenticular lamination in this facies suggests that the silt, clay and sand sediment was deposited rapidly during the migration of current ripples. Deposition occurred via traction transport with some deposition via suspension (Potter, 1980) during episodes of high velocity conditions, such as periodic flooding.

The occasional soft sediment deformation disrupting lamination represents down slope shear due to gravitational instability (Allen, 1982). Thus Facies E was most likely deposited in a subaqueous shallow marine environment exposed to rapid changes in energy, and small scale slope instabilities e.g. alternating periods of current activity in tidal processes.



Figure 4.15: Outcrop of Frc indicating ripple marks with strong interference of cleavage.

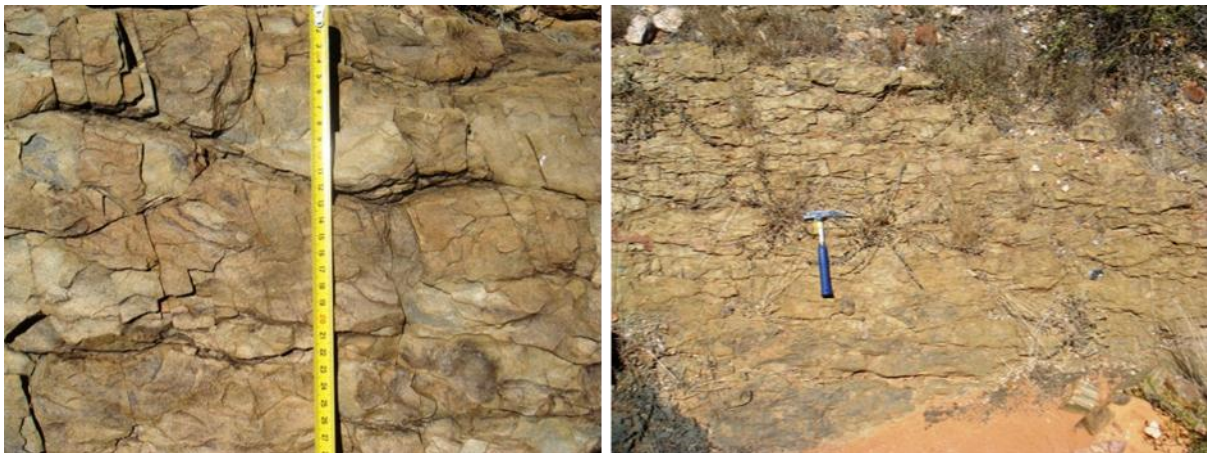


Figure 4.16: Ripple marks on bedding plane of lithological unit Frc.

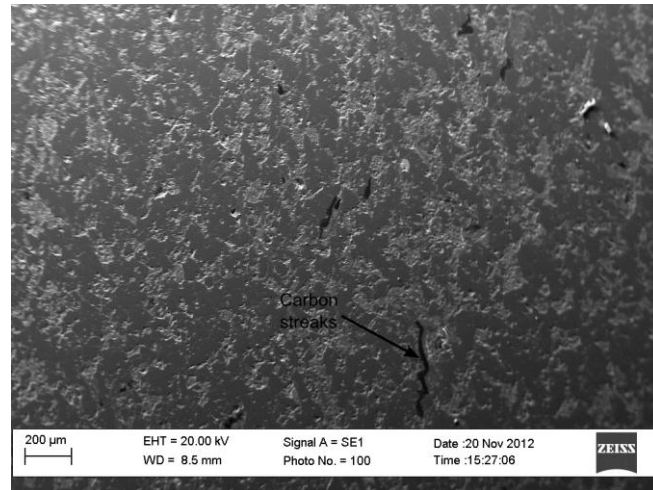


Figure 4.17: SEM image indicating organic carbon streaks in between matrix of Frc.

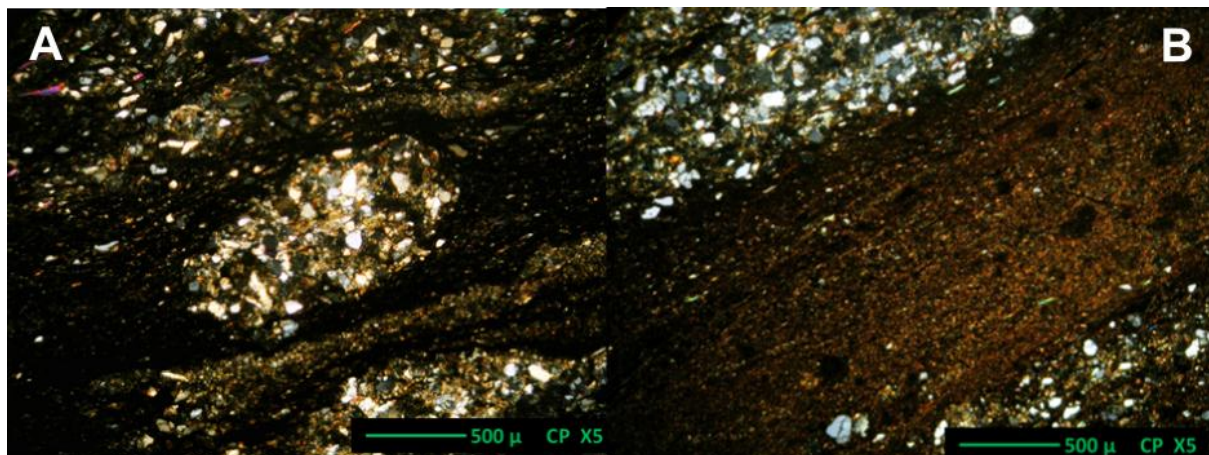


Figure 4.18: A - Lenticular lamination of fine sand/silt lenses surrounded by clay in Frc. B - Close up of clay (Illite) layer in Frc.

4.7 Facies F

4.7.1 Description

Facies F is represented by a massive sandstone (Smr) and a laminated sandstone (Slr) separated by sharp erosional contact. This facies is only present at Swaylands.

Smr is dark in colour and has a gravelly texture. The only structural features visible are a few quartz veins cutting perpendicular through beds. The outcrop width is 0.5 m, which is also the bed thickness since only one discontinuous bed is visible. Only on the surface bed plane there is a mixture of pebbles (1mm – 5mm) in no preferred orientation covering the face (Fig 4.19). For the first 5cm inside the bed, from the surface plane, the same pebbles can be seen, but they then grade into a structureless bed with no coarse grained pebbles (Fig 4.20.). Asymmetrical interference current ripple marks are also present on the bedding plane. Depositional structures present, in the first 5 cm of bed, are trough cross lamination which are defined by two light and dark layers with the pebbles/granules mostly restricted to the darker layer. Smr is poorly sorted with a mean grain size of coarse to fine sand (40% cs; 57% fs; 3% sl + cl). Grain shape varies from subrounded to angular with grain contacts being concavo-convex. Coarse grains are mixed with medium sand and medium to fine sand (Fig 4.21). The mineral composition consists of 98% mono – and polycrystalline quartz, which show straight, wavy and undulosed extinction as well as biotite and rutile inclusions. The matrix (<30 μ) consists of quartz, chlorite and biotite. Heavy minerals include garnet, magnetite and rutile.

Slr is a light brown sandstone which weathers to a medium to light brown colour. The outcrop in the riverbed is 5m wide, with the individual beds ranging from 1 cm to 6 cm in thickness. Beds are parallel and continuous. The only structural aspects observed are a few quartz veins running perpendicular to strike. Depositional structures present are low angle planar lamination within the beds (Fig 4.22). On the surface of the bedding planes are small bumps or very small ripples which could be either adhesion ripples (Fig 4.23) or another kind erosional structure, hence the erosional contact between Smr and Slr. Slr is composed of well sorted medium sand (97% s; 3% sl + cl). Grains are angular and more elongated than round in shape, with sutured grain contact relations (Fig 4.24). Signs of fabric are defined by long axis of grains orientated parallel to each other, which are responsible for the planar lamination observed in field outcrop.



Figure 4.19: Mixture of pebbles on the surface bedding plane of Smr.



Figure 4.20: Sample of Smr indicating the abrupt change in grain size from fine grained (below line) to coarse grained (above line). Arrow indicates "way up" of bedding.

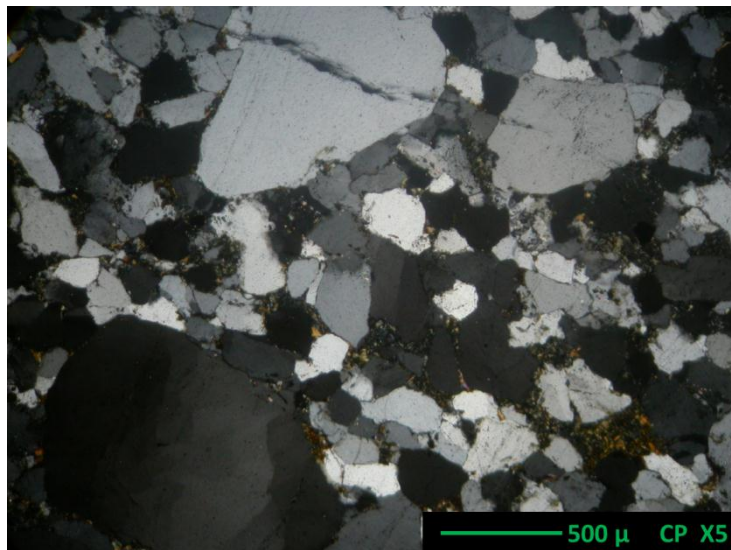


Figure 4.21: Overview of gravelly quartz arenite Smr showing coarse sand grains surrounded by fine sand size grains.



Figure 4.22: Beds of Si r showing low angle horizontal lamination.

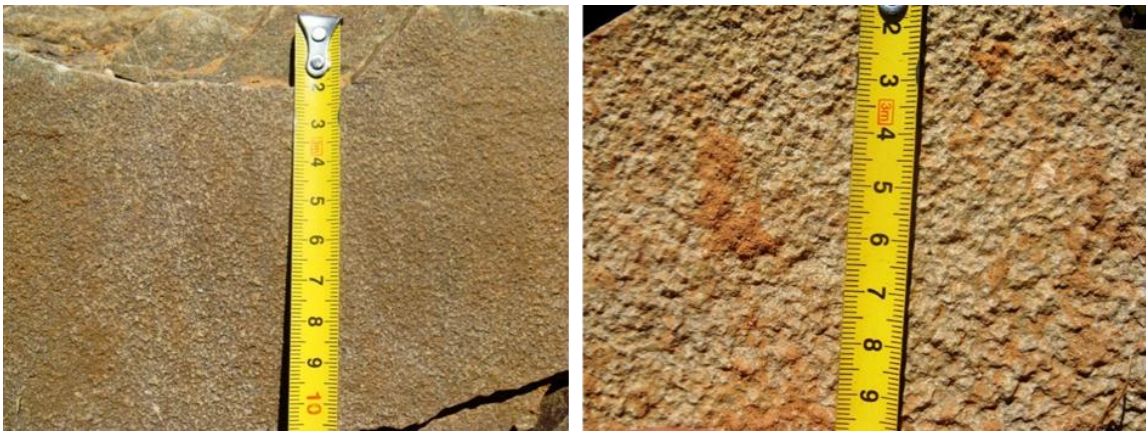


Figure 4.23: Bedding plane of Si r indicating small adhesion ripples.

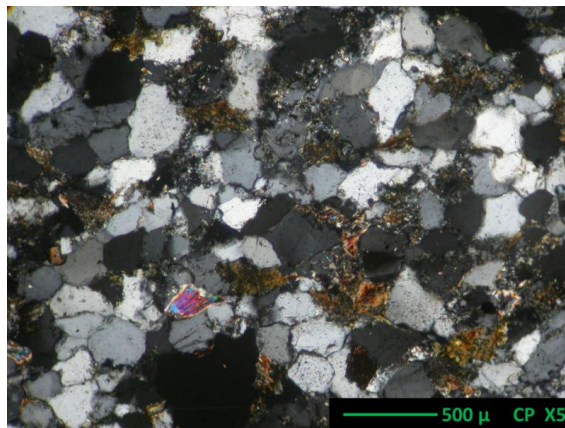


Figure 4.24: Overview of quartz arenite Si r showing quartz with chlorite cement.

Mineral composition consists of 97 % mono – and polycrystalline quartz, which show straight, wavy and undulosed extinction as well as garnet and rutile inclusions. The quartz grains are cemented together by chlorite (3%). Other heavy minerals present include rutile, garnet, apatite and zircon.

4.7.2 Interpretation

The massive structure of Smr suggests a deposition of sand size sediment through rapid suspension and the lack of traction. This explains the angular to subrounded grain size and poor sorting. The 5 cm gravelly section is evidence of a reworked surface moved by the interference current ripples on the surface plane of Smc. This could be due to high energy stormy conditions.

Slr was deposited with lower energy and traction transport than Smr. The laminated beds represent periodic sedimentation events. The adhesive ripples develop when wind is blown over a damp surface and is usually seen in a sandy beach or inter tidal flats (Allen, 1982)

Due to the limited outcrop at Swaylands the geometry of the facies is difficult to determine, and it is thus speculative. It is apparent that though Smr overlies Slr disconformably and is discontinuous. This Facies was deposited during episodic events of fluctuating energy and sediment supply, found in beach and tidal flat environments with partial subaqueous and subaerial exposure.

4.8 Facies G

4.8.1 Description

Facies G is represented by a white quartzitic sandstone (Smq), which is structureless. Vague appearance of low angle cross lamination is visible although due to the quartzitic nature it is difficult to identify. This facies is only visible at Swaylands. The outcrop is about 7m wide, but the unit is most likely thicker since parts are covered in vegetation. Bed thickness varies between 50cm – 70cm and is parallel and continuous with each other. It is a sandstone which consists of fine to coarse grained sand, with dominantly medium to coarse sand (80%). Grains are subrounded to subangular in shape and have concavo-convex contact relations with each other. Smq is grain supported with all grains randomly orientated. The mineral composition is composed of 99% monocrystalline quartz (a few polycrystalline

grains), with straight – and occasional undulosed extinction. Quartz shows process of quartz overgrowth and pressure solution (4.25). Other heavy minerals (<1%) are present as individual grains and inclusions such as rutile, zircon and Ilminite.

No fossils are present in this facies. No paleocurrent indicators are present.

4.8.2 Interpretation

Due to the very distinctive quarzitic nature of Facies G, most of the sedimentary structures in this outcrop have been overwritten. Massive and slightly low angle cross lamination indicates deposition under low energy conditions via traction transport. With almost 100% quartz composition and associated heavy minerals it can suggest beach sand deposits.

4.9 Facies H

4.9.1 Description

Facies H is represented by a massive siltstone (Fm), and a deformed mudrock (Fdp). Both Fm and Fdp are present at Swaylands only.

Fm is a medium brown siltstone. There are no signs of sedimentary structures, though there are, at the basal part of the unit, calcitic nodules (1cm). It is a moderately sorted siltstone (80% sl; 20% cl) with angular to subrounded grains. Silt size grains are in point contact with each other and show no preferred distribution or orientation (Fig 4.26). Mineral composition is composed of all silt size grains as monocrystalline quartz with straight and wavy extinction. Matrix consists of smectite and some heavy minerals, zircon and rutile.

Fdp is a yellowish brown mudrock unit, which show some significant changes throughout the profile with regards to grain size and sedimentary structures. Sedimentary structures include cross lamination, horizontal lamination, carbonate bands, lenticular lamination, through cross bedding, slumping and soft sediment deformation (Fig 4.27, Fig 4.28). Occasional calcitic nodules are also present (Fig 4.27). The grain sizes vary constantly between silty mudrock to clay-rich, back to a sandy siltstone and then extremely clayish mudstone. This mudrock consists of 50% silt size and 50% clay size grains. Grain shape varies between

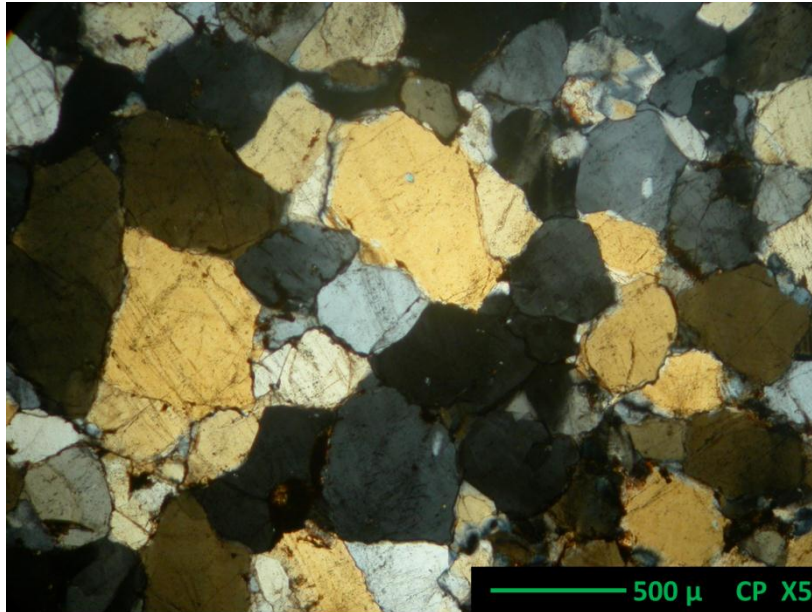


Figure 4.25: Overview of Smq quartzite indicating pressure solution and quartz overgrowth .

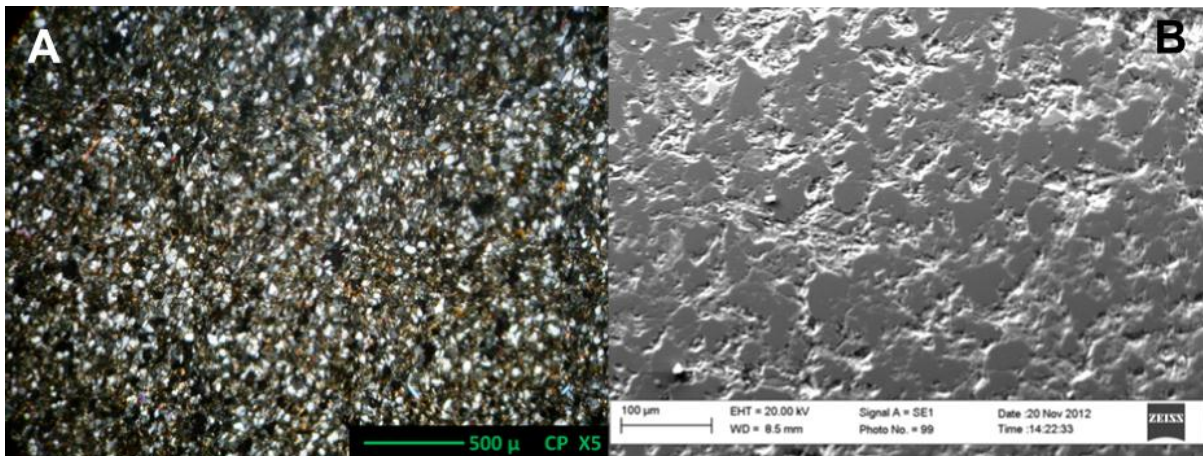


Figure 4.26: A - Overview of Fm. B - SEM close up image of Fm showing random distribution of silt grains.

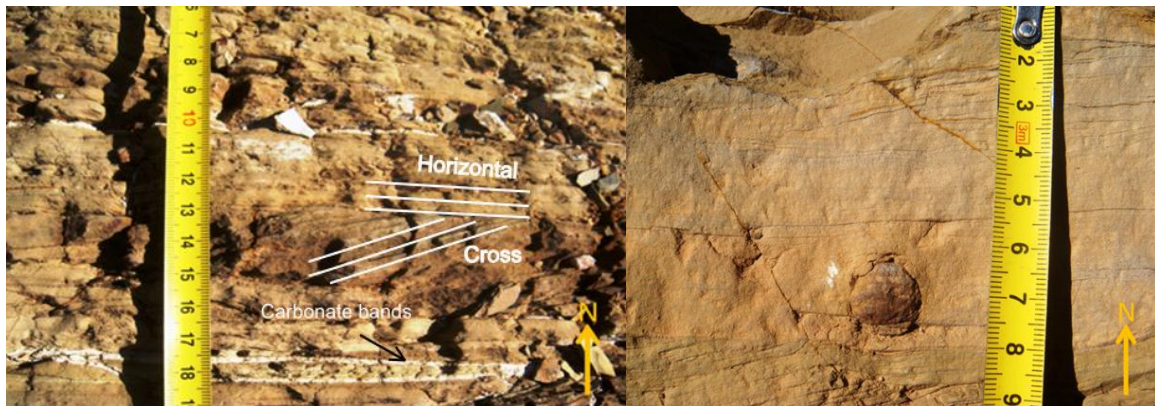


Figure 4.27: Left - Horizontal - , cross lamination and carbonate bands in Fdp. Right - Nodule in Fdp.

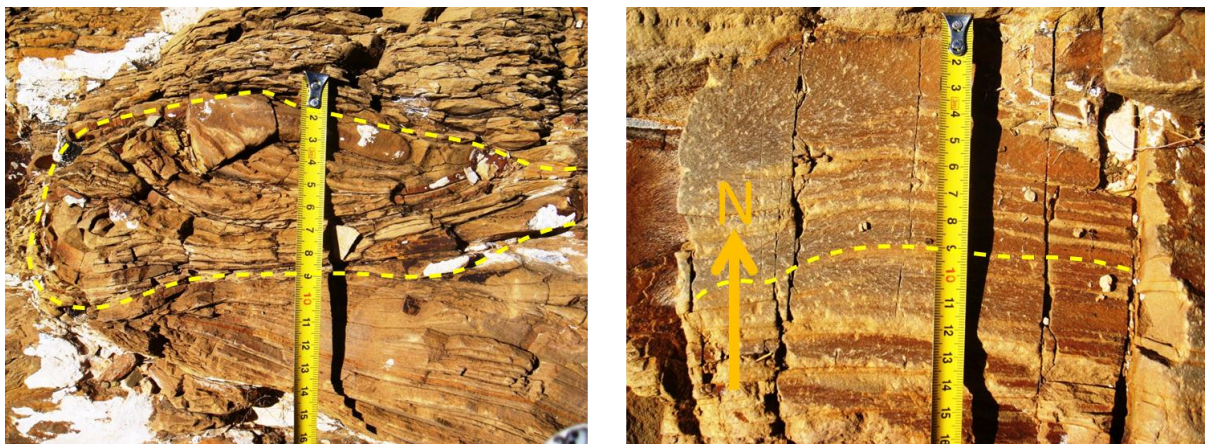


Figure 4.28: Left – slumping in Fdp; Right – distorted horizontal lamination.

subangular to subrounded grains. Grains that are elongated are orientated with their long axis parallel to the fabric. Silt size grains seem to be suspended in clay. Mineral composition is composed of quartz (all silt size grains), muscovite, biotite, rutile, feldspar, smectite and calcite (Fig 4.29).

4.9.2 Interpretation

The change in sedimentary structures from cross -, horizontal -, lenticular - to trough cross lamination and grain size (clay: silt) represents episodic periods of high and low energy deposited through suspension. The interbedded carbonate layers between the muds suggest that sedimentation may have seized periodically, allowing for the precipitation of carbonatic material. This precipitation is possibly due to the circulation in a saline water body or by suspended carbonatic material sourced from adjacent environment. Sediment instability or slope failure can be assigned to the variations of sediment deformation. It is thus suggested that Facies H represents an inclined slope environment exposed to fluxuations in sedimentation rates.

4.10 Facies I

4.10.1 Description

Facies I is represented by a rippled mudrock (Frt), laminated calcareous mudrock (Flp) and a fissile mudstone (Ffb). Both Frt and Flp are located at Campherspoort.

Frt is a brown to greyish rippled mudstone. Visible outcrop extends over 40 m. The bed thickness alternates between thin (10 cm) and thick (36 cm) beds, with wavy and non-parallel bed boundaries. Low angle cross lamination, trough cross lamination and distorted cross lamination is made visible by alternating light and dark brown layers in the beds (Fig 4.30). The alternating layers are exceptionally visible where it seems as if it consists of fine sand to silt layers. Current ripples seem to be visible on the bedding surface with the paleocurrent being either to the East or West (due to outcrop quality it is difficult to determine) (Fig 4.31). On the bedding surface there are markings that can possibly be grazing trail marks of trace fossils (pascichnia) (Fig 4.32). There is textural variation within the beds thus two layers are identified, due to their change in grain size.

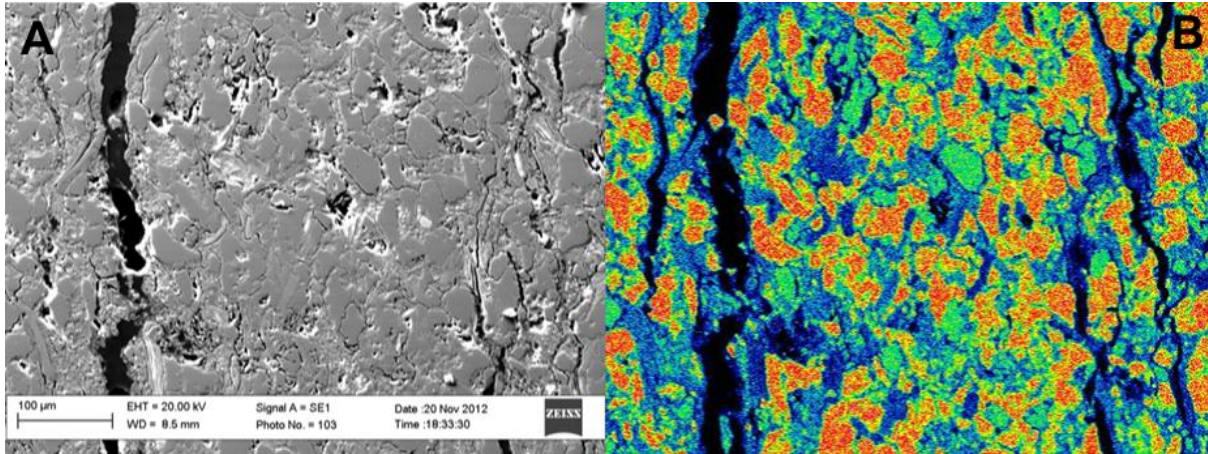


Figure 4.29: A - SEM image of Fdp showing clay grains wrapping around silt size grains. B - Mineralogy indicating silica content with bright orange colours being quartz grains. Green and blue and black are lower levels with black being the lowest.

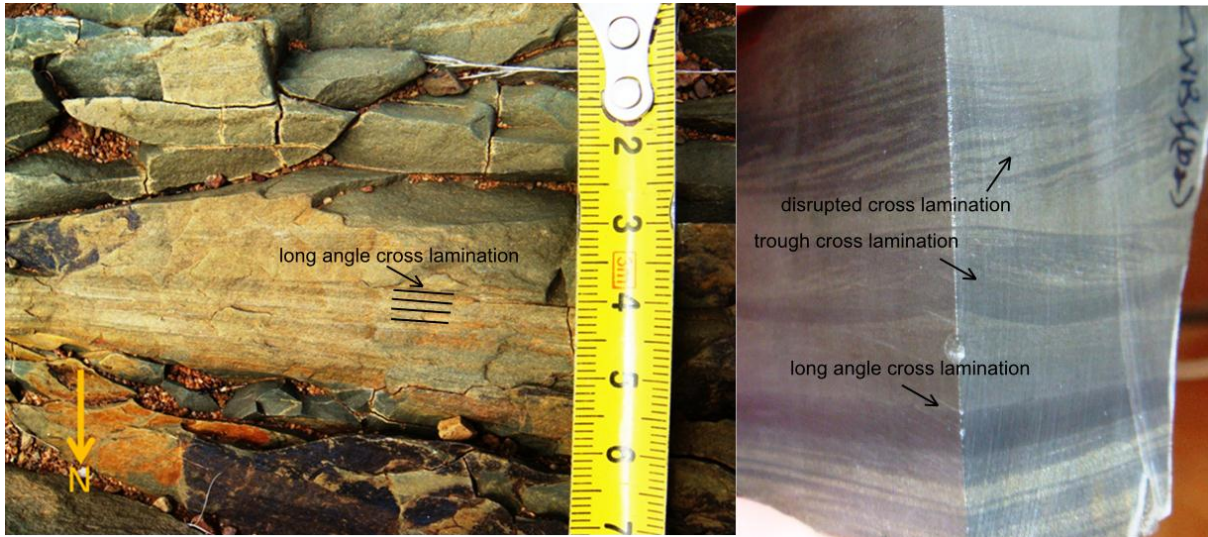


Figure 4.30: Depositional structures in Frt.

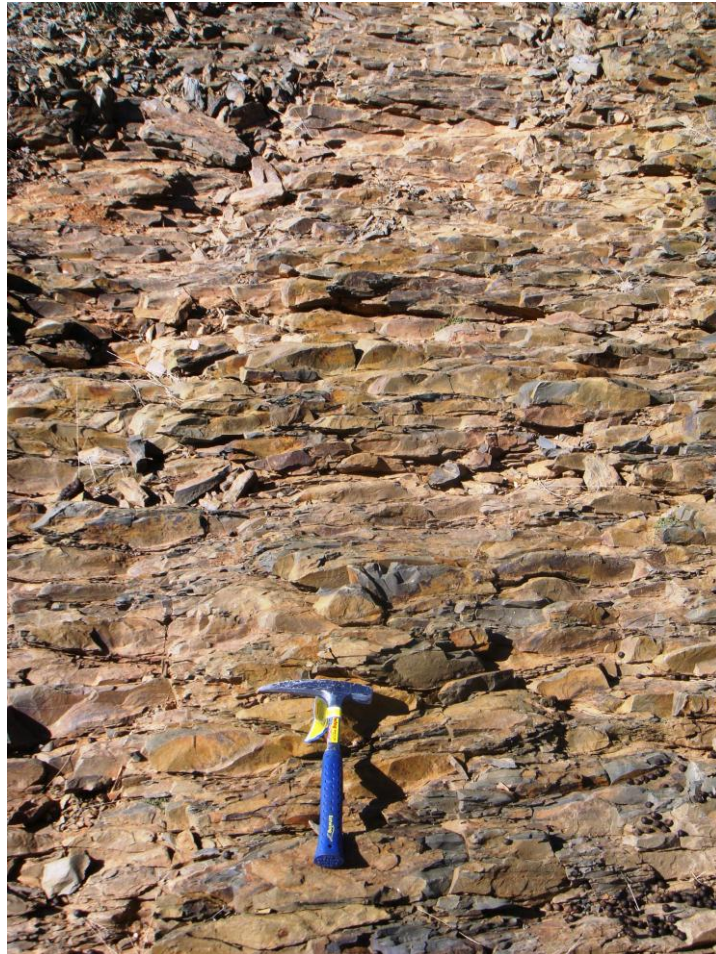


Figure 4.31: Outcrop of Frt showing asymmetric current ripples on surface plane.



Figure 4.32: Surface marks (grazing trail marks) on bedding plane of Frt.

Layer 1 consists mainly of fine sand size grains with some silt, whereas layer 2 mostly has silt-size grains with a little fine sand. The layers alternate and vary in thickness throughout different parts of the outcrop. Layer 1 is composed of 70% silt and 30% clay. The grain shape is angular to subrounded. Lamination is visible due to alteration between orientation of silt and clay size grain. The mineral composition is composed of barite, apatite, quartz, chlorite, biotite rutilite and k-feldspar. Layer 2 has more clay (40% sl; 60% cl) and has larger silt size grains. Lamination is defined by variation in silt and clay size grains, with elongated clay minerals orientated parallel to lamination. Mineral composition is the same as Layer 1, except that there is no feldspar or calcite present.

Flp is a 6m outcrop that consists of 3 alternated layers (1, 2 and 3), which all have different colours, composition, grain size and range between 10cm – 20 cm in thickness (Fig 4.33). Boundaries between these layers are sharp and continuous. Layer 1 is dark grey, with dominantly silt size grains (50% sl; 50 % cl), whereas layer 2 is black with a finer clayish texture (10% sl; 90% cl) and layer 3 is white calcitic. The layering does not continue in a specific order. Layer 1 and 2 are more dominant with the occasional layer 3 in between. No other sedimentary structures are clear due to the nature of the outcrop. The mineral composition of layer 1 consists of smectite, biotite, chlorite and quartz. Layer 2 has a similar mineral composition, except less quartz and no calcite. Layer 3 consists of a 100% clay size grains which is dominantly calcite in mineral composition, with small amounts of quartz and biotite.

Ffb is a fine grained black mudstone, which is easily identified by its fissile texture and "pencil like" cleavage. The outcrop is 4m wide and seems to be parallel and continuous in geometry. The bed thickness is 5mm with sharp boundaries between beds. Due to fissile texture it is difficult to determine what sedimentary structures are present, but it seems to be horizontal lamination, with occasional bioturbation. Flame structures are also present between finer and coarser grained material (Fig 4.34). The shale consists of 80% clay and 20% silt. Grains are well sorted, angular and needle like in shape. Main mineral composition is smectite/illite, chlorite, biotite and quartz (restricted to silt size grains).

4.10.2 Interpretation

Sedimentation of Frt occurred via traction with episodic changes in high to low energy, presented by the alternation of low angle cross lamination to trough cross lamination. The distorted cross lamination suggests possible sediment instability. Shallow water levels are

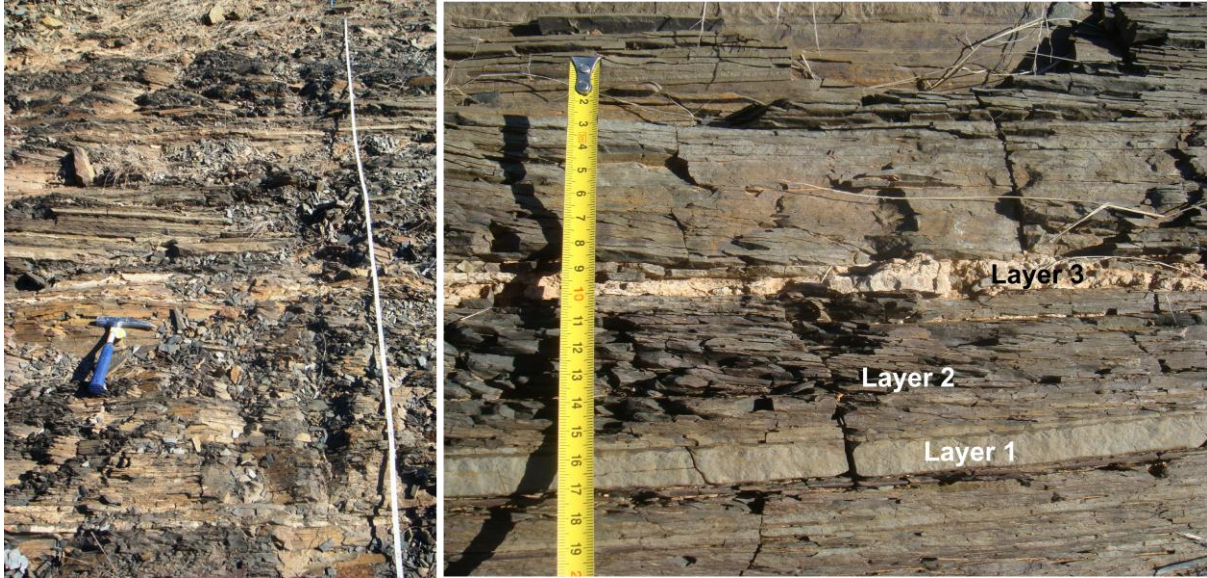


Figure 4.33: Left - Outcrop of Flp. Right – Close up view of alternating layers 1,2 and 3.

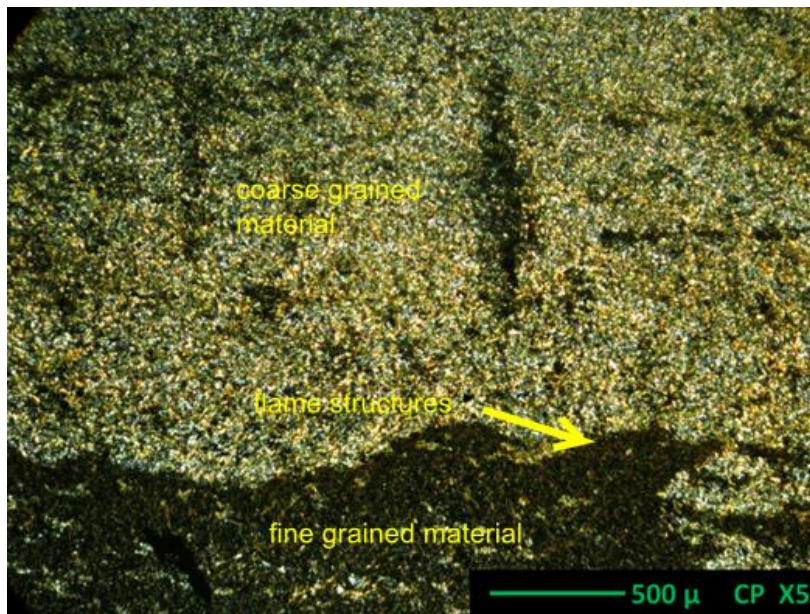


Figure 4.34: Flame structures in mudstone Ffb, with bioturbation.

assigned to formation of current ripples on the surface (Tye et al., 1989). The trace fossil grazing marks is also a clear indication of a shallow water environment.

The layering of Flp is due to change in sedimentation rate influencing change in transport via suspension. The interbedded carbonate layers between the muds are similar to those interpreted in Facies H.

The horizontal lamination represents sedimentation from suspension in relatively quiet water, where bottom currents are weak and mud was deposited in a quiet subaqueous environment (Potter et al., 1980). This suggests that Ffb was deposited in a distal, but shallow subaqueous marine/pro-delta environment.

Facies I represents a succession of shallowing sedimentation from a more distal quiet environment (marine prodelta) to a shallow active subaqueous setting with episodic changes in sedimentation and energy (lower delta front)

4.11 Facies J

4.11.1 Description

Facies J is represented by laminated sandstone (Slm) which is only present at Campherspoort. Slm is a medium to fine textured sandstone unit. The outcrop width is about 40m and the beds, which have sharp boundaries and are parallel and continuous to each other, alternate in thickness from 14cm – 57cm,. There seems to be an alternation between low angle cross laminated beds and massive beds (Fig 4.35). Massive beds show no internal structures, with no evidence of diagenesis or bioturbation, which could have destroyed any signs of internal structures. Low angle planar lamination is prominent in some beds (Fig 4.36). Small nodules are occasionally present, but are very scarce. The nodules vary in size from 5mm – 1 cm. Slm is a moderately sorted sandstone (20% ms; 77% fs; 3% sl + cl) with angular to subrounded grains. Grain contacts are concavo-convex and grains show no significant fabric or lamination. All grains are randomly orientated and distributed (Fig 4.37). Mineral composition consists of 50% quartz, 10% chert, 30% feldspar (k-feldspar and microcline), 1% biotite and 9% heavy minerals (garnet and sphene). The quartz is mostly monocrystalline with occasional polycrystalline grains. The extinction is straight with occasional wavy and undulosed. Garnet (almandine and pyrope) grains range in size from sand to silt, with occasional quartz inclusions.



Figure 4.35: Low angle cross lamination (bottom, CL) and massive bed (top, M) in SIm.



Figure 4.36: Low angle planar lamination in SIm.



Figure 4.37: Overview of SIm.

4.11.2 Interpretation

The sedimentation of Facies J occurred via low velocity suspended load transport (low angle planar lamination), although occasional higher transport rates were present (massive bedding). This is based on the assumption that the massive beds through single high energy sand suspension event due to the lack of internal structures. The nodules in this facies suggest the calcification of some or other organic matter. Although the outcrop is very extensive (stretching over a few kilometres) it is not very wide. It can be assumed that Facies J represents a subaqueous sheet-like sand body influenced by distal channel flow.

CHAPTER FIVE

FACIES ASSOCIATIONS AND MODELS

5.1 Facies associations

The sedimentary facies that were outlined in the previous chapter, together with the investigation of (1) the mechanism/energy responsible for the transport and deposition of the facies, and (2) diagenetic processes that the facies have undergone (to distinguish between syn – and post depositional information), will provide information to define related facies associations (Table 5.1). This provides a review of the depositional sub-environments. Figure 5.1 provides an overview of the spatial orientation of facies associations of the stratigraphic profiles at each location. Do note that the scale of each profile varies. For detailed view of profiles refer to Fig 4.1.

5.1.1 Distal glacio-marine deposits (FA1)

This association is represented by facies A and B. FA1 is present at all four locations (Volstruisleegte, Miller, Swaylands and Campherspoort) and overlies all the other facies associations (Fig 5.1). This makes it an extensive and large scale association (especially facies A), since the distance between Volstruisleegte and Miller is about 80 km. The boundary between facies A and B (where it is visible) is sharp and conformable (Fig 5.2).

FA1 can be interpreted as a distal indirect glacial marine environment as described in chapter 2. Facies B represents the distal marine environment which was deposited by suspension settling of silt and clay, with facies A being interpreted as debris flows along the basal slope. Although dropstone features are not clear in facies A, its presence is noticed in facies B, which suggest “rain-out” deposits. The deposition of FA1 can thus be described as a distal marine environment where glacial sediments were transported from floating icebergs from a proximal marine environment. These ice rafts floated over unstratified muddy marine sediments (facies B). Individual rock fragments glacially transported sediments dropped from melting ice rafts into these muddy deposits forming diamictites (facies A). Similar facies are described by Visser (1991). The smaller scale massive sandstone bodies in facies

Table 5.1: Summary of the main features of the facies and facies associations.

Locations	Facies Associations	Facies	Facies divisions	Depositional processes	Depositional environment	Diagenic processes
Volstruisleepte, Miller, Swaylands, Campherspoort	FA1 (Glacio - marine rain-out deposits)	A	Dcm	Cohesive debris flow, en-masse deposition, sediment "rain out"	Subaqueous, indirect glacial environment with floating ice bergs. Steep wall channels depositing sand bodies.	Recrystallization of calcite; Chlorite - low grade metamorphism
Volstruisleepte, Miller, Swaylands			Sm	Rapid traction transport, lightly reworked sediment		Shallow burial; Chlorite - exposure to low grade metamorphism
Volstruisleepte, Miller		B	Ffd	Episodic deposition from suspension with occasional bottom current action	Subaqueous, quite marine/prodelta environment	Compaction (fissility)
Volstruisleepte, Miller	FA2 (Proximal slope deposits)	C	Dmm	moderate to weak cohesive debris flow, en-masse deposition	Subaqueous, slope failure in shallow marine environment	Recrystallization of calcite
Miller			Smc	deposition from suspension due to non cohesive flow		?
Volstruisleepte, Miller		D	Sl	Deposition from hyperconcentrated density flow. Deformation due to gravitational slumping		Shallow burial; meteoric qrtz/calcite cementation
Miller, Swaylands	FA3 (Beach barrier and tidal flats deposits)	E	Frc	Rapid deposition of migrating current ripples; sedimentation from traction with suspension	Subaqueous shallow water environment, periodic flooding possibly due to current activity in tidal processes	Shallow depth burial
Swaylands		F	Srm	Deposition from suspension and lack of traction, High energy and episodic sedimentation	subaqueous shallow waters, reworked scour channel	Chlorite - low grade metamorphism
			Slr	Low energy, episodic sedimentation through traction transport	Subaerial and subaqueous, intertidal beach sand	
Swaylands	G	Smq	Low energy traction transport	Beach sand	Shallow burial metamorphism destroyed all sedimentary lamination (qrtz overgrowth)	
Swaylands	FA4 (Delta front and prodelta deposits)	H	Fm	Suspension sedimentation controlled by episodic events with changes in energy. Deformation due to slope failure	marine slope environment	Calclitic nodules - compaction
			Fdp			Nodules due to burial (shallow); circulation of sea water - precipitation of carbonate bands
Campherspoort		I	Frt	transport via suspension of episodic sedimentation in a low to high energy environment	marine shallow water, delta front	
			Ffp	Transport via suspension and alternating sedimentation rates	marine shallow water, lower delta front	Circulation of sea water - precipitation of carbonate bands; low grade metamorphism - chlorite
			Ffb	Low energy suspension sedimentation	Marine , prodelta	Compaction (fissility)
Canpherspoort		J	Slm	Suspension, sediment loading, low energy	subaqueous shallow waters, fan sand body close to channel	Calclitic nodules - compaction

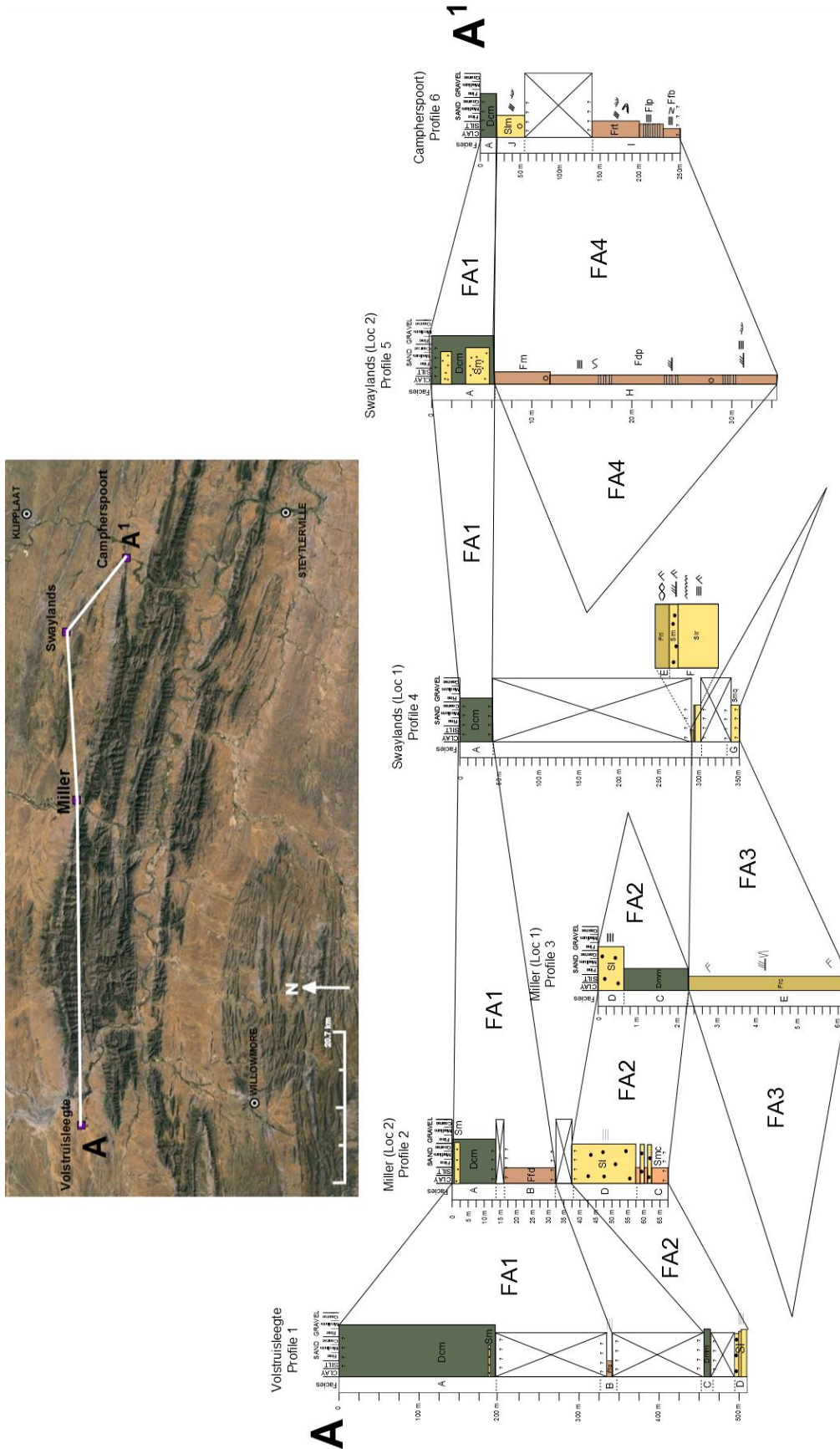


Figure 5.1: The relations between the facies associations over the stratigraphic profiles at all four locations. Please note the difference in scale for each profile. Profiles can be viewed in more detail in Fig 4.1

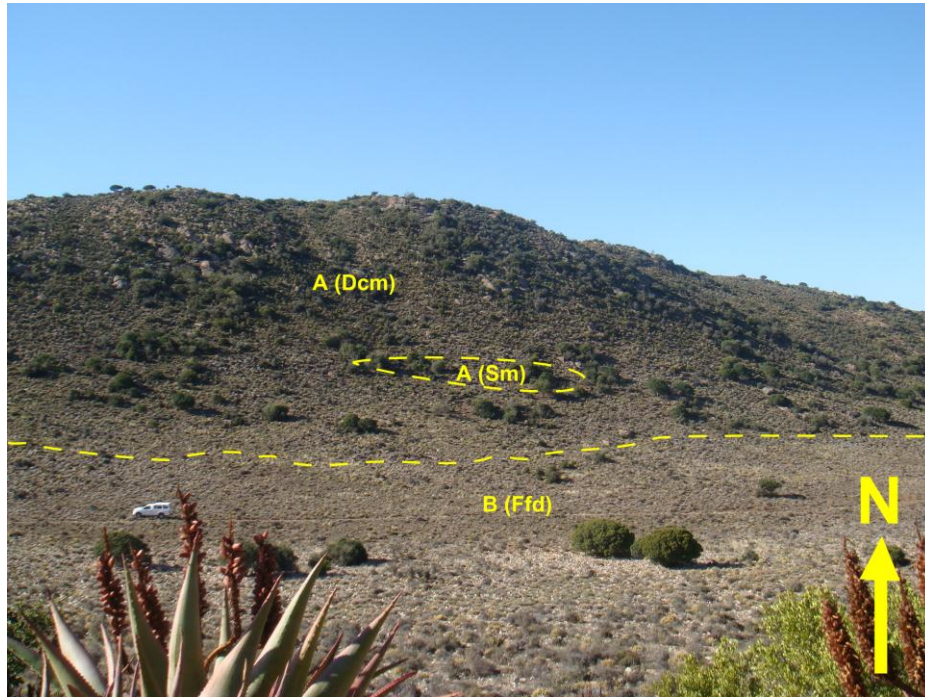


Figure 5.2: Estimated boundary relation between facies A and B at Volstruisleegte.

A represent possible reworked sediment due to wave/wind shear currents or turbidity currents which can co-exist with subaqueous debris flows (Eyles *et al.*, 1985).

5.1.2 Proximal slope deposits (FA2)

This association is represented by facies C and D and underlies FA1 at Volstruisleegte and Miller (Fig 5.3). Facies C and D is intertongued with each other forming sharp irregular boundaries (Fig 5.4). FA2 stretches over approximately 40km between Volstruisleegte and Miller. It laterally pinches out towards the east with a decrease in thickness from approximately 80 m at Volstruisleegte to less than 2 meters at Miller (Fig 5.1). At Miller it overlies FA3 which is marked by a very distinct and sharp nonconformity (Fig 5.4).

The mixture of sediments (diamictite and silty sandstone) can be assigned to debris flow deposits due to surges along the slopes of a water body. The post deposition soft sediment deformation present in the sandstone of facies D could be responsible as the trigger for these surges due to slope failures (Woodcock, 1976; Strasser *et al.*, 2007). The debris flow deposit in the study area is relatively large in size and is laterally discontinuous, thinning outwards. According to Major (1997) there is no evidence to distinguish between en-masse deposition and multiple surges of debris flows, thus both options can be taken into consideration. The dispersed clasts associated with facies D could be due to placement of debris in sandy "levees" around surges of the debris flow deposit as described by Bridge *et al.*, 2008.

5.1.3 Beach barrier and tidal flats deposits (FA 3)

This association is a very small section of the whole study area and is defined by facies E, F and G. Facies E is laterally continuous over Miller and Swaylands. Although Profile 3 at Miller only allows exposure of facies E, the assumption is made that facies F and G, which is covered by vegetation also present and also laterally continuous over all four locations.

The evidence for tidal flat conditions is limited in the study area since it is only represented by the outcrop at Miller and Swaylands. The key aspect for assigning this association to a tidal environment is the presence of well-defined changes from flaser -, lenticular -, wavy

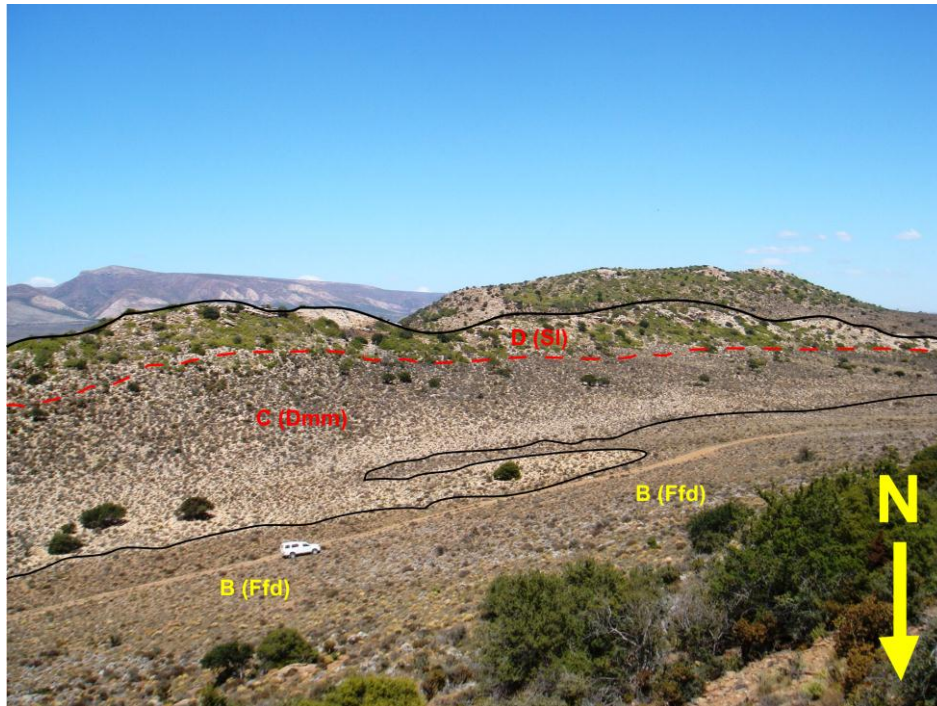


Figure 5.3: Sharp boundary between facies B and C (Boundary between FA1 and FA2). Estimated contact between facies C and D at Volstruisleegte.

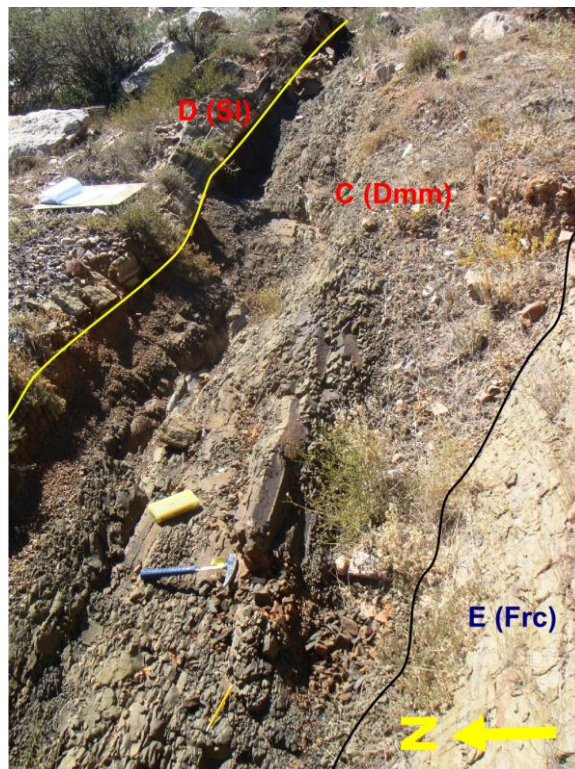


Figure 5.4: Erosional boundary between facies E (FA3) and C (FA2). Irregular sharp boundary between facies C and D (FA2) at Miller.

bedding and bimodal current ripple marks in very shallow subsurface facies E (Chakrabarti 2005; Daidu, 2013). Facies E and F form a sharp irregular surface boundary at Swaylands, which is due to the exposure of facies F to current activity (current ripple marks on surface) (Fig 5.5 and Fig 5.6). The adhesion ripples in Slr, formed when a weak wind blew over a damp surface, this suggests an environment of subaqueous conditions, partially exposed to subaerial events. Srm possibly represents an outwash surge over the sand barrier (facies G), flowing over Slr's eroded and exposed surface into the more subaqueous environment of facies F, where it is exposed to current action from the shallow tidal flats area. This is why there is a clear irregular and erosional boundary between the two, Slr and Srm (Fig 5.7).

5.1.4 Delta front and prodelta deposits (FA 4)

Facies association FA4 is represented by facies H, I and J. From the geological map and cross section in Fig 1.6 it can be seen that profile 4 was taken on the northern limb of a syncline. For the purpose of facies analysis, profile 4 in Fig 4.1 and Fig 5.1 was rotated to represent the unfolded strata that correspond with the other profiles. Figure 5.8 shows the northern limb of the syncline, with Facies A representing the centre.

Facies I is represented by the prodelta muds of Ffb which gradually grades upwards into a distal delta front environment, via alternating silt and clay layers (Flp and facies H), into coarser silty muds with a decrease in clay content (Frt). Sediments are deposited by suspension deposition with episodic changes in high to low energy, which is responsible for the formation of low angle planar beds. Due to low water levels sediments are also transported by currents forming trough cross lamination and current ripples on the surface (Tye et al., 1989). The grazing trace fossil trail marks found in facies SI is a clear indication of biological activity on the ocean floor of a shallow marine environment.

In general pro-delta muds are deposited in a low energy water body on the shelf slope. The change in composition between silt and clay layers suggest episodic periods of high and low energy due to flood variation of sedimentation supply from upper delta plain and delta front. During high energy supply silt size grains travel further down slope towards the prodelta than during low energy events when only fine clay size material are deposited. This change

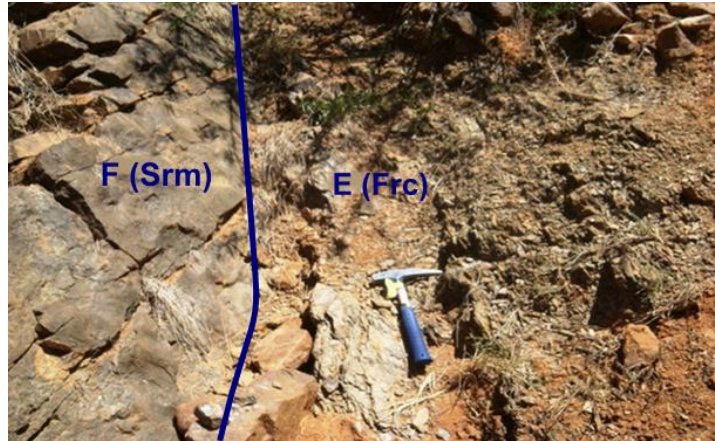


Figure 5.5: Sharp irregular surface boundary between facies E and F at Swaylands.

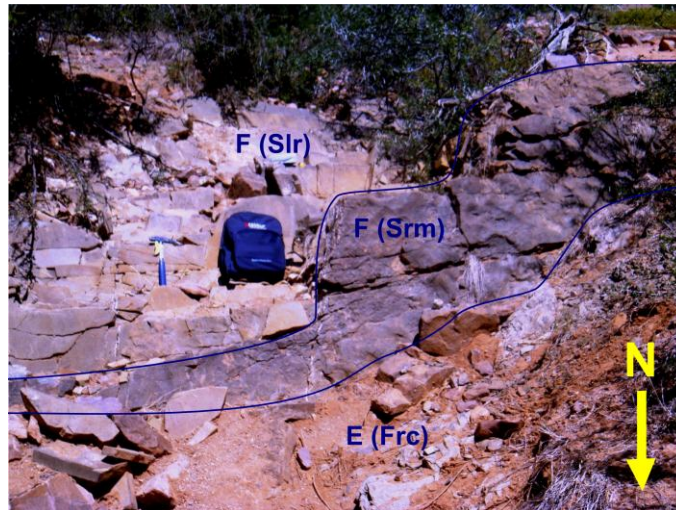


Figure 5.6: Contact relations between tidal flat facies E and F. Both boundaries are sharp and erosional.

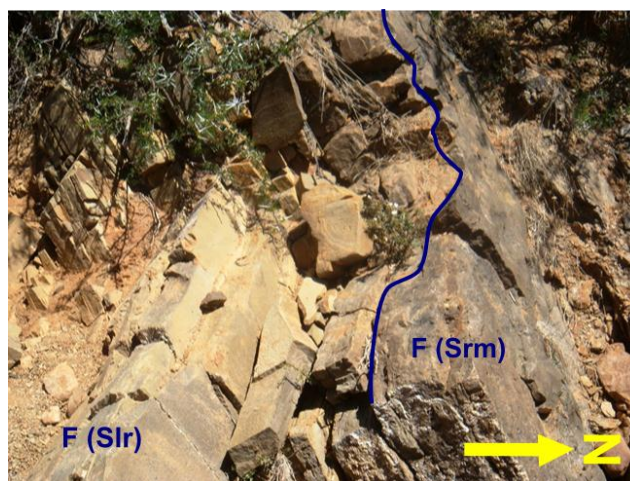


Figure 5.7: Erosional boundary surface with scours between Srm and Slr at Swaylands.

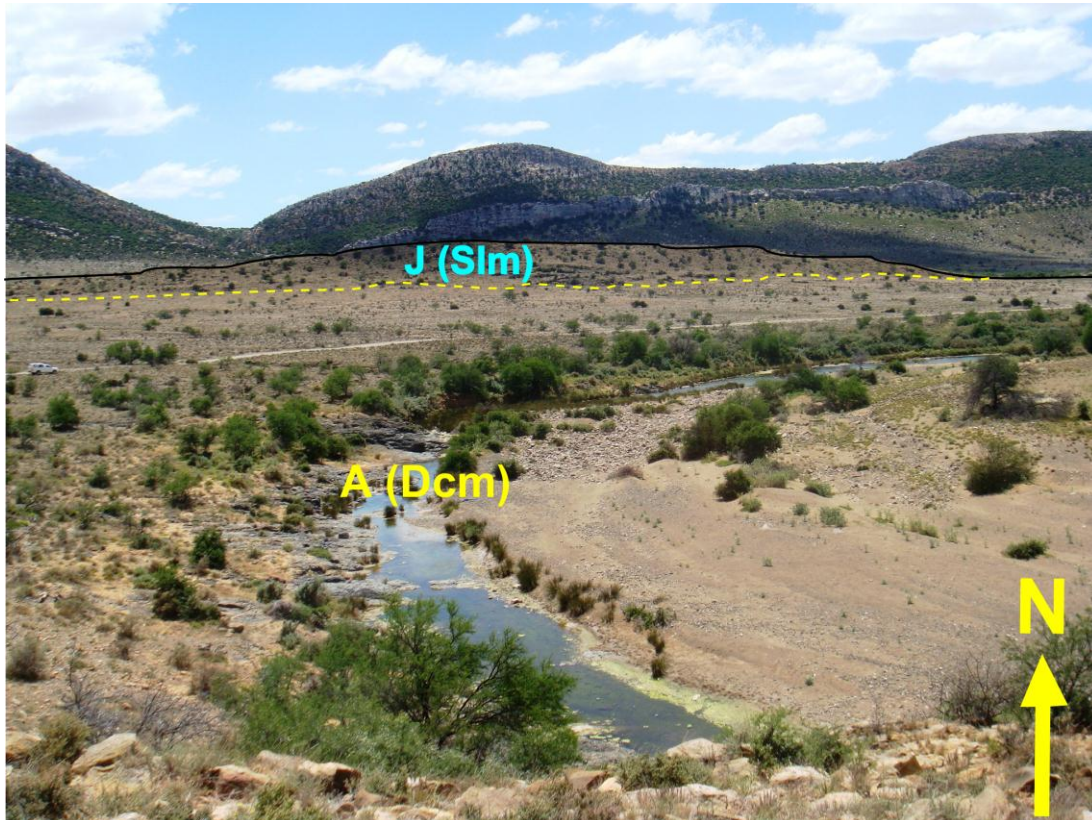


Figure 5.8: Small ridges formed by facies J with facies A on the lower edges covered by vegetation at Campherspoort syncline.

in energy in the delta front, in facies H and I, from bottom to top, is evident in the rock record due to vertical change in lamination from planar -, massive - and trough cross lamination. The soft deformation and slump structures in facies H confirm slope failure on the upper steeper parts of the slope as described by Allen (1982) and Nemec (1990). The interbedded carbonate layers between the muds suggest that silicate sedimentation may have seized periodically, allowing precipitation of carbonates in saline water. The sediment supply may have seized due to a change in the feeder system (e.g. lobe switching) which is responsible for suspended sediment supply to the prodelta.

Facies J with its lateral continuity in the area of Campherspoort can be interpreted as the lower part of the delta front which lies more distal from distributary channels, but provides sedimentation to the further parts of the delta slope.

FA4 is only present at Campherspoort and partly at Swaylands, which may suggest that FA4 pinches out and is laterally discontinuous towards the east or that there is an erosional disconformity between FA4 and overlying FA1 (Fig 5.9).

5.2 Facies model

Sedimentological data presented in the facies and facies associations are synthesised in order to gain better understanding of the depositional environment during the sedimentation of the Kommadagga Subgroup and Dwyka Group. Previous authors have debated whether sedimentation seized after the closing of the Cape Basin, which resulted in an hiatus where erosion took place before the opening of the Main Karoo Basin (Visser, 1991; Catuneanu et al., 1998; Tankard et al., 2009) or whether the Kommadagga Subgroup actually represents a period of continuous sedimentation during the closing of the Cape Basin and opening of the Main Karoo Basin thus allowing uninterrupted sedimentation (Rust, 1973; Dunley and Hiller, 1979).

The results of this study represents only a partial (western side) area of the Kommadagga sub-basin and exposure of the relevant stratigraphic units are of poor quality, because this leads to speculation of contact relations between units, it has been decided to present two facies models of the study area.

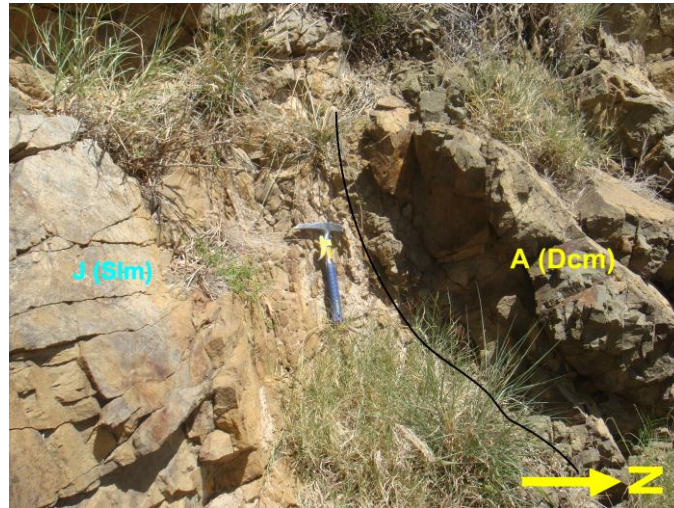


Figure 5.9: Unconformable contact between facies A and facies J at Campherspoort.

The first model will represent a continuous sedimentation cycle that does not support a hiatus between Kommadagga Subgroup deposits and Dwyka Group deposits, whereas the second model will demonstrate a break between the two groups.

5.2.1 Model 1

Kommadagga deposits represent continuous sedimentation during hiatus:

The succession of FA1 and FA2 at Volstruisleegte and Miller can be interpreted as a proximal glacio-marine environment (Fig 5.10). FA2 represents the close contact boundary where grounded glacial body, lying towards the south, is in contact with open marine waters towards the north (FA1). Ice sheet movement, which confirm movement towards the north, has been documented by Smith et al. (1993).

FA2 represents the debris flow and sediment outwash where melting took place at the foot of the glacier and formed underwater channel surges of debris. Floating ice sheets broke off from the main lobe in the south carrying debris into open marine waters towards the north, which deposited "rain-out" sediments in between finely laminated distal mud deposits (FA1). This succession suggests a period of transgression where sediment supply was limited and due to the melting of grounded ice sheets and icebergs the sea level most likely raised.

This interpretation is quite convincing if only taking into consideration the successions at Volstruisleegte and Miller. FA3 and FA4 represent beach barrier, tidal flats and an intermediate to distal deltaic environment. These environments commonly co-exist (Daidu, 2013), although the glacial influence in FA1 and FA2 is lacking in FA3 and FA4. At this point it is also necessary to state that FA2 was most likely not deposited through direct glacial contact, but rather was exposed to glacial influences post deformation, if at all so. Evidence is discussed in detail by Bell (1981).

The absence of facies B towards the east of the study area, at Swaylands and Campherspoort would suggest shallowing of sedimentary environment. Although the profiles at Swaylands and Campherspoort show a state of regression, it is not possible to co-exist with the retrogradation on the western side of the study area.

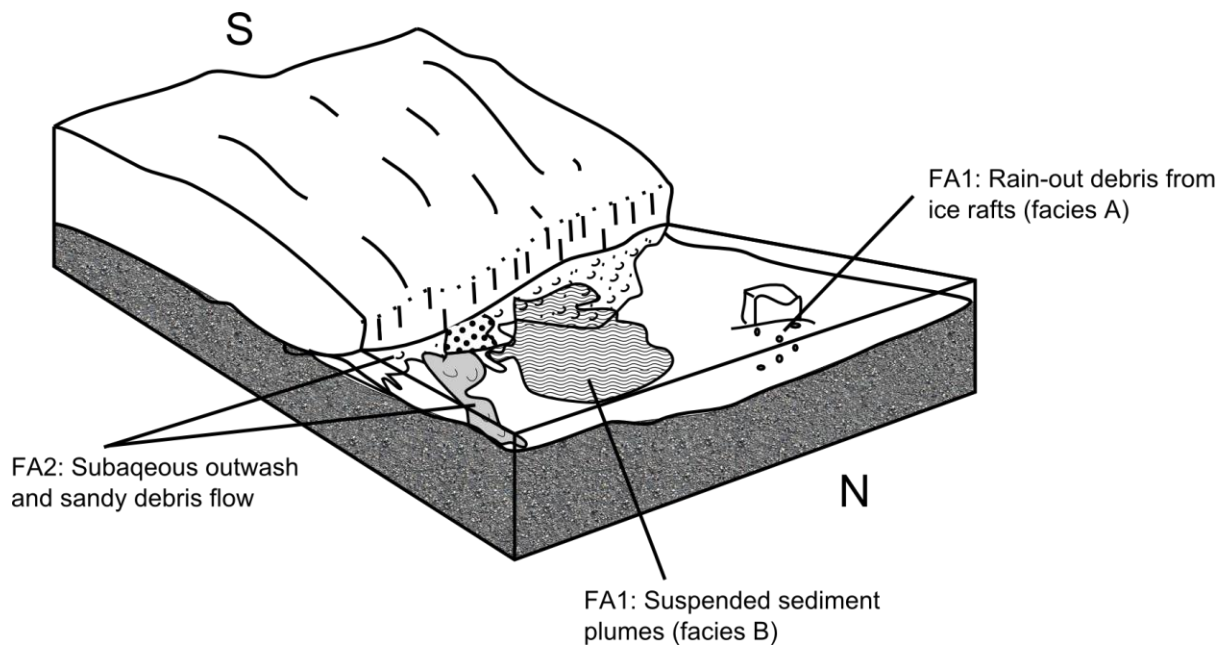


Figure 5.10: Hypothesized sedimentary environment of Model 1 representing FA1 and FA2.

5.2.2 Model 2

Kommadagga deposits represent the closing of the Witteberg basin with an erosional hiatus before the opening of the Main Karoo basin:

The sedimentation sequence of Model 2 can be divided into 3 stages, each representing a particular change in depositional environments over a period of time.

Stage 1: The Floriskraal - and Waaipoort Formation are represented by the beach barrier and tidal flats facies association (FA3, Table 5.2). According to Swart (1982) the beach barrier (facies G) was towards the south with a tidal flat environment (facies E) towards the north (Fig 5.11). During periods of storm wave conditions the beach barrier was breached by wash-over marine water and reworked beach sand (facies F) was transported into the tidal flat zone. This interpretation of Swart (1982), based on outcrops outside of this study area, will be used since profile 2 and 4 only displays partial information of the Floriskraal – and Waaipoort Formation due to poor accessibility of outcrops in the study area.

Stage 2: The second stage was a period of regression (coarsening upward in profile 6 of FA4) during which time the Kommadagga Subgroup was deposited. This is represented by the deltaic deposits of the Miller -, Swartwaterspoort -, Soutkloof - and Dirkskraal formation (Fig 5.11 and Table 5.2,). The Soutkloof - and Dirkskraal formation (FA4) represent the lower to upper parts of the slope, demonstrating an upwards facies change by progradation of the shallow marine slope. The prodelta deposits of facies I (Ffb) are marked by their fine laminated muds formed out of suspension. According to Wright (1978) and Elliot (1978) this is typical for prodelta muds. The current ripples, soft sediment deformation and change in energy activity along the slope represent the delta front environment (facies I, J and H). There is almost an absence of bioturbation or biological activity. According to Swart (1982) this lack in body fossils is due to the fact that these deposits formed in a narrow basin with restricted circulation, increasing salinity levels to a level which is too high for the development of abundant life.

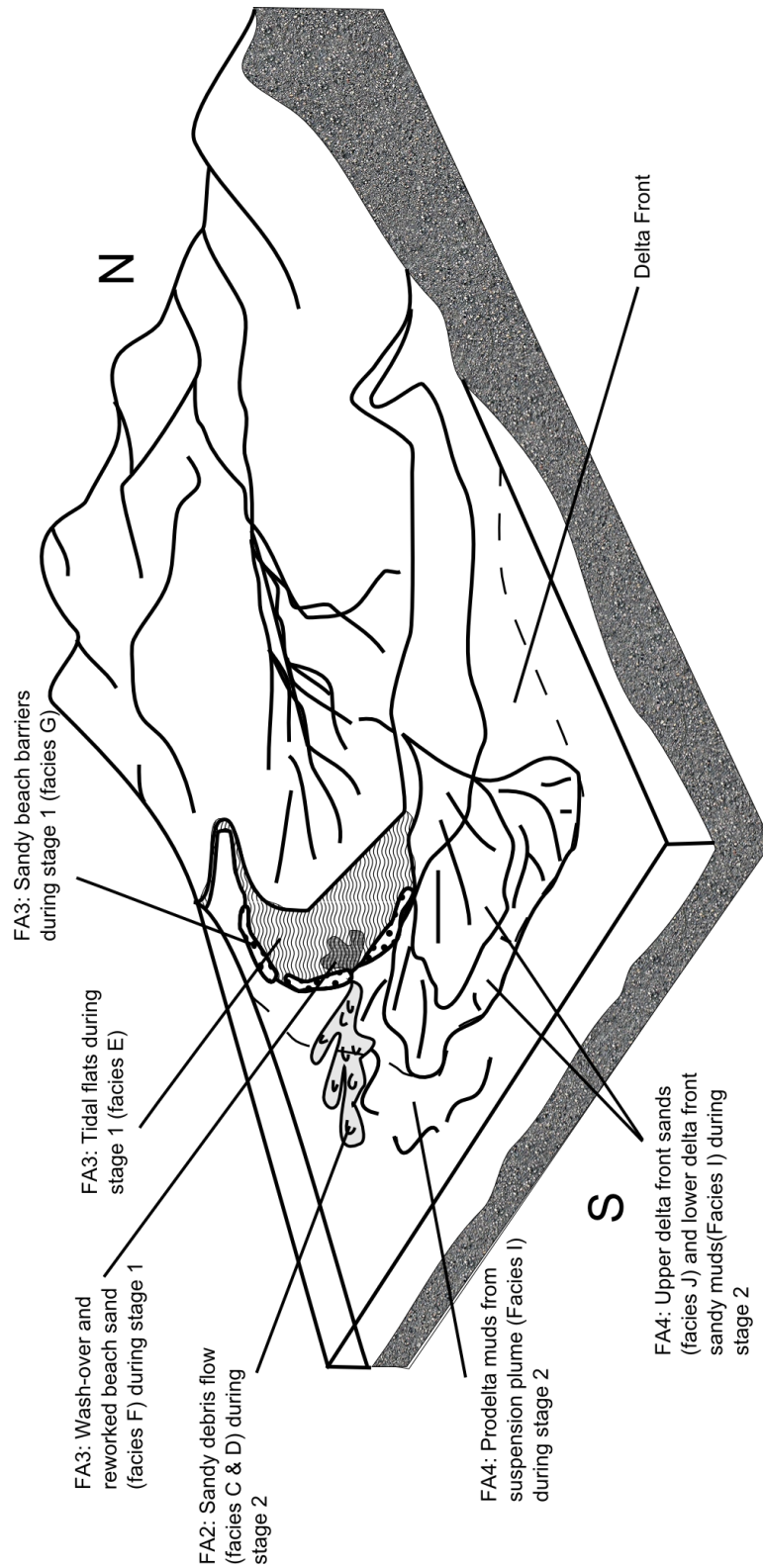


Figure 5.11: Hypothesized sedimentary environment of Model 2 representing Stage 1 followed by Stage 2.

Table 5.2: Correlation between stratigraphic groups and facies associations.

Group	Formation	Facies (Facies divisions)	Facies Association
Dwyka	Elandsmei	A	FA1 (Glacio - marine rain-out deposits)
		B	
Kommadagga Sub-group	Dirskraal	I (Frt, Flp), J, H	FA4 (Delta front)
	Soutkloof	I (Ffb)	FA4 (Prodelta)
	Swartwaterspoort	D	FA2 (Proximal slope deposits)
	Miller	C	
Lake Mentz Sub-group	Waaipoort	E, F	FA3 (Beach barrier and tidal flats deposits)
	Floriskraal	G	

Due to the lack in paleocurrent indicators it is difficult to determine the direction of the debris flow and related deposits of the Miller – and Swartwaterspoort formation (FA2), but it was most likely in a northeast to a southwest direction due to the pinching out of FA2 towards the east. The Kommadagga sediments filled in the last of the Witteberg basin due to the fall in sea-level and increase in sediment supply from the north, where sedimentation then ceased (Visser, 1991; Catuneanu et al., 1998; Tankard et al., 2009).

According to Mcpherson et al. (1987) the subaerial components of fan-deltas and braid deltas are the key features to use to distinguish between these two kinds of deltas. The type of distributary system and subaerial components are the main feature used to distinguish between the different types, but unfortunately this data is not represented in the rock record of the study area. When comparing the delta front and prodelta deposits in this study to the classifications of Mcpherson et al. (1987) and Postma (1990) it can be speculated that the Kommadagga deposits represents more a shallow marine braided-delta type due to the following reasons: boulders and cobbles are uncommon, clast shape in general is subrounded to rounded, facies changes are gradual and simplistic, lateral continuity is moderate to high; grain size decreases from delta front to prodelta, size of deposits are sheet like and are up to hundreds of km² (if taking into consideration the Kommadagga deposits outside of the study area (Rossouw, 1953; Swart, 1982)) close lateral relations with beach and tidal flat deposits (FA3). Due to the presence of slope failure (FA2) the gradient is most likely moderate rather than too flat. This slope dipped towards the south.

Stage 3: After sedimentation ceased, erosion took place which is evident in the disconformable contact of FA1 and FA4 at Campherspoort, as well as the fact that FA1 unconformably overlies all the other facies associations in the study area (Fig 5.1).

The Dwyka glaciation and deglaciation stage followed (Schematically presented in Fig 3.7). The Dwyka deposits (FA1) represent the advance and retreat of the major glacial ice sheets from the north moving towards the south in an open marine environment (Swart, 1982) due to the proglacial deposits (facies division Sm and facies B) interbedded in between the main diamictite (Dcm). Due to the majority of "rain out" diamictite in FA1 it is evident that the environment was exposed to floating icebergs which broke off from more distal ice sheets in the north. This is also confirmed by Dunley and Hiller (1979).

CHAPTER SIX

DISCUSSION AND CONCLUSION

Diamictites are classified as matrix-supported conglomerates according to their textural composition as defined in Fig 2.2. In general, they are complex deposits due to their various styles of deposition and are present in extremely contrasting environments. For debris flow diamictites, the internal controls that are involved in the mode of deposition are the sediment clay/sand ratio, water content and viscosity of debris. This influences the strength of the flow and will determine the size and thickness of the deposit. The external controls involved are effects of the surrounding sedimentary environment, such as slope angle and floor topography. For direct glacial diamictites the deposition depends on the frictional drag between the glacier/sediment contact, as well as the melting rate and release of sediment inside the glacier. Table 2.2 provides an adequate summary of the characteristics involved to determine whether a diamictite was deposited due to glacial influences or not.

By re-evaluating the facies in this study and creating a new facies model of the Kommadagga Subgroup and Dwyka Group, it can be concluded that the Miller diamictite can indeed, be labelled as a diamictite due to its facies characteristics. This corresponds to the similar conformation of Bell (1981) and Swart (1982). Although cold temperatures and glacial conditions likely occurred during the closing of the Witteberg basin, there is no evidence of the Miller diamictite being a product of direct glacial contact, therefore it cannot be called a tillite as interpreted by Loock (1967) and Rossouw (1953). This study agrees with the views of Crowell (1957) and Bell (1981) that the Miller diamictite is a debris flow deposit formed in a deltaic environment with non glacial connotations.

Of the two facies models that were presented in the previous chapter, the preferred facies model for the deposition of the Kommadagga Subgroup and Dwyka Group is model 2. This is based on the following arguments: Model 1 can only be used to partially interpret the study area, and does not allow all four of the established facies associations to co-exist (only FA1 and FA2) within continuous sedimentation; since only true glacial evidence

can be established in FA1, the lack thereof, in the other associations, is not convincing enough to group all of them in a glacial environment as described in Model 1; Model 2 provides a systematic representation of the change in environments as described by all the facies associations (FA1 to FA4).

According to Model 2, deposition of the massive, clast poor sandy Miller diamictite (facies divisions Dmm) occurred within a deltaic system which fed into a large body of water, which is possibly an open marine environment. The delta was dominated by a prograding braid delta that transported sediments from the distal alluvial environment in the north into a marine setting towards the south. The shallow basin trends in a northeast to southwest direction and is rather narrow (Swart, 1982).

The Kommadagga sub-basin represents the final infilling and closing of the Cape Basin due to the regression in stage 3, described in Model 2. Deposition seems to have occurred in a rather stable basin during the mantle extension (as discussed in chapter 3) process of the Cape Basin (Tankard et al, 2009). The Kommadagga sub-basin was only exposed to minor faulting. Evidence of erosion after the closing of the basin is confirmed by erosional disconformities and the unconformable manner of deposition of the Dwyka Group over the Witteberg sediments (Fig 5.1). The duration of the erosional time period is not certain; Tankard et al (2009), Catuneanu et al. (1998) and Visser (1991) have suggested a hiatus representing a time gap of about 20 to 30 Ma.

After the hiatus, the Dwyka Group, including the Dwyka diamictite which represents a massive, clast rich muddy diamictite (subfacies Dcm), was deposited in an indirect distal glaciomarine environment (Fig 2.7). It is suggested that there were major tectonic (switch from rifting to subduction) and climatic changes (decrease in temperature) in the basin. This influenced the change in deposition environment from deltaic Kommadagga deposits to glacio-marine Dwyka deposits. This is not concluded from this study, but contributes to the findings of Visser (1991), Smith et al., (1993) and Catuneanu et al., (1998).

With a preference for the use of Model 2, it is concluded that the Cape – and Karoo sedimentation is not continuous and that the Miller - and Dwyka diamictite are not related

to each other. Their sediments were derived from different environments which correspond to different sedimentary processes. The sediments for the Miller diamictite were supplied from inside the small basin by distal deltaic processes from the upper slope, whereas the sediments for the Dwyka diamictite were supplied from highlands in the north thousands of kilometres away from the depositional area (Eyles, 1993). This highlights the contrast in the variety of environmental conditions that can generate diamictite deposits which emphasises the importance of the need to understanding all the processes involved in the deposition of a diamictite.

It is suggested that an additional facies analysis should be done in the most eastern part of the Kommadagga sub-basin (close to Grahamstown). The facies analysis of the eastern part should be compared with this study and the confirmed preferred facies model in this study, since this study area only represents the western half of the Kommadagga sub-basin. Detailed mapping of the Kommadagga Subgroup would be a great contribution to this study as well as detailed tectonic controls on this sub-basin. Currently the only geological maps available, group the Kommadagga Subgroup and Lake Mentz Subgroup together, for this reason it is difficult to see the true presence of the Kommadagga Subgroup and its formations over the basin.

REFERENCES

- Adams, A., Mackenzie, W., & Guilford, C. (1984). *Atlas of sedimentary rocks under the microscope*. London: Prentice Hall.
- Allen, J. (1982). *Sedimentary structures: Their character and physical basis*. Amsterdam: Elsevier.
- Bell, C. (1981). Soft-sediment deformation of sandstone related to the Dwyka glaciations in South Africa. *Sedimentology*, 28, 321-329.
- Benvenuti, M. (2003). Facies analysis and tectonic significance of lacustrine fan-deltaic successions in the Pliocene–Pleistocene Mugello Basin, Central Italy. *Sedimentary Geology*, 157, 197-234.
- Bertan, P., Hetu, B., Texier, J., Van Stein, H. (1997). Fabric characteristics of subaerial slope deposits. *Sedimentology*, 44, 1-16.
- Boggs, S. J. (1992). *Petrology of sedimentary rocks*. New York: Merrill/ Macmillan.
- Boggs, S. J. (2006). *Principles of sedimentology and stratigraphy (4 ed)*. USA: Pearson Prentice Hall.
- Booth, P.W.K., Shone, R.W. (2002). A review of thrust faulting in the Eastern Cape Fold Belt, and the implications of the current lithostratigraphic interpretation of the Cape Supergroup. *Journal of African Earth Sciences*, 34, 179 – 190.
- Bridge, J.S., Demicco, R.V. (2008). *Earth surface processes, landforms and sediment deposits*. New York: Cambridge University Press.
- Broquet, C. (1992). The sedimentary record of the Cape Supergroup: a review. *In: de Wit, M.J. and Ransome, I.G.D. (Eds.), Inversion tectonics of the Cape Fold Belt*,

Karoo and Cretaceous Basins of Southern Africa. A.A. Balkema Publ., Rotterdam, Brookfield, pp.159-183.

Carozzi, A. (1993). *Sedimentary petrography*. New Jersey: PTR Prentice-hall.

Catuneanu, O., Hancox, P.J., Rubidge, B.S. (1998). Reciprocal flexural behavior and contrasting stratigraphies: a new basin development model for the Karoo retroarc foreland system, South Africa. *Basin Research*, 10, 417-439.

Chakrabarti, A. (2005). Sedimentary structures of tidal flats: A journey from coast to inner estuarine region of eastern India. *Journal of earth system science*, 114, 353-368.

Chakraborty, C., Ghosh, S.K. (2008). Pattern of sedimentation during the Late Paleozoic, Gondwanaland glaciation: An example from the Talchir Formation, Satpura Gondwana basin, central India. *Journal of Earth System Science*, 4, 499-519.

Colella, A., Prior, D.B. (1981). Deltaic environments of deposition. *Am. Assoc. Petroleum Geologists*, 139.

Coleman, J.M. , Wright, L.D. (1975). Modern river deltas: variability of processes and sand bodies. In E. B. Broussard, *In: Deltas: Models for Exploration* (pp. 99-149). Houston: Houston Geological Society.

Crowell, J. (1957). Origin of pebbly mudstone. *Bulletin of geological Society of America*, 68, 993-1010.

Crowell, J.C., Frakes, L.A. (1972). Late Paleozoic Glaciation: Part V, Karroo Basin, South Africa. *Geological Society of America Bulletin*, 83, 2887-2912.

Daidu, F. (2013). Classifications, sedimentary features and facies associations of tidal flats. *Journal of Paleogeography*, 2, 66-80.

Deer, W., Howie, R., & Zussman, J. (1992). *The rockforming minerals* . Harlow: Pearson education limited.

- Du Toit, A. (1921). The Carboniferous glaciation of South Africa. *Trans. Geol. Soc. S. Afr.*, 24: 188-22.
- Dunley, J.N. and Hiller, N. (1979). The Witteberg- Dwyka boundary in the south-western Cape. *Trans. Geol. Soc. S.Afr.*, 82, 251-256.
- Elliot, T. (1978). Deltas. In H. Reading, *Sedimentary environments and facies* (pp. 97-142). New York: Elsevier.
- Ethridge, F.G., Wescott, W.A. (1984). Tectonic setting, recognition and hydrocarbon reservoir potential of fan-delta deposits. In E. K. Steel, *Sedimentology of Gravels and Conglomerates* (pp. 10, 217-235). Mem. Can. Soc. Petrol. Geol.
- Eyles, C.H., Eyles, N., Miall, A.D. (1983). Lithofacies types and vertical profile models; an alternative approach to the description and environmental interpretation of glacial diamict and diamictite sequences. *Sedimentology*, 30, 393-410.
- Eyles, C.H., Eyles, N., Miall, A.D. (1985). Models of Glaciomarine sedimentation and their application to the interpretation of ancient Glacial Sequences. *Palaeogeography, Palaeoclimatology, Palaeoecology*, 51,15-84.
- Eyles, N. (1993). Earth's glacial record and its tectonic setting. *Earth-Science Reviews*, 35, 1-248.
- Fagereng, A. (2012). A note on folding mechanisms in the Cape Fold Belt, South Africa. *South African Journal of Geology* , 115.2, 137–144.
- Fagereng, A. (2014). Significant shortening by pressure solution creep in the Dwyka diamictite, Cape Fold Belt, South Africa. *Journal of African Earth Sciences*, 97, 9–18.
- Felix, M., Peakall, J. (2006). Transformation of debris flows into turbidity currents:mechanisms inferred from laboratory experiments. *Sedimentology*, 53, 107-123.

- Fourie, P.H., Zimmermann, U., Beukes, N.J., Naidoo, T., Kobayashi, K., Kosler, J., Nakamura, E., Tait, J., Theron, J.N. (2011). Provenance and reconnaissance study of detrital zircons of the Palaeozoic Cape Supergroup in South Africa:revealing the interaction of the Kalahari and Rio de la Plata cratons. *Int J Earth Sci (Geol Rudsch)*, 100, 527-541.
- Frakes, C. (1987). Diamicite. In R. B. Fairbridge, *The Encyclopedia of Sedimentology* (pp. 262-263). Stroudsburg: Dowden, Hutchinson & Ross.
- Franks, P. (1969). Nature, origin, and significance of cone-in-cone structures in the Kiowa Formation (Early Cretaceous), north-central Kansas. *Journal of sedimentary research*, 39, 1438-1454.
- Friedman, G. (2003). Classification of sediments and sedimentary rocks. In G. Middleton, *Encyclopedia sediments and sedimentary rocks* (p. 134). Springer.
- Galloway, W. (1975). Process framework for describing the morphology and stratigraphic evolution of the deltaic depositional systems. In M. Broussard, *Deltas: Models for Exploration* (pp. 87-98). Houston: Houston Geological Society.
- Ghibaudo, G. (1992). Subaqueous sediment gravity flow deposits:practical criteria for their field description and classification. *Sedimentology*, 39, 423-454.
- Hambrey, M. (1994). *Glacial Environments*. Vancouver: University of British Columbia Press and London: UCL Press.
- Hambrey, M.J., Glasser, N.F. (2003). Glacial sediments: Process, environments and facies. In G. Middleton, *Encyclopedia of sediments and sedimentary rocks* (p. 325). Springer.
- Hampton, M. (1972). The role of subaqueous debris flow in generating turbidity currents. *Journal of Sedimentary Petrology*, 42, 775-793.

- Holmes, A. (1965). *Principles of Physical Geology*. London, 1288 pp.: 2nd edn. Thomas Nelson.
- Isbell, J. L. (2008). Carboniferous-Permian glaciation in the main Karoo Basin, South Africa: Stratigraphy, depositional controls, and glacial dynamics. *Resolving the Late Paleozoic Ice Age in Time and Space: Geological Society of America Special Publication*, 441, 71-82.
- Johnson, M. (1976). *Stratigraphy and sedimentology of the Cape and Karoo sequences in the Eastern Cape Province*. Rhodes Univ. Grahamstown. 336 pp.: Phd. Thesis (unpubl).
- Johnson, M. (1991). Sandstone petrography, provenance and plate tectonic setting in Gondwana. *South African J. Geol.*, v. 94, pp137-154.
- Johnson, M. A. (2006). *The geology of South Africa*. Pretoria: Geological Society of South Africa, Johannesburg/Council of Geoscience, 691 pp.
- Leigh, N.S., Hartley, A. (1992). Mega-debris flow deposits from the Oligo-Miocene Pindos foreland basin, western mainland Greece: implications for transport mechanisms in ancient deep marine basins. *Sedimentology*, 39, 1003-1012.
- Loock, J. (1967). *The stratigraphy of the Witteberg – Dwyka contact beds*. Stellenbosch Univ. pp 139.: M.Sc. thesis.
- Mail, A. (1977). A review of the braided-river depositional environment. *Earth-Science Reviews*, 13, 1-62.
- Major, J. (1997). Depositional processes in Large-Scale Debris-Flow Experiments. *The Journal of Geology*, 105,345-366.
- Major, J. (2003). Debris flow. In G. Middleton, *Encyclopedia of sediments and sedimentary rocks* (p. 744). Springer.

- Marr, J.G., Harff, P.A., Shanmugam, G., Parker, G. (2001). Experiments on subaqueous sandy gravity flows: The role of clay and water content in flow dynamics and depositional structures. *Geological Society of America Bulletin*, 113, 1377-1386.
- Mcperson, J.G, Shanmugam, G., Moiola, R.J. (1987). Fan-deltas and braid deltas: Varieties of coarse-grained deltas. *Geological Society of America Bulletin*, 3, 331-340.
- Menzies, J. (2003). Till and tillites. In G. Middleton, *Encyclopedia of sediments and sedimentary rocks* (p. 744). Springer.
- Mulder, T., Alexander, J. (2001). The physical characteristics of subaqueous sedimentary density flows and their deposits. *Sedimentology*, 48, 269-299.
- Nemec, W. (1990). Deltas - remarks on terminology and classification. In D. P. A. Colella., *Coarse-grained Deltas:International Association of Sedimentologists, Special Publication 10* (pp. 3-12). Oxford: Blackwell Scientific publications.
- Posamentier, H.W., Walker, R. G. (2006). *Facies models revisited*. Laura j. Crossey and Donald S. Mc Neill, Editors of Special Publications; SEPM Special Publication 84.
- Postma, G. (1990). Depositional architecture and facies of river and fan deltas: a synthesis. In A. P. Colella, *Coarse-grained Deltas* (pp. 10,13-27). Oxford: Spec. Publ. I.A.S., Blackwell Scientific Publication.
- Pye, K. (1994). *Sediment transport and depositional processes*. London: Blackwell Scientific Publications.
- Reimond, W.U., Brunn, V., Koeberl, C. (1997). Are diamictites Impact Ejecta? - No supporting evidence from South Africa Dwyka Group Diamictite. *The Journal of Geology*, 105, 517 - 530.

- Rossouw, P. (1953). The Southern Karroo. *In : Haughton, S.H. Et al, Results of an investigation into the possible presence of oil in Karoo rocks in Part of the Union of South Africa. Mem. Geol Surv. S. Afr., 45, 14-36.*
- Rossouw, P. (1970). The Witteberg-Dwyka contact in the Willowmore and Steytlerville district. *In: Haughton, S.H. (Ed.), Proceedings of the 2nd Gondwana Symposium. CSIR, South Africa, , pp. 205-207.*
- SACS (South African Committee for Stratigraphy). (1980). Stratigraphy of South Africa. Part 1. (Compiled by Kent, L.E.). *Lithostratigraphy of the Republic of South Africa, South West Africa/Namibia, and the Republics of Bophuthatswana, Transkei and Venda. Handbook of the Geological Survey of South Africa 8, 690 p.*
- Selley, R. (2000). *Applied Sedimentology, 2nd Ed.* San Diego: Academic press.
- Shone, R.W., Booth, P.W.K. (2005). The Cape Basin, South Africa: A review. *Journal of African Earth Sciences, 43, 196-210.*
- Smith R.M.H., Eriksson P.J., Botha W.J. (1993). Review of the stratigraphy and sedimentary environments of the Karoo-aged basins of Southern Africa. *Journal of African Earth Sciences, Vol. 16, No. 132, pp. 143-169.*
- Stow, D. (2006). *Sedimentary rocks in the field.* London: Manson publishing.
- Strasser, M.; Stegmann, M.; Bussmann F.; Anselmetti, FS.; Rick, B.; Kopf, A. (2007). Quantifying subaqueous slope stability during seismic shaking: Lake Lucerne as model for ocean margins. *Marine geology, 240, 77-97.*
- Stratigraphy), S. (. (1980). *Stratigraphy of South Africa. Part 1. (Compiled by Kent, L.E.). Lithostratigraphy of the Republic of South Africa, South West Africa/Namibia, and the Republics of Bophuthatswana, Transkei and Venda. Handbook of the Geological Survey of South Africa 8, 690 p.*

- Swart, R. (1982). *The stratigraphy and sedimentology of the Kommadagga Subgroup and contiguous rocks*. Grahamstown: M.Sc thesis (unpubl). Rhodes Univ. 120 pp.
- Tamura, T., Masuda, F. (2003). Shallow-marine fan delta slope deposits with large-scale cross-stratification: the Plio-Pleistocene Zaimokuzawa formation in the Ishikari Hills, northern Japan. *Sedimentary Geology*, 158, 195-207.
- Tankard, A., Welsink, H., Aukes, P., Newton, R., Stettler, E. (2009). Tectonic evolution of the Cape and Karoo basins of South Africa. *Marine and Petroleum Geology*, 26, 1379-1412.
- Treagus, S. T. (2002). Studies of strain and Rheology of conglomerates. *Journal of Structural Geology*, 24, 1541-1567.
- Tye, R.S; Coleman, J.M. (1989). Depositional processes and stratigraphy of fluvially dominated lacustrine deltas; Mississippi delta plain. *Journal of Sedimentary Research*, 59,973-996.
- Visser, J. (1986). Lateral lithofacies relationships in the glaciogene Dwyka Formation in the western and central parts of the Karoo Basin. . *Trans. Geol. Soc. S. Afr.*, 89, 373 - 383.
- Visser, J. (1989). The Permo-Carboniferous Dwyka Formation of southern Africa: Deposition by a predominatly subpolar marine ice sheet. *Palaeogeography, Palaeoclimatology, Palaeoecology*, 70, 377-391.
- Visser, J. (1991). Self-destructive collapse of the Permo-Carboniferous marine ice sheet in the Karoo Basin: evidence from the southern Karoo. *South African Journal of Geology*, 94, 255–262.
- Visser, J. (1991). Self-destructive collapse of the Permo-Carboniferous marine ice sheet in the Karoo Basin: evidence from the southern Karoo. *South African Journal of Geology*, 94, 255–262.

- Visser, J. (1997). Deglaciation sequences in the Permo=Carboniferous Karoo and kalahari basins of southern Africa: a tool in analysis of cyclic glaciomarine basin fills. *Sedimentology*, 44, 507-521.
- Visser, J.N.J., Young, G.M. (1990). Major element geochemistry and paeoclimatology of Permo Carboniferous glacigene Dwyka Formation and post-glacial mudrocks in southern Africa. *Palaeogeography, Palaeoclimatology, Palaeoecology*, 81, 49-57.
- Woodcack, N. (1976). Structural style in slump sheets: Ludlow Series, Powys, Wales. *Journal of the Geological Society (London)*, 132,399-415.
- Woodcock, N. (1976). Structural style in slump sheets: Ludlow Series, Powys, Wales. *Journal of the geological Society*, 132, 399-415.
- Wright, L. (1978). River Deltas. In R. Davis, *Coastal Sedimentary Environments* (pp. 5-68). New York: Springer verlag.

APPENDIX A

STUDY LOCATIONS AND GPS COORDINATES

Table A1: GPS coordinates of facies divisions, samples and thin sections of each location.

W P	S	E	Facies divisions	Volstruisleegte:			
				Unit/Contact	Dip	Hand Sample	Thin section
1	33°07.15 3	023°25.88 6	Dcm	VD	outcrop not suitable for measurement	VLD1	VLD1
2	33°07.25 5	023°25.91 5	Sm	VWA	003/66	VLWA1	VWA1
3	33°07.31 4	023°25.94 1	Ffd	VWB	003/66	VLWB1	VLWB1
4	33°07.38 9	023°25.89 4	Sl	VWCb	353/71; 348/81; 310/63		
5	33°07.39 2	023°25.83 6	Dmm	VWD	outcrop not suitable for measurement		
6	33°07.39 4	023°25.83 1	Dmm	VWD	outcrop not suitable for measurement		
7	33°07.39 7	023°25.82 9	Dmm	VWD	outcrop not suitable for measurement		
8	33°07.39 7	023°25.82 2	Dmm	VWD	000/53	VLWD1	VLWD1
9	33°07.42 0	023°25.81 9	Sl	VWCa	355/66	VLWCa1	VLWCa1
10	33°07.41 9	023°25.81 2	Sl	VWCb	335/50	VLWCb1	VLWCb1
11	33°07.42 5	023°25.80 9	Dmm	VWD	outcrop not suitable for measurement		
12	33°07.43 9	023°25.79 7	Ffd	VWB			
13	33°07.53 0	023°24.46 5	Sl	VWCa			
14	33°07.52 3	023°24.47 9	Sl	VWCa	336/55		
15	33°07.52 7	023°24.51 5	Sl	VWCb	358/45	VLWCb2	
16	33°07.52 8	023°24.51 4	Dmm/Sl	Contact between VWD and VWCb			
17	33°07.39 5	023°24.47 2	Dcm	VD	outcrop not suitable for measurement	VLD2	
18	33°07.34 9	023°24.44 9	Dcm	VD	outcrop not suitable for measurement		

Miller (Location 1):							
W P	S	E	Facies divisions	Unit/Contact	Dip	Hand Sample	Thin section
44	33°05.11 8	023°55.31 3	Frc/Dmm/S l	Contact between MWE and MWD & contact between MWD and MWC	MWE: 020/35; 355/35 MWD: 002/51; 015/35 MWC: 003/31; 340/31	MWE1 MWD1 MWC1	MWE1 MWD1 MWC1

Miller (Location 2):							
W P	S	E	Facies divisions	Unit/Contact	Dip	Hand Sample	Thin section
45	33°04.90 5	023°54.769 .	Sm	MWA	034/75	MWA1	MWA1
46	33°04.90 7	023°54.773 .	Dcm/Sm	Contact between MWB and MWA	outcrop not suitable for measurement		
47	33°04.91 4	023°54.77 6	Ffd/Sl	Contact between MWF and MWD	outcrop not suitable for measurement		
48	33°04.92 5	023°54.75 2	Smc/Ffd	Contact between MWC and MWF	outcrop not suitable for measurement		
49	33°04.93 0	023°54.73 7	Smc	MWC	outcrop not suitable for measurement		

Table A1: GPS coordinates of units, samples and thin sections of each location (continue).

Miller (Location 2):							
W P	S	E	Facies divisions	Unit/Contact	Dip	Hand Sample	Thin section
50	33°04.92 7	023°54.73 5	Smc	MWC	outcrop not suitable for measurement		
51	33°04.92 1	023°54.75 4	Sl/Ffd	Contact between MWD and MWF	outcrop not suitable for measurement		
52	33°04.93 2	023°54.73 4	Smc/Sl	MWC interbedded with MWD	outcrop not suitable for measurement	MWC2	MWC2
53	33°04.92 2	023°54.74 5	Sl	MWD	outcrop not suitable for measurement	MWD2	MWD2
54	33°04.91 9	023°54.74 0	Ffd	MWF	outcrop not suitable for measurement	MWF2	MWF2
55	33°04.90 8	023°54.76 8	Dcm	MWB	outcrop not suitable for measurement	MWB1	MWB1
Swaylands (Location 1):							
W P	S	E	Facies divisions	Unit/Contact	Dip	Sample	Thin section
56	33°04.27 6	024°09.85 5	Smq	SWQ		SWQ1	SWQ1
57	33°04.31 2	024°09.93 8	Slr/Srm/Fr c	Contact between SWZ and SWY & contact between SWY and SWX	SWZ: 005/50; 006/49 SWY: 010/55; 350/54 SWX: 015/40	SWZ1 SWY1 SWX1	SWZ1 SWY1 SWX1
58	33°04.11 3	024°10.24 5	Dcm	SD	outcrop not suitable for measurement	SD2	SD2
Swaylands (Location 2):							
W P	S	E	Facies divisions	Unit/Contact	Dip	Sample	Thin section
43	33°07.47 7	024°10.26 2	Fdp	SWB(b7) SWB(b6) SWB(b4) SWB(b3) SWB(b2) SWB(b1) SWA SD(a2) SD(a3) SD(a1)	outcrop not suitable for measurement	SWB(b7) SWB(b6) SWB(b4) SWB(b3) SWB(b2) SWB(b1) SWA SD(a2) SD(a3) SD(a1)	SWB(b7) SWB(b6) SWB(b4) SWB(b3) SWB(b2) SWB(b1) SWA SD(a2) SD(a3) SD(a1)

Table A1: GPS coordinates of units, samples and thin sections of each location (continue).

WP	S	E	Facies divisions	Campherspoort:		Sample	Thin section
				Unit/Contact	Dip		
19	33°08.926	024°15.208	Dcm	CD		CD1	CD1
20	33°09.057	024°15.220	Dcm	CD	027/56	CD2	
21	33°09.059	024°15.230	Slm/Dcm	Contact between CWA and CD			
22	33°09.069	024°15.209	Slm	CWA	003/61	CWA1	CWA1
23	33°08.679	024°15.129	Slm	CWA	172/35	CWA2	
24	33°08.708	024°15.118	Slm/Dcm	Contact between CWA and CD			
25	33°08.718	024°15.325	Slm/Dcm	Contact between CWA and CD	194/70 (CWA)	CWA3 CD3	
27	33°09.199	024°15.960	Slm	CWA	010/55	CWA4	
28	33°09.208	024°16.057	Slm	CWA	015/55	CWA5	
29	33°08.801	024°16.417	Slm	CWA	195/35	CWA6	
30	33°08.756	024°16.472	Frt/Slm	Contact between CWB and CWA			
31	33°08.761	024°16.414	Frt	CWB			
32	33°08.744	024°16.348	Frt/Slm	Contact between CWB and CWA			
33	33°08.736	024°16.260	Frt/Slm	Contact between CWB and CWA			
34	33°08.729	024°16.469	Frt	CWB			
35	33°08.735	024°16.376	Frt	CWB	197/58		
36	33°08.726	024°16.343	Frt	CWB	194/70; 185/64	CWB1(b1) CWB1(b2)	CWB1(b1) CWB1(b2)
37	33°08.733	024°16.354	Frt	CWB	outcrop not suitable for measurement		
38	33°08.735	024°16.380	Frt	CWB	187/55; 194/65	CWB2(b2)	
39	33°08.733	024°16.446	Frt	CWB	192/60; 191/60	CWB3(b2)	
40	33°08.715	024°16.614	Frt	CWB	190/65	CWB4(b2)	
41	33°08.701	024°156.614	Flp	Transition zone C1, 2,3	outcrop not suitable for measurement	C1; C2; C3	C1; C2; C3
42	33°08.695	024°16.614	Ffb	CWC	outcrop not suitable for measurement	CWC1	CWC1

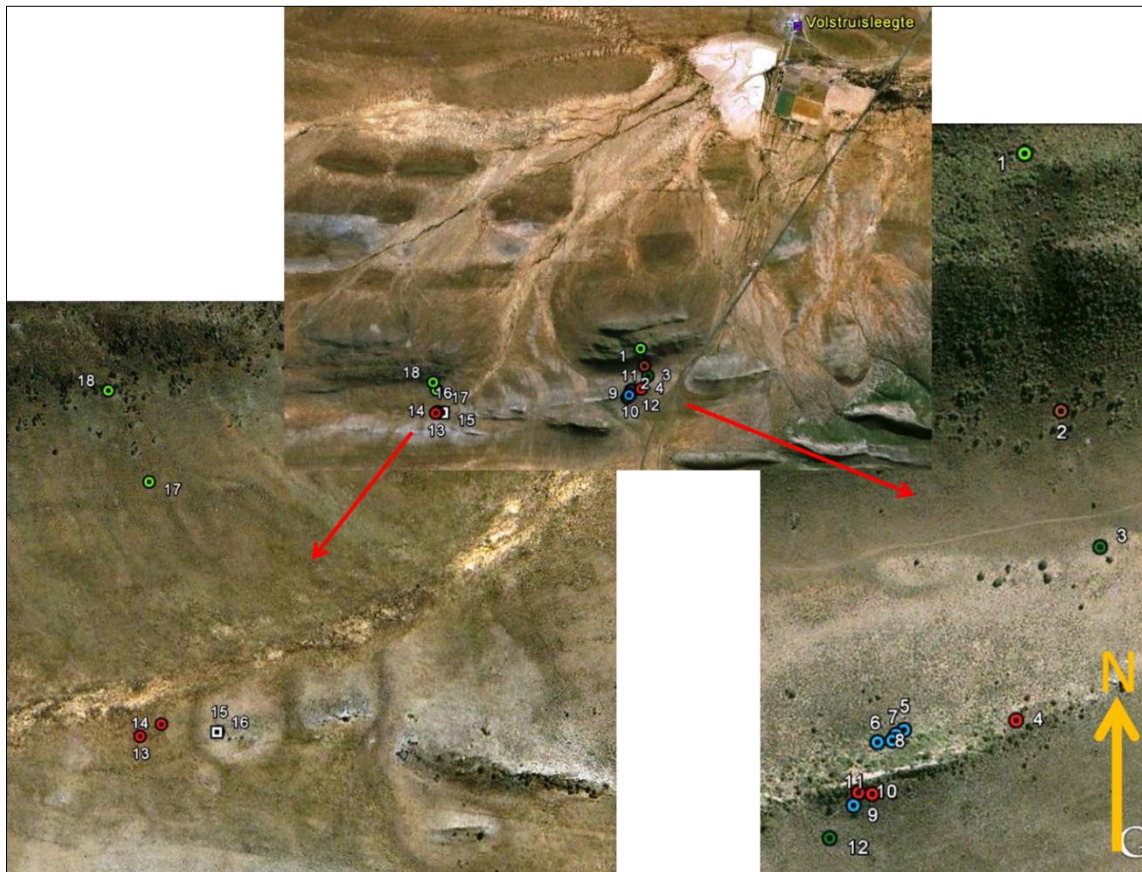


Figure A1: Overview of Volstruisleegte with GPS points corresponding to the different lithological units.

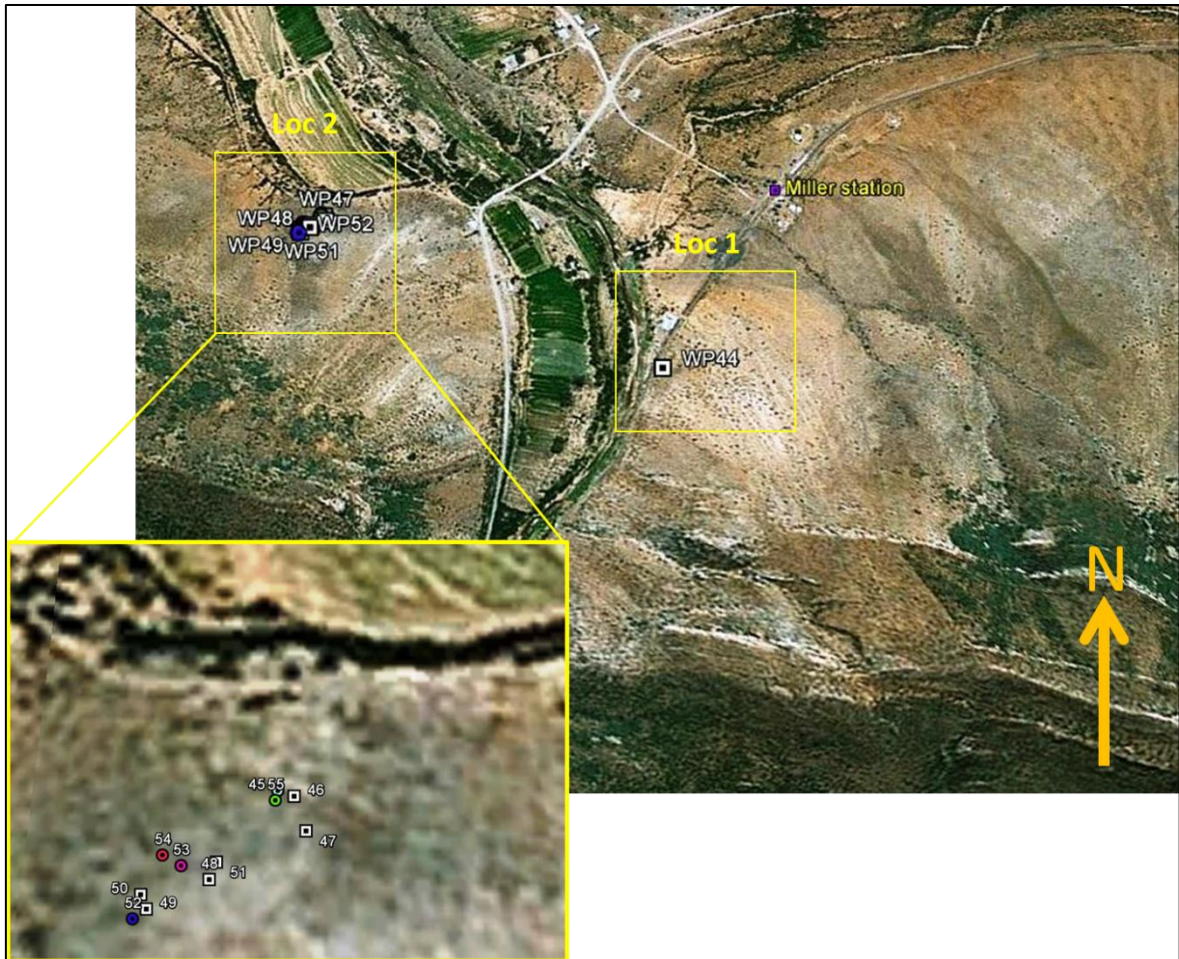


Figure A2: Overview of Miller station indicating GPS point.

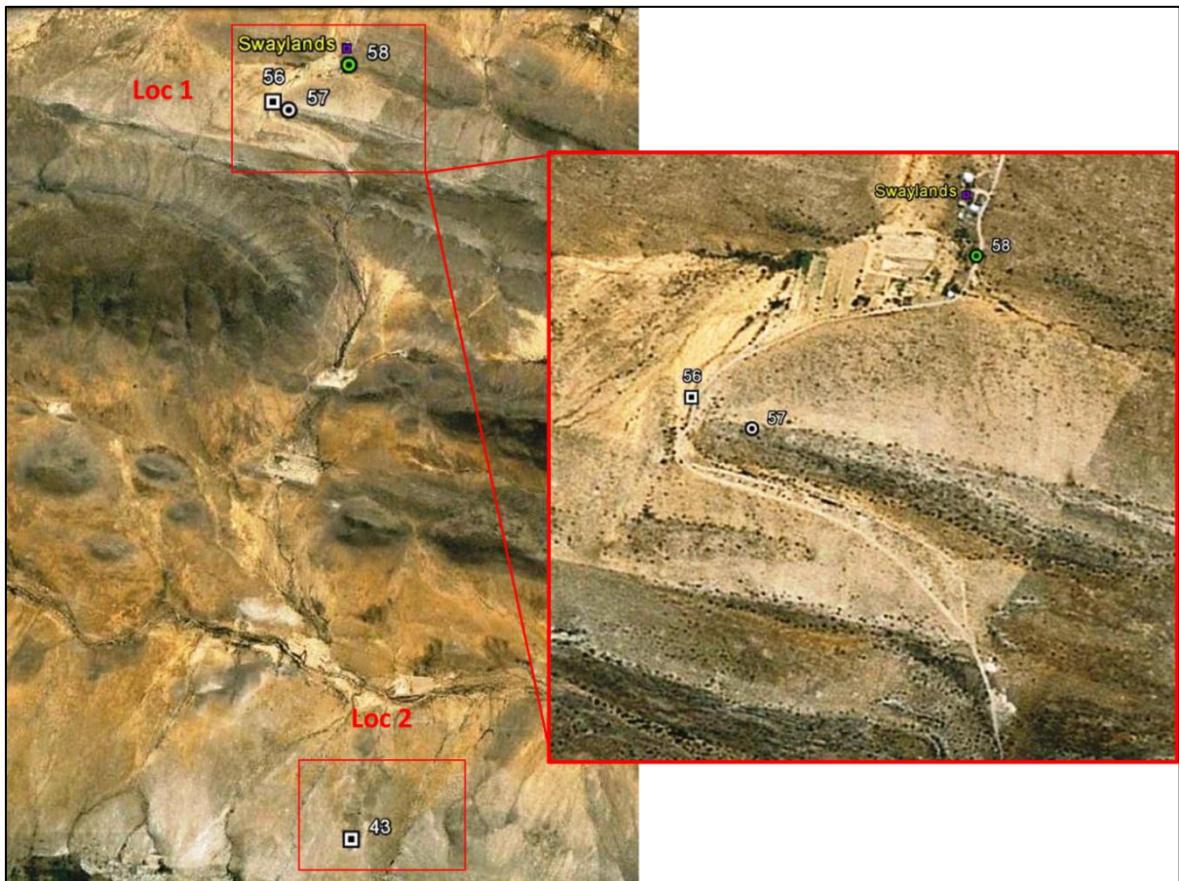


Figure A3: Overview of Swaylands with GPS points.



Figure A4: Overview of Campherspoort with GPS points corresponding to the different lithological units.

APPENDIX B

GRAIN SIZE SCALE

Table B1: The Udden-Wentworth grain-size classification scale (Boggs, 2006).

	U.S. Standard sieve mesh	Millimeters	Phi (ϕ) units	Wentworth size class
GRAVEL	Use wire squares	4096	- 12	Boulder
		1024	- 10	
		256	256 _____ - 8	Cobble
		64	64 _____ - 6	
		16	_____ - 4	Pebble
	5	4	4 _____ - 2	
	6	3.36	_____ - 1.75	Granule
	7	2.83	_____ - 1.5	
	8	2.38	_____ - 1.25	
	10	2.00	2 _____ - 1.0	
SAND	12	1.68	_____ - 0.75	Very coarse sand
	14	1.41	_____ - 0.5	
	16	1.19	_____ - 0.25	
	18	1.00	1 _____ 0.0	Coarse sand
	20	0.84	_____ 0.25	
	25	0.71	_____ 0.5	Medium sand
	30	0.59	_____ 0.75	
	35	0.50	1/2 _____ 1.0	
	40	0.42	_____ 1.25	Fine sand
	45	0.35	_____ 1.5	
	50	0.30	_____ 1.75	
	60	0.25	1/4 _____ 2.0	Very fine sand
	70	0.210	_____ 2.25	
	80	0.177	_____ 2.5	
	100	0.149	_____ 2.75	
	120	0.125	1/8 _____ 3.0	Coarse silt
	140	0.105	_____ 3.25	
170	0.088	_____ 3.5		
200	0.074	_____ 3.75		
230	0.0625	1/16 _____ 4.0	Medium silt	
270	0.053	_____ 4.25		
325	0.044	_____ 4.5	Fine silt	
	0.037	_____ 4.75		
SILT		0.031	1/32 _____ 5.0	Very fine silt
		0.0156	1/64 _____ 6.0	
MUD	Use pipette or hydro-meter	0.0078	1/128 _____ 7.0	Clay
		0.0039	1/256 _____ 8.0	
		0.0020	_____ 9.0	
		0.00098	_____ 10.0	
		0.00049	_____ 11.0	
		0.00024	_____ 12.0	
	0.00012	_____ 13.0		
	0.00006	_____ 14.0		

APPENDIX C

THIN SECTION IMAGES

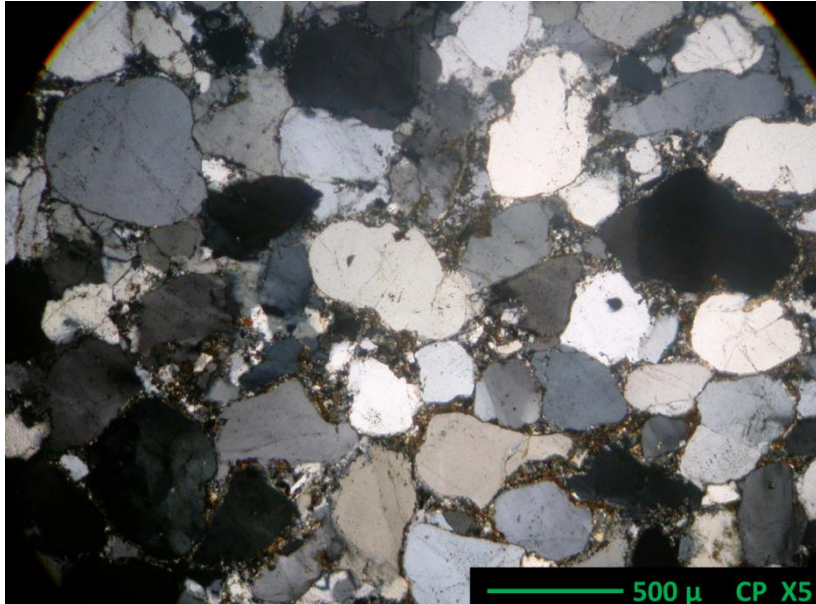


Figure C1: Overview of Sl.

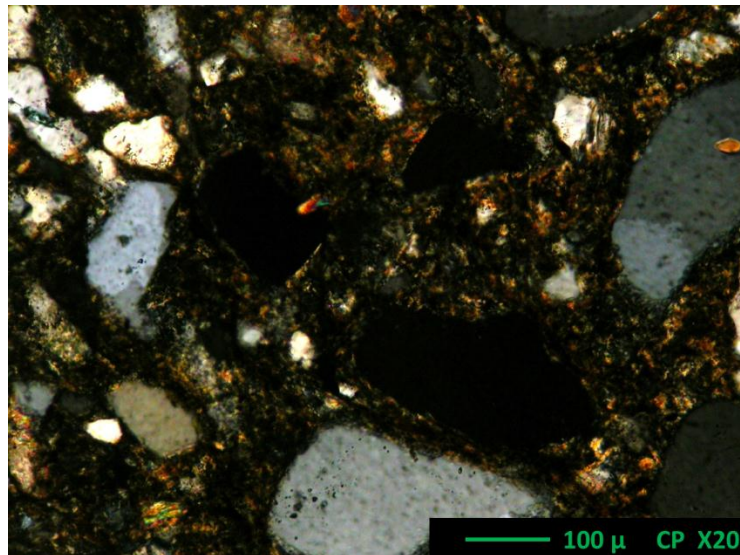


Figure C2: Matrix (<63 u) between sand size grains in Dmm.

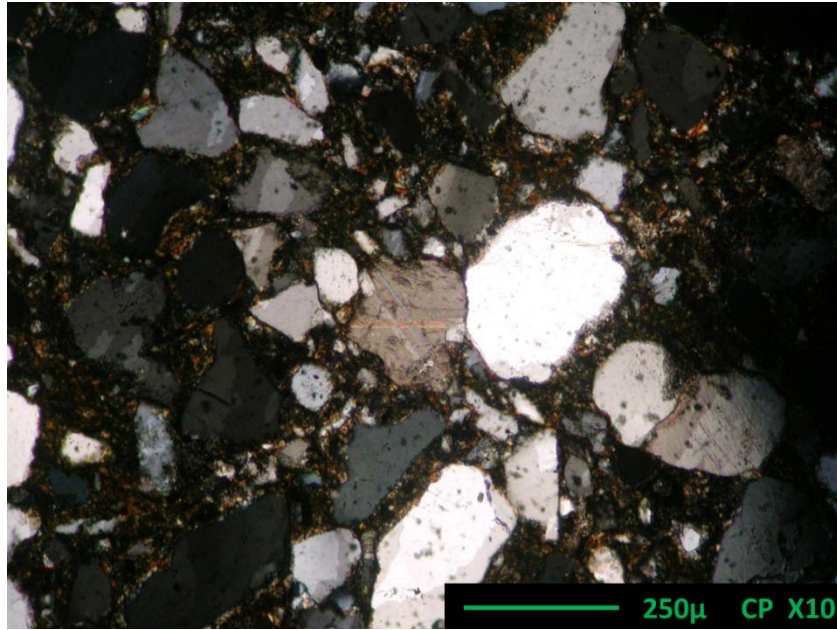


Figure C3: Sand - size calcite grain in Dmm.

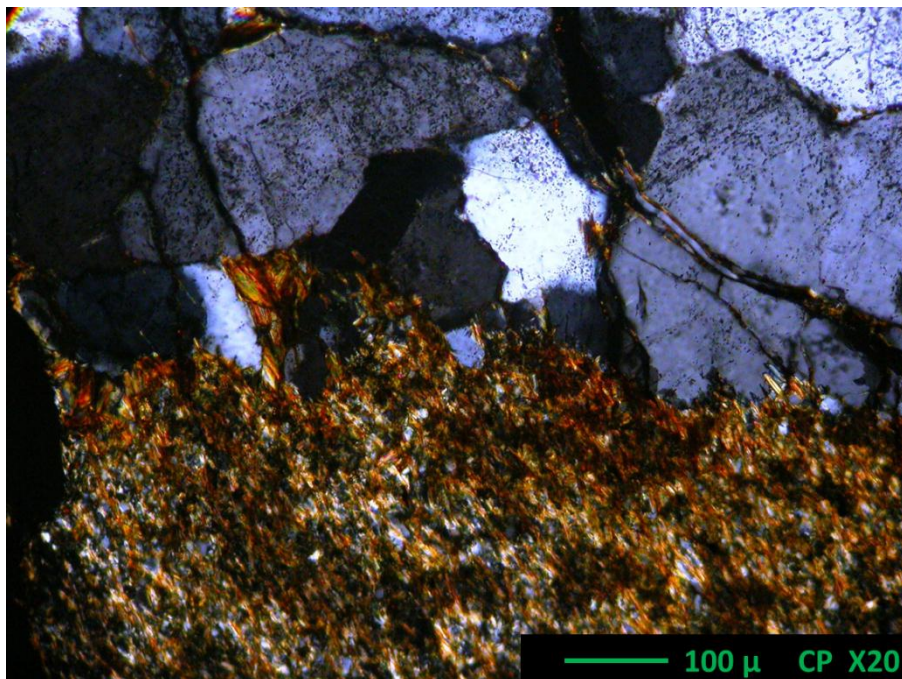


Figure C4: Quartz vein (top) cutting through Ffd (bottom).

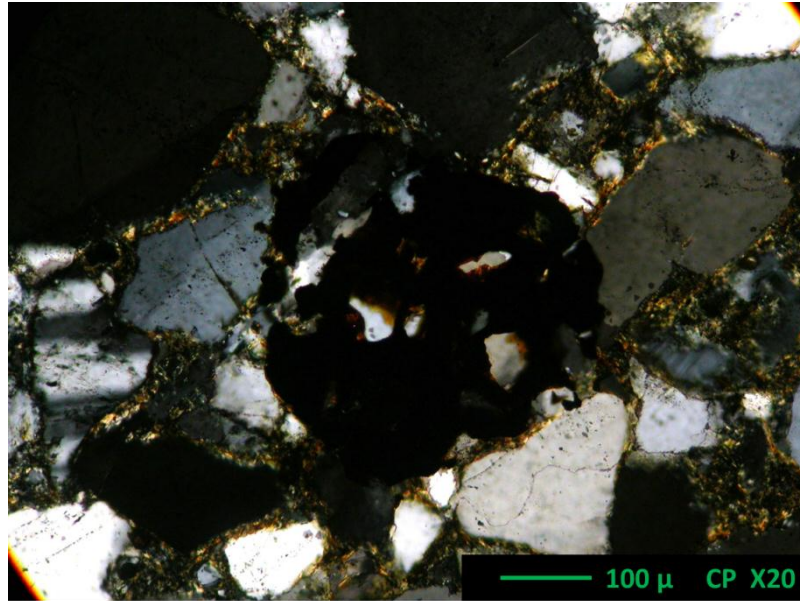


Figure C5: Magnetite - quartz - biotite grain in Sm.

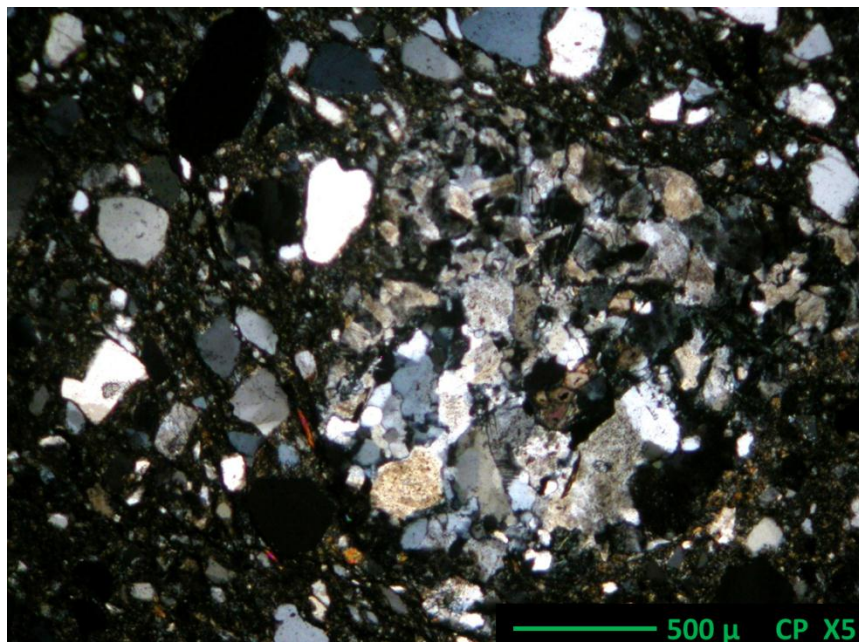


Figure C6: Plutonic rock fragment situated in interstitial material of Dcm.

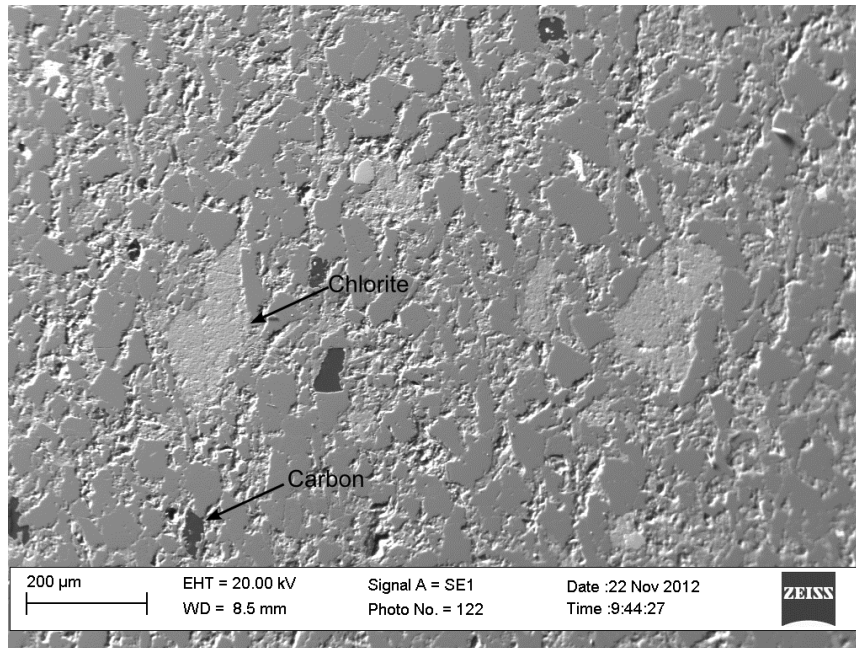


Figure C7: Overview of Smc.

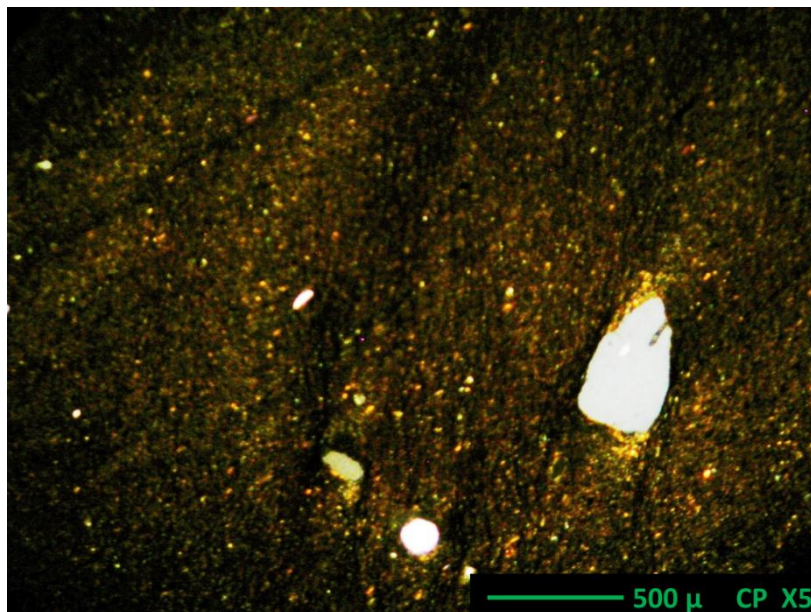


Figure C8: Overview of Ffd with dropstone clasts.

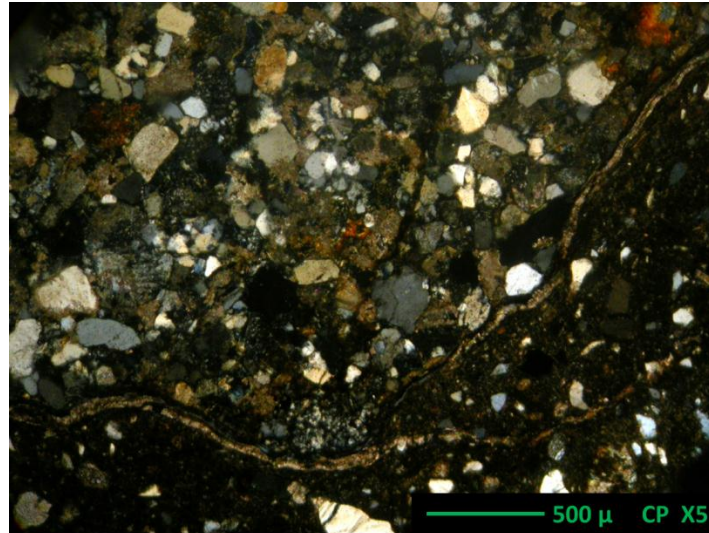


Figure C9: Calcite rim around rock fragment in Dcm.

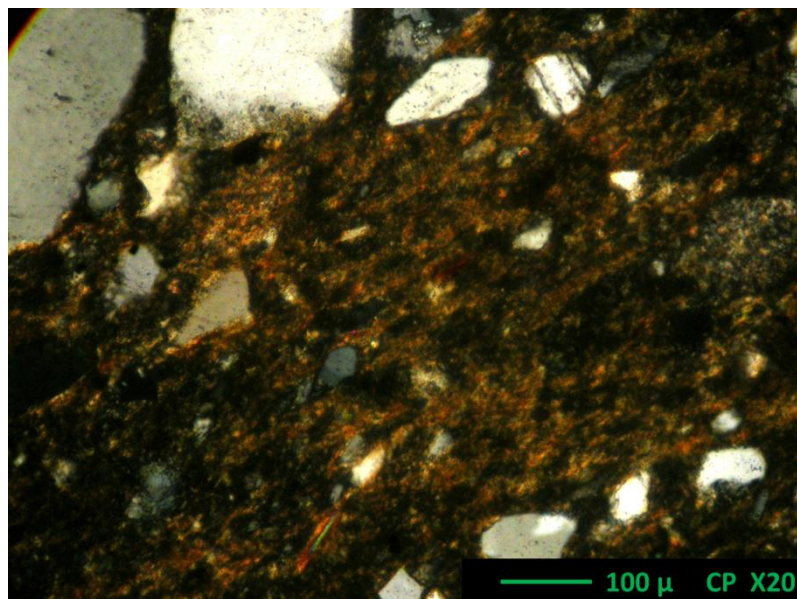


Figure C10: Close up of matrix of Dcm.

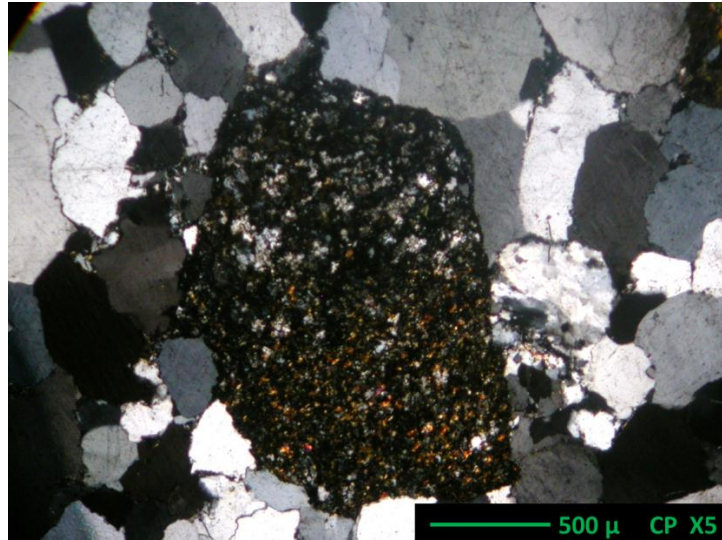


Figure C11: Granitic rock fragment in Sm.

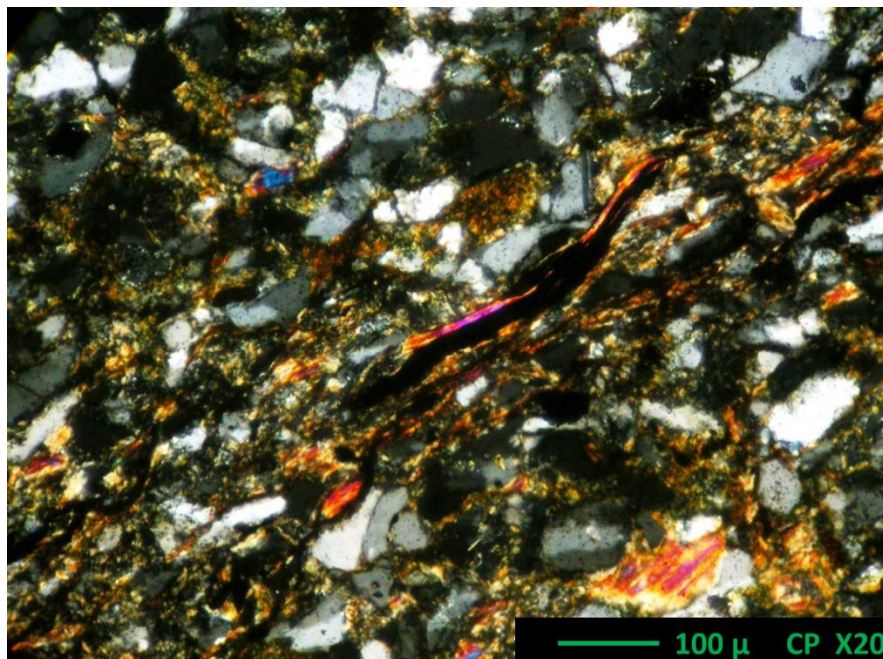


Figure C12: Close-up of Frc show fine sand grains and matrix with carbon streak.

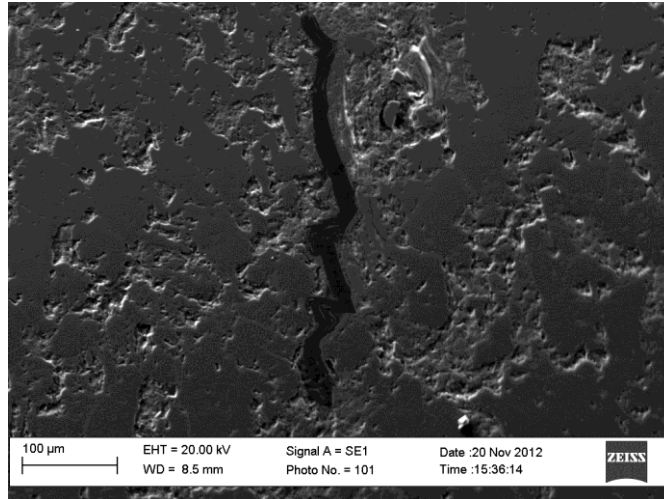


Figure C13: Close-up SEM image of folded carbon streak in Frc.

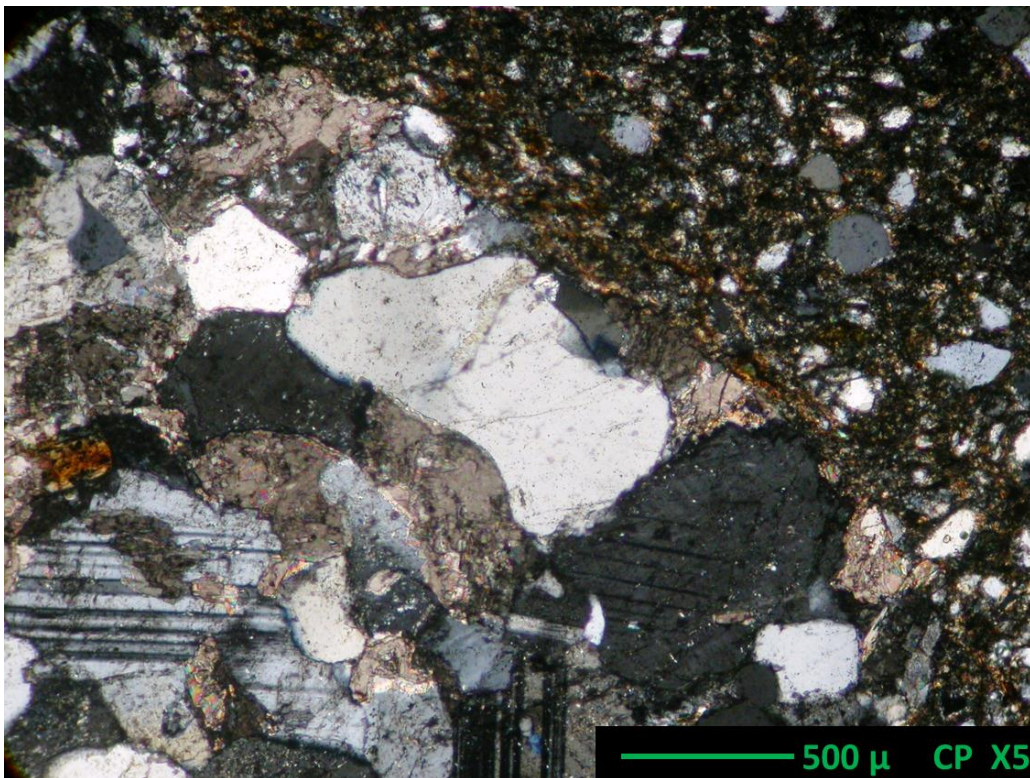


Figure C14: Large rock fragment surrounded by interstitial material of Dcm.

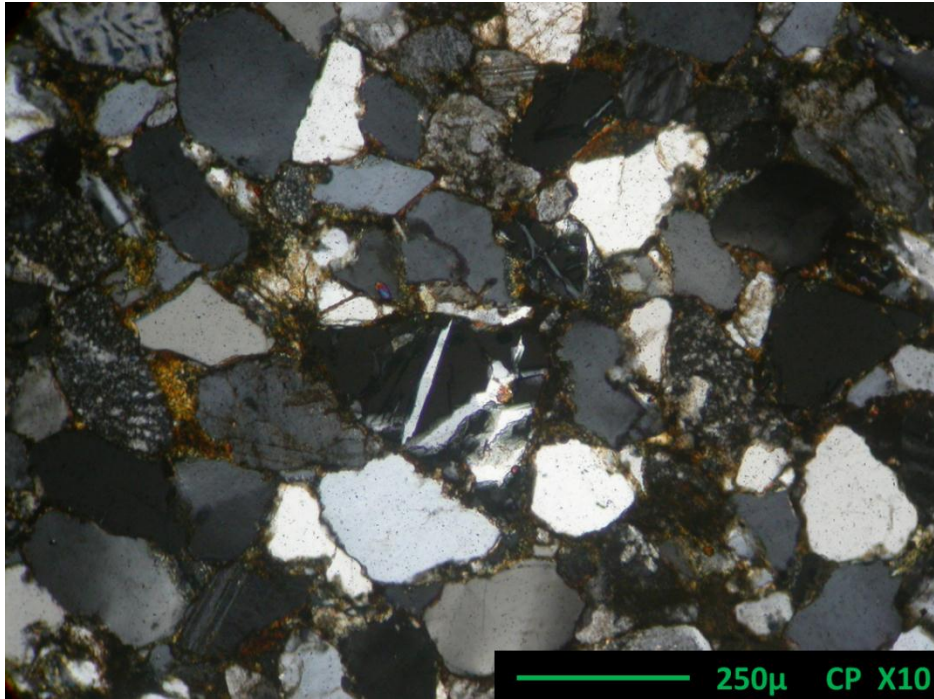


Figure C.15: Close-up of SIm with garnet and quartz grain in centre.